universität wien

# DISSERTATION / DOCTORAL THESIS

Titel der Dissertation /Title of the Doctoral Thesis

„Interaction partners and post-translational modifications of cohesin in *Tetrahymena thermophila*“

verfasst von / submitted by

Emine Ibriam Ali

angestrebter akademischer Grad / in partial fulfilment of the requirements for the degree of

Doctor of Philosophy (PhD)

Wien, 2018 / Vienna, 2018

| | |
|---|---|
| Studienkennzahl lt. Studienblatt / degree programme code as it appears on the student record sheet: | A 794 685 490 |
| Dissertationsgebiet lt. Studienblatt / field of study as it appears on the student record sheet: | Molekulare Biologie |
| Betreut von / Supervisor: | ao. Univ. Prof. Dr. Josef Loidl |

# Table of Contents

## Acknowledgment

First of all, I would like to thank my supervisor, Prof. Dr. Josef Loidl, for the opportunity to work on this interesting project and for his support and input during my PhD study. I would like to thank Rachel Howard-Till for providing me with professional and personal guidance. Her insightful comments and encouragements have made it possible to overcome numerous challenges I have been facing through my research.

I would like to thank all members of the lab, Miao Tian, Takahiko Akematsu, and Bradley Till, for the wonderful atmosphere and lovely discussions. I am grateful to all members of our department and campus who in one way or another contributed to the completion of my projects.

Finally, I would also like to thank my family and my friends for the encouragement and moral support. Special thanks to Yeserin Yildirim, Kaya Akyuz, Elcin Golbasi, Fatma Akin, Hilal Ates, and Hulya Ulusoy for their patience and endless support through writing this thesis.

# Abstract

Cohesin is a conserved protein complex required for chromosome segregation, genome organization, DNA repair, and gene regulation. The complex consists of Smc1, Smc3, an $\alpha$-kleisin and a HEAT repeat subunit. Most eukaryotes have different variants of cohesin subunits that form specific complexes to perform distinct functions. However, only a single cohesin complex is used in the protist *Tetrahymena thermophila*. *Tetrahymena* has two genomes: a transcriptionally silent germline nucleus and a transcriptionally active somatic nucleus. Cohesin has been detected only in the germline nucleus, which undergoes mitosis and meiosis. To understand how a single cohesin complex is able to function in different cellular processes, we investigated the interaction partners and post-translational modifications that regulate cohesin function.

We showed that a putative homolog of the HEAT repeat protein Scc3 is able to interact with all known cohesin subunits. Depletion of Scc3 by RNA interference showed that Scc3 is required for meiotic DNA double-strand break repair (DSB), phosphorylation of the kleisin (Rec8), and chromatin association of both Smc1 and Rec8. Next, we studied a homolog of Scc2 which, in other organisms, is part of the Scc2/Scc4 cohesin loader complex. Scc2 depletion revealed that it is essential for faithful chromosome segregation in mitosis as well as meiotic progression and DSB repair. Although *Tetrahymena* Scc2 interacts with both Scc3 and Rec8, it is not required for their localization on chromatin, suggesting that Scc2 might have a different role in cohesin function in *Tetrahymena*. Finally, we found multiple post-translationally modified residues on different cohesin subunits. To study the effect of reduced cohesin SUMOylation, we fused the catalytic domain of Ulp1 (SUMO isopeptidase) to Rec8. Cells expressing the fused protein showed meiotic defects and decreased chromatin association of Rec8 (or cohesin).

In summary, this study demonstrates numerous peculiarities of the minimal cohesin apparatus in the evolutionarily distant model *Tetrahymena thermophila*.

# Zusammenfassung

Cohesin ist ein konservierter Proteinkomplex mit Funktionen bei der Chromosomensegregation, Genomorganisation, DNA Reparatur und Genregulation. Dieser Komplex besteht aus Smc1, Smc3, einem α-Kleisin und einer HEAT-Repeat Untereinheit. Bei den meisten Eukaryoten bilden unterschiedliche Untereinheiten unterschiedliche Varianten des Komplexes mit spezifischen Funktionen, jedoch nur eine Variante findet sich beim Protisten *Tetrahymena thermophila*. *Tetrahymena* hat zwei Genome: einen transkriptorisch inaktiven Keimbahn-Kern, welcher Mitosen und Meiose durchführt, und einen aktiven Soma-Kern; Cohesin wurde nur im Keimbahn-Kern gefunden. Um zu verstehen, wie ein Organismus mit einem einzigen Cohesin-Komplex auskommt, untersuchten wir die Interaktionspartner und post-transkriptionelle Modifikationen, die die Funktionen von Cohesin regulieren.

Wir zeigen, dass ein vermutliches Homologes des HEAT-Repeat Proteins Scc3 mit allen bisher bekannten Cohesin-Untereinheiten interagieren kann. Der Entzug von Scc3 durch RNA-Interferenz zeigte, dass Scc3 für die Reparatur von meiotischen DNA Doppelstrangbrüchen (DSBs), die Phosphorylierung des Kleisins Rec8, und die Chromatin-Assoziation von Smc1 und Rec8 nötig ist.

Weiters untersuchten wir ein Homologes von Scc2, welches bei anderen Organismen Teil des Scc2/Scc4 Cohesin Lade-Komplexes ist. Der Entzug von Scc2 enthüllte seine essentielle Rolle bei der mitotischen Chromosomensegregation, der meiotischen Teilung und der DSB Reparatur. Obwohl *Tetrahymena* Scc2 mit Scc3 und Rec8 interagiert, ist es nicht für ihre Assoziation mit Chromatin nötig, daher mag es eine andere Bedeutung für die Funktion des Cohesins haben.

Schließlich haben wir zahlreiche post-transkriptionell modifizierte Reste an verschiedenen Cohesin-Untereinheiten gefunden. Um die Effekte reduzierter Cohesin SUMOylierung zu untersuchen, fusionierten wir die katalytische Domäne der SUMO Isopeptidase Ulp1 mit Rec8. Zellen mit dem Fusionsprotein zeigten meiotische Defekte und verminderte Chromatin-Assoziation von Rec8 bzw. Cohesin.

Zusammenfassend zeigt dieser Beitrag die zahlreichen Unterschiede zwischen dem minimalistischen Cohesin Apparat des evolutionär weit entfernten Modellorganismus *Tetrahymena* und dem der traditionell studierten Organismen auf.

# Introduction

## Overview of Mitosis and Meiosis

The accurate transmission of the genetic information is vital for the survival of every species. This process is driven by two types of cell divisions: mitosis, which is used for somatic or non-sexual cell division, and meiosis, which produces sexual gametes. In mitosis, the parental genomic content is duplicated and segregated into the daughter cells. In meiosis, however, DNA replication is followed by two consecutive rounds of segregation which reduce the genomic content by half. Moreover, recombination between homologs and the random segregation of the chromosomes during meiosis provides genomic diversity during the generation of haploid gametes. Errors in meiosis result in aneuploidy and birth defects, whereas the deregulation of mitosis can result in cancer.

After completion of DNA replication, a cell contains two copies of each chromosome, called sister chromatids. An evolutionarily conserved protein complex known as cohesin provides a physical connection between the sister chromatids. This physical linkage is known as cohesion, and it is important for subsequent stages of mitosis and meiosis (Brooker and Berkowitz, 2014; Peters and Nishiyama, 2012)
Mitosis can be divided into the stages of prophase, metaphase, anaphase and telophase (Figure 1). During prophase, chromosomes condense and the nuclear envelope breaks down. The microtubules emerging from opposite ends of the cell attach to the centromere-associated kinetochores of sister chromatids. Cohesion at the centromere resists the pulling forces of the microtubules until all kinetochores are correctly attached (biorientation) at metaphase. Completion of attachment is followed by spindle assembly checkpoint silencing, removal of cohesin and separation of sister chromatids at anaphase (reviewed in (Hauf and Watanabe, 2004; Sacristan and Kops, 2015)). In telophase, separated chromatids decondense and the nuclear envelope reassembles.

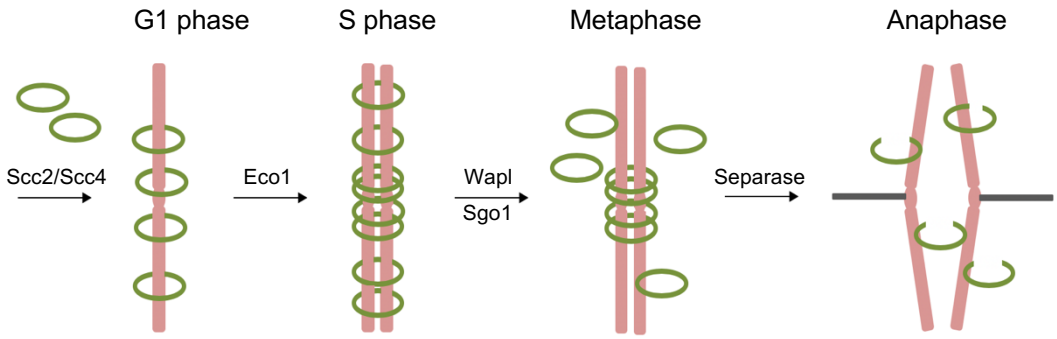


**Figure 1. General illustration of mitosis.**
After DNA replication, cohesion is established between sister chromatids with multiple cohesin complexes (green). During mitosis of mammalian cells, most of the cohesin on the chromosome arms is dissociated during prophase while a subset of cohesin is protected and remains at the centromeres. At the onset of anaphase, the cleavage of cohesin allows sister chromatid segregation.

The segregation of chromosomes in meiosis occurs in two rounds of division, meiosis I and meiosis II (Figure 2). Each division consists of prophase, metaphase, anaphase, and telophase. During prophase of meiosis I, homologous recombination leads to genomic exchange and the formation of chiasmata that establish a physical connection between homologous chromosomes. In most organisms, these processes depend on the pairing of homologs with the help of a protein structure called the synaptonemal complex (SC). Based on the chromosome morphology, prophase I is further subdivided into leptonema, zygonema, pachynema, diplonema and diakinesis. By the end of DNA replication, chromosomes are organized into loops that are connected by chromosome axis proteins and cohesin to form loop/axis structure. The assembly of the chromosome axes continues during leptotenema and the proteins of SC are recruited to form lateral elements. At the same time, multiple DNA double strand breaks (DSBs) are introduced by Spo11 (Keeney, 2008). By zygonema, the telomeres cluster together to form a bouquet-like structure which is thought to be important for the pairing of the homologs (Scherthan, 2007; Zickler and Kleckner, 2015; Loidl, 2016). Meanwhile, the assembly of transverse filaments starts to connect the lateral elements of the homologs. At pachynema, the SC assembly is complete and the DSBs are repaired through either crossover or non-crossover pathways. SC disassembly and condensation of the chromosomes are initiated by pachynema. In diakinesis, chromosomes condense to form pairs of connected homologs, known as bivalents. At metaphase I, the bivalents align at the metaphase plate with the

kinetochores of sister chromatids attached to the microtubules from the same pole (mono-orientation). Crossed-over chromatids that are held together by cohesion form chiasmata. Chiasmata hold the homologs together and ensure attachment of homolog centromeres to microtubules from opposite poles. At anaphase I, cohesin dissociates from chromosome arms (but not from the centromeres) to allow for resolution of crossovers and the segregation of homologous chromosomes. Similar to mitosis, biorientation of the sister kinetochores occurs during meiosis II. It is followed by the removal of the remaining cohesin from chromosomes, leading to sister chromatid separation at the onset of anaphase II.

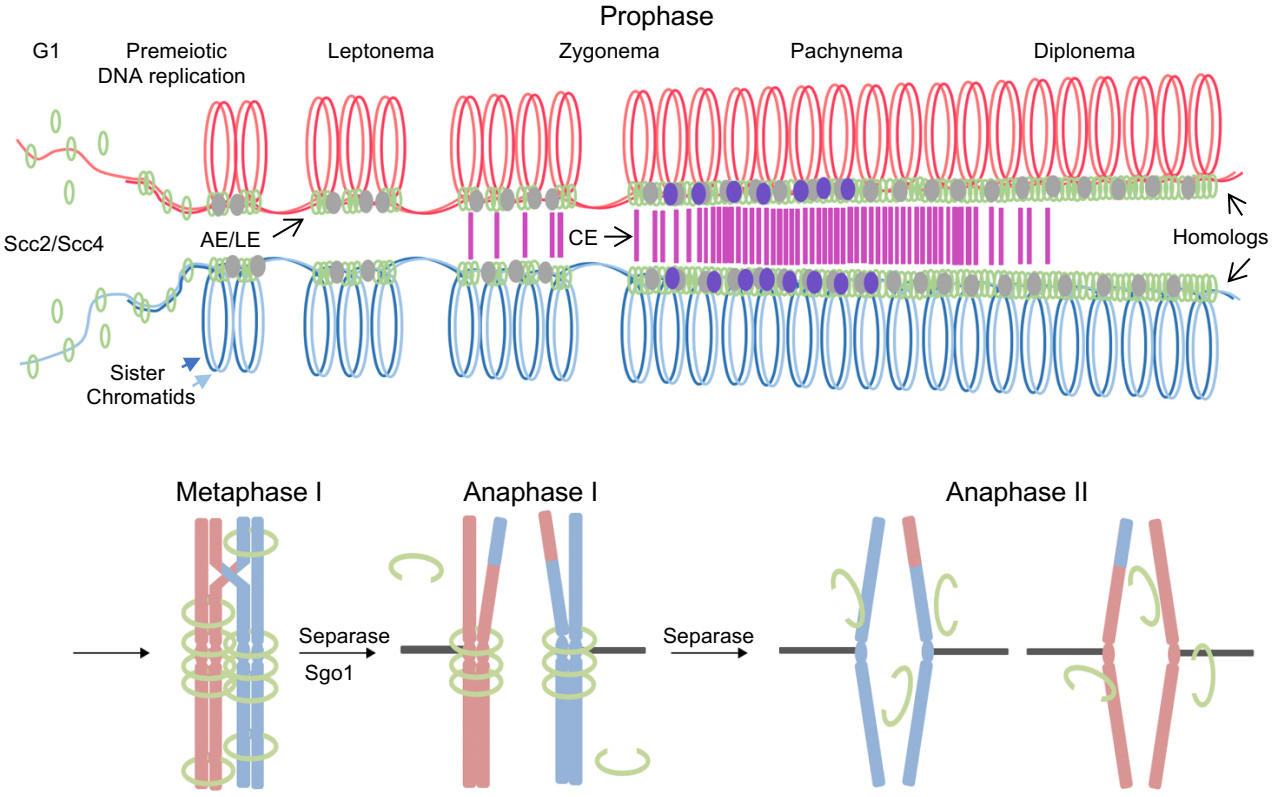


**Figure 2. General illustration of meiosis.**
In meiosis, the chromosome segregation occurs at two rounds. For simplicity, only four stages of meiosis are shown. During prophase I, chromosome axis and SC assembly promote programmed DSBs formation and pairing of homologous chromosomes. In meiosis I, most of the cohesin is cleaved and removed from chromosome arms while centromeric cohesion is protected. Homologous chromosomes are segregated during anaphase I. Cleavage of cohesin at the centromeres promotes sister chromatid segregation during meiosis II. AE: axial element, LE: lateral element, CE: central element

# The Cohesin Complex

The role of cohesin has been well documented for different nuclear processes, including chromosome segregation, genome organization, and DNA repair (Nasmyth and Haering, 2009; Seitan and Merkenschlager, 2012; Ström et al., 2007). Cohesin is critical to maintaining genome stability; a large number of studies have identified mutations in the genes encoding cohesin subunits and cohesin regulators in different cancer types (Hill et al., 2016; Banerji et al., 2017; Mazumdar and Majeti, 2017). Cohesin is also implicated in a number of developmental disorders known as cohesinopathies. Numerous studies indicate that, in many of these disorders, reduced cohesin function primarily affects chromatin organization and gene transcription, which can have profound effects during development (Mazumdar and Majeti, 2017).

## Structure of the cohesin complex

The cohesin complex is composed of four conserved subunits: Smc1, Smc3, an $\alpha$-kleisin (Scc1/Mcd1/Rad21), and a HEAT repeat protein (Scc3/SA1/2) (Losada et al., 1998, 2000; Michaelis et al., 1997). The polypeptides of both Smc1 and Smc3 (structural maintenance of chromosomes) proteins fold on themselves to form a hinge domain, an antiparallel coiled-coil and a nucleotide binding domain (NBD). The interaction of Smc1 and Smc3 at their hinge domains creates a V-shaped heterodimer (Haering et al., 2002), and the two NBDs join to form an ATPase with two ATP binding sites (reviewed in (Nasmyth and Haering, 2009)). The $\alpha$-kleisin binds asymmetrically to the Smc dimer, with its N-terminal end at the coiled-coil region next to the Smc3 NBD domain and its C-terminal end at the Smc1 NBD domain (Gligoris and Löwe, 2016; Gligoris et al., 2014, Huis in ’t Veld et al., 2014) . The HEAT repeat subunit, Scc3/SA1/2, is recruited to the complex via the $\alpha$-kleisin (Haering et al., 2002; Roig et al., 2014).

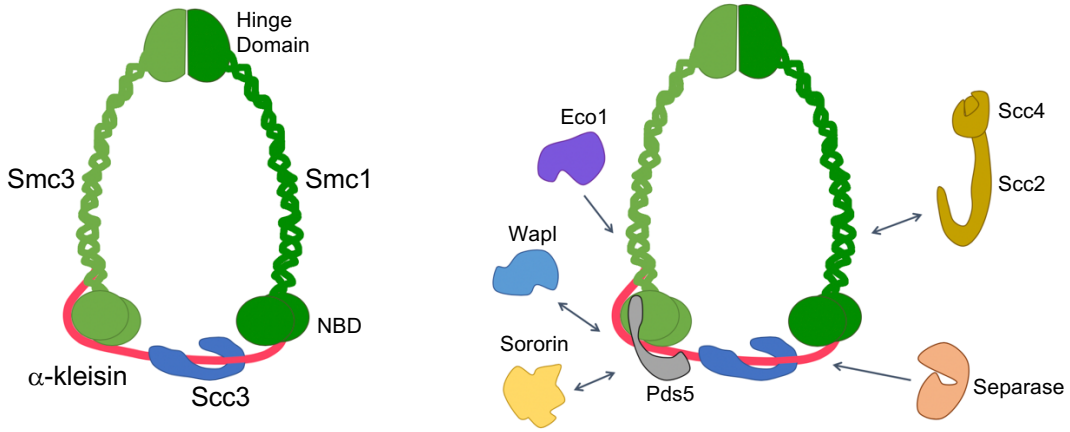


**Figure 3. The cohesin architecture and interacting proteins.** See the text for details.

In addition to binding Scc3, the α-kleisin functions as a binding platform for another HEAT repeat containing protein, Pds5. Although the function of Pds5 can vary between species, it has been shown that it is required for both the maintenance of cohesion and the dissociation of cohesin from chromosomes (reviewed in (Mehta et al., 2012; Haarhuis et al., 2014)). The interaction of Pds5 with Wapl mediates cohesin dissociation from chromosomes (see below). However, the binding of Pds5 to vertebrate specific Sororin inhibits the function of Wapl (Nishiyama et al., 2010). Cohesin also interacts with the Scc2/Scc4 complex, which mediates its loading onto chromosomes (see below).

Biochemistry and electron microscopy has revealed that the cohesin complex forms a ring-like structure (Anderson et al., 2002; Gruber et al., 2003; Huis in 't Veld et al., 2014; Hons et al., 2016). Moreover, it has been shown that DNA is topologically entrapped within the cohesin ring (Ivanov and Nasmyth, 2005). Several models have been proposed for the role of cohesin in mediating sister chromatid cohesion (reviewed in (Nasmyth and Haering, 2009)). The ring model predicts that both sister chromatids are held together within a single cohesin ring (Ivanov and Nasmyth, 2005; Haering et al., 2008). The handcuff model, on the other hand, proposes that each chromatid is entrapped by a single cohesin complex and these complexes interact in order to mediate sister chromatid cohesion (Zhang et al., 2008b).

## The HEAT repeat protein Scc3

The HEAT repeat protein subunit of cohesin (Scc3/SA1/SA2/STAG3) interacts with the α-kleisin (Haering et al., 2002; Roig et al., 2014). Mitosis and meiosis specific forms of this subunit are encoded in some organisms. For instance, vertebrates have three homologs, SA1/STAG1 and SA2/STAG2 for somatic cells and STAG3 for meiosis. The SA1 containing cohesin is essential for telomere cohesion, and SA2 cohesin is required for centromere cohesion (Canudas and Smith, 2009; Remeseiro et al., 2012). Meiosis specific STAG3 is required for the synapsis of homologous chromosomes and meiotic DSB repair during meiotic prophase (Fukuda et al., 2014; Hopkins et al., 2014; Winters et al., 2014). In yeast cells, Scc3 functions in both mitosis and meiosis. It interacts with the Scc2/Scc4 loader complex and promotes the association of cohesin with chromatin (Hu et al., 2011; Murayama and Uhlmann, 2014). Moreover, it helps to maintain sister chromatid cohesion (Roig et al., 2014), but also plays a role in cohesin's dissociation from chromatin (Hauf et al., 2005; Losada et al., 2000). Meiosis in the absence of Scc3 results in defective chromosome axis formation, sister chromatid cohesion and meiotic progression (Fukuda et al., 2012, 2014; Sakuno and Watanabe, 2015; Winters et al., 2014).

## Scc2 as a subunit of the cohesin loader complex

Scc2 (Mis4 in fission yeast, Nipbl in mammals) was initially identified in budding yeast (Michaelis et al., 1997). Scc2 is composed of multiple HEAT repeats (Kikuchi et al., 2016; Neuwald, 2000), and structural studies show that the C-terminal end of Scc2 folds into a hook-like structure (Chao et al., 2017; Kikuchi et al., 2016). Moreover, the C-terminal end contains multiple conserved residues that are important for the interaction with cohesin subunits. Interestingly, these same residues are mutated in cohesinopathies (Chao et al., 2017; Kikuchi et al., 2016). Emphasizing the importance of these residues is the finding that Scc2 alone, or even just the C-terminal end, is sufficient for cohesin loading in vitro (Murayama and Uhlmann, 2014). Although the N-terminal end of the protein is unstructured, it is required for forming a complex with Scc4 (Ssl3 in fission yeast, MAU2 in mammals) (Chao et al., 2015; Woodman et al., 2014). Scc4 is a TPR (tetratricopeptide repeat) containing protein that is important for targeting the complex to specific genomic regions (Watrin et al., 2006; Chao et al., 2015; Hinshaw et al., 2015).

## The association of cohesin with chromosomes during mitosis and meiosis

The interaction of cohesin with chromatin is a dynamic process. Protein-protein interactions and post-translational modifications regulate cohesin association with chromatin during cell cycle progression. This process is known as cohesin cycle. Although there are organism-specific differences, the cycle can be divided to three parts: loading of cohesin, establishment of cohesion, and dissociation of cohesin.

### Loading of cohesin

The initial association of cohesin with chromatin occurs at late G1/early S phase in budding yeast, and at telophase in vertebrates (Darwiche et al., 1999; Michaelis et al., 1997; Sumara et al., 2000; Uhlmann et al., 1999). Loading depends on the hydrolysis of ATP by the NBDs of Smc1 and Smc3 (Arumugam et al., 2003; Hu et al., 2011; Weitzer et al., 2003). The ATPase activity of cohesin is stimulated by the Scc2/Scc4 loader complex which results in the entrapment of DNA (Murayama and Uhlmann, 2014; Petela et al., 2018). Based on mutation studies and artificial blocking of different cohesin interfaces, it has been suggested that the Smc1-Smc3 hinge interface might act as the DNA entry gate in human and budding yeast (Buheitel and Stemmann, 2013; Gruber et al., 2006; Kurze et al., 2011; Mishra et al., 2010). However, it is unknown how ATP hydrolysis at the NBD domains stimulates hinge opening at the opposite end of the complex.

### Establishment of cohesion

Loading of cohesin is not sufficient for the establishment of sister chromatid cohesion at later stages of the cell cycle. It has been observed that mammalian cohesin has a short residence time on chromatin before DNA replication (Gerlich et al., 2006). This dynamic behavior of cohesin during interphase has been suggested to be due to the anti-establishment activity of Wapl (Kueng et al., 2006). The stable association of cohesin occurs during DNA replication both in mammals and yeast (Gerlich et al., 2006; Haering et al., 2004). During DNA replication, the conserved K112 and K113 residues of budding yeast Smc3 (K105 and K106 in mammals) are acetylated by Eco1 acetyltransferase (Esco1 and Esco2 in mammals) (Ben-Shahar et al., 2008; Unal et

al., 2008; Zhang et al., 2008a). Acetylation antagonizes the anti-establishment function of Wapl and Pds5 (Gandhi et al., 2006; Kueng et al., 2006; Rowland et al., 2009; Tedeschi et al., 2013). In vertebrates, the maintenance of cohesins' stable interaction with DNA also depends on Sororin (Nishiyama et al., 2010; Schmitz et al., 2007).

Cohesion can also be established independently of DNA replication in mitotically dividing cells. In the presence of DNA damage, the Scc2/Scc4 complex promotes the loading of cohesin around the DNA damage sites, as well as through the genome (Ström et al., 2004, 2007; Unal et al., 2007) . The acetylation of cohesin by Eco1 is important for damage induced cohesion. In this case, however, Mcd1 (the budding yeast kleisin subunit), not Smc3, is the target for modification. Mcd1 is phosphorylated at S83 by checkpoint kinase1 (Chk1), and this modification is required for the subsequent acetylation of K84 and K210 by Eco1 (Heidinger-Pauli et al., 2008, 2009).

## The dissociation of cohesin

The connection between sister chromatids needs to be released in order to allow sister chromatid separation. In mitotically dividing budding yeast, all cohesin is removed at the onset of anaphase by the thiol protease separase (Uhlmann et al., 2000). During the cell cycle, separase is kept inactive by its interaction with securin and by inhibitory phosphorylation. Once the correct attachment of the chromosomes to opposing microtubules is achieved, the anaphase-promoting complex (APC/C) adds ubiquitin to the securin. Ubiquitination stimulates securin degradation and the activation of separase (reviewed in (Kamenz and Hauf, 2017)). The active separase cleaves the phosphorylated $\alpha$-kleisin subunit and leads to the release of cohesin from chromatids (Uhlmann et al., 2000).

In vertebrate cells, the bulk of cohesin is released from chromosome arms prior to anaphase, during mitotic prophase (Sumara et al., 2000; Waizenegger et al., 2000). This so-called "prophase pathway" depends on the phosphorylation of the SA2 (Scc3) subunit of cohesin by polo-like kinase (Plk1) (Hauf et al., 2005; Sumara et al., 2002). Wapl/Pds5 interacts with phosphorylated SA2 and promotes the release of cohesin through the Smc3/$\alpha$-kleisin interface (Buheitel and Stemmann, 2013; Chan et al., 2012; Eichinger et al., 2013; Hauf et al., 2005). The cohesin at the centromeres is

protected from the prophase pathway by the protein phosphatase 2A (PP2A). Shugoshin (Sgo1) recruits PP2A to the centromeres, where SA2 is dephosphorylated and the dissociation function of Wapl is inhibited (Hara et al., 2014; Kitajima et al., 2006; McGuinness et al., 2005). At anaphase, the remaining centromeric cohesin is cleaved by separase and sister chromatids are pulled to opposite sides of the cell.

During meiosis, the mitosis specific cohesin subunits are replaced with meiosis specific subunits. Most notable is the presence of meiosis specific Rec8 as the kleisin subunit. The dissociation of cohesin from chromosomes is a step-wise process. In meiosis I, Rec8 is phosphorylated by casein kinase 1 and Dbf4-dependent kinase. At the onset of anaphase I, the activated separase cleaves the phosphorylated Rec8 from chromosome arms and allows the homologous chromosomes to segregate (Brar et al., 2006; Buonomo et al., 2000; Katis et al., 2010). A small pool of cohesin at the centromeres is protected from cleavage by Shugoshin protein (Katis et al., 2010; Kitajima et al., 2003). Shugoshin recruits PP2A phosphatase to the centromeres, which removes the phosphorylation on cohesin and inhibits its recognition by separase, thus preventing Rec8 cleavage and cohesin dissociation (Kitajima et al., 2006; Riedel et al., 2006). In meiosis II, the protection of cohesin at centromeres is lost, which allows the separase cleavage and removal of cohesin.

## Post-translational regulation of cohesin

Post-translational modifications (PTMs) of non-histone proteins are fundamental for all cellular processes. The modification of one or more residues can regulate protein-protein interactions, localization, stability, and enzymatic activity of the target proteins. Cohesin is not an exception. More and more studies have shown how different PTMs regulate cohesin function in diverse processes. As mentioned above, acetylation is required for the establishment of cohesion, and phosphorylation for the dissociation of cohesin from chromosomes. DNA damage, on the other hand, induces not only phosphorylation and acetylation but also SUMOylation of cohesin, which is described in further detail below.

## Cohesin SUMOylation

SUMOylation is a reversible modification that is based on the covalent attachment of a small ubiquitin-related modifier (SUMO) polypeptide to the lysine residues of a target protein. The process is mediated via an enzymatic cascade that includes E1 SUMO activating, E2 SUMO conjugating and E3 SUMO ligase enzymes (reviewed in (Johnson, 2004)). The lysine residues of SUMO polypeptides can also be SUMOylated, which results in the formation of SUMO chains. SUMOylation can act as a binding interface for proteins containing SUMO-interacting motifs (SIMs) and modulate enzymatic activity or subcellular localization of the modified protein. Moreover, SUMOylation can be recognized as signal for the protein degradation (Cubeñas-Potts and Matunis, 2013). SUMOylation can be reversed by SUMO specific proteases/isopeptidases that remove SUMO from the substrate protein (reviewed in (Nayak and Müller, 2014)) .

The SUMOylation of all cohesin subunits has been detected during mitosis in budding yeast. The increase of cohesin SUMOylation during DNA replication has been proposed to be involved in the establishment of cohesion (Almedawar et al., 2012). It has also been suggested that the cell cycle dependent SUMOylation of Pds5 might promote the dissociation of cohesin at mitotic anaphase in budding yeast (Stead et al., 2003). In budding yeast, polySUMOylaton of Mcd1 ($\alpha$-kleisin) in the absence of Pds5 results in the ubiquitination and subsequent degradation of the protein (D'Ambrosio and Lavoie, 2014) .

In addition, the SUMOylation of budding yeast Mcd1 is required for de novo establishment of cohesion in the presence of DNA damage (McAleenan et al., 2012). However, in human cells the SUMOylation of Scc1 ($\alpha$-kleisin) is required for DNA repair but not for cohesion (Wu et al., 2012). Moreover, a recent study in mice proposes the involvement of SUMO in the maintenance of centromeric cohesion prior meiosis II (Ding et al., 2018).

## The advantages of *Tetrahymena thermophila* as a model organism

*Tetrahymena thermophila* is a free-living, freshwater, unicellular ciliate. Its unique features as a model organism have allowed for important findings, including the discovery of self-splicing RNAs, dynein, telomeric repeats and telomerase (Blackburn and Gall, 1978; Cech et al., 1981; Gibbons and Rowe, 1965; Greider and Blackburn, 1985).

*Tetrahymena* contains two nuclei within a single cell. The small germline nucleus is transcriptionally silent during vegetative growth and resides within a pocket on the surface of the larger somatic nucleus. Although the somatic nucleus is derived from the germline nucleus during sexual reproduction (see below), the genome composition of the two nuclei is very different from each other. The germline nucleus is diploid and contains five chromosomes, while the somatic nucleus contains approximately 50 copies each of ~225 chromosomes (Eisen et al., 2006; Hamilton et al., 2016).

The nuclear dualism of *Tetrahymena* presents an advantage to study lethal mutations. Homozygous mutations can be introduced into the germline nucleus without affecting the cell viability, and the phenotype can be expressed only in the sexual progeny carrying the mutation. In addition, tagged protein fusions and knock-out strains can be created by homologous recombination, and gene knockdowns are possible using inducible RNAi (Howard-Till and Yao, 2006; Kataoka et al., 2010; Hayashi and Mochizuki, 2015). These applications are possible because of the availability of the genome sequence of both nuclei (Eisen et al., 2006; Hamilton et al., 2016). Furthermore, fast cell growth and synchronous mating enables the analysis of different biological processes easily.

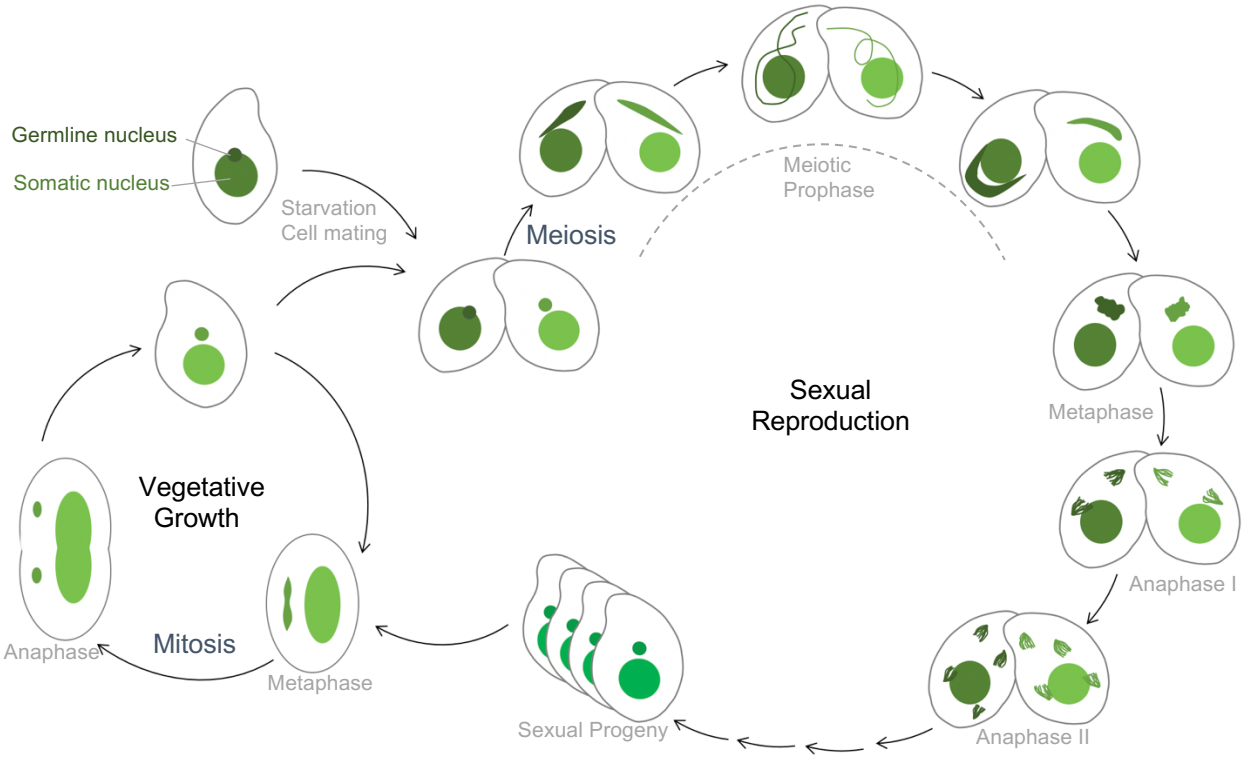


**Figure 4. Schematic illustration of the life cycles of *Tetrahymena thermophila.*** See the text for details.

The *Tetrahymena* has two life cycles: vegetative and sexual reproduction (Figure 4). In the presence of nutrients, the germline nucleus of vegetatively growing cells undergoes mitosis while the somatic nucleus undergoes amitosis, in which chromosomes are randomly split between daughter cells.

The sexual reproduction stage can be induced by starvation, after which *Tetrahymena* cells of different mating types can form a pair. The germline nuclei of both cells undergo synchronous meiosis. Similar to fission yeast, *Tetrahymena* does not utilize an SC during meiotic prophase (Loidl, 2016). However, the induction of programmed DSBs by Spo11 triggers the elongation of the germline nuclei and the formation of a crescent like structure (Mochizuki et al., 2008; Loidl and Mochizuki, 2009). The clustering of telomeres and centromeres to the opposite ends of the elongated nuclei facilitates the formation of a bouquet-like structure and promotes the pairing of the homologous chromosomes (Loidl et al., 2012). At the end of meiosis, one of the four meiotic products undergoes a mitotic division to form pronuclei, and the remaining nuclei are degraded. A reciprocal exchange of pronuclei between paired cells leads to cross-fertilization and zygote formation. The zygotes undergo two additional rounds of mitotic divisions to give rise to four post-zygotic nuclei. Programmed genome

rearrangements occur in two of these nuclei to form the new somatic nuclei. Meanwhile, the parental somatic nuclei are degraded. During the somatic nuclei development the germline specific chromosomes are fragmented at chromosome breakage sites, IESs sequences are removed, and the chromosomes are replicated to form the polyploid somatic nuclei (reviewed in (Noto and Mochizuki, 2017)).

# Aims of the thesis

In *Tetrahymena*, a single cohesin complex has been identified to be essential during mitosis and meiosis (Howard-Till et al., 2013). The complex has been detected only in the transcriptionally silent germline nucleus. In contrast to other eukaryotes, not all proteins regulating the function of cohesin in different nuclear processes have been identified. The goals of this study were to identify and characterize proteins and PTMs required for cohesin function. Most of the experiments presented in the chapter 1 and 2 have been published in (Ali et al., 2018).

Aim 1- Characterization of *Tetrahymena* homologs of Scc3 and Scc2 (Chapter 1 and 2)

The initial goal was to identify cohesin interacting proteins by MS analysis. The approach did not lead to identification of conserved or *Tetrahymena* specific proteins. However, a Scc2 homolog was identified and its role in cohesin function was studied. In addition, the functional conservation of Scc3 homolog which has been identified but not characterized was investigated (Howard-Till et al., 2013).

Aim 2- Identification of PTMs of cohesin (Chapter 3)

The cohesin machinery in *Tetrahymena* appears to be relatively parsimonious. The question we explored in chapter 3 is how a single complex is able to function in different cellular processes for which other organisms need dedicated versions of the complex. As a possible explanation of the versatility of this complex, we aimed to search for PTMs of cohesin subunits at different stages of the *Tetrahymena* life cycle.

# Results

## Chapter 1. Scc3 is essential for the chromatin association of cohesin in *Tetrahymena*

The interaction of Smc1, Smc3, and an α-kleisin forms a tripartite ring which entraps DNA (Nasmyth and Haering, 2009; Rankin and Dawson, 2016). The HEAT repeat protein Scc3 is recruited to cohesin through its interaction with the α-kleisin subunit (Haering et al., 2002; Roig et al., 2014). In yeast and mammals, Scc3 is required for the association of cohesin with chromatin (Hu et al., 2011; Murayama and Uhlmann, 2014), the maintenance of sister chromatid cohesion (Roig et al., 2014), and for cohesin's dissociation from chromatin (Hauf et al., 2005; Losada et al., 2000). In addition, chromosome axis formation, sister chromatid cohesion and meiotic progression are defective in the absence of Scc3 (Fukuda et al., 2012, 2014; Sakuno and Watanabe, 2015; Winters et al., 2014). In *Tetrahymena*, a putative homolog of Scc3 was identified based on homology at the conserved STAG domain (Howard-Till et al., 2013). In this part of the project, the goal was to further characterize the involvement of *Tetrahymena* Scc3 in cohesin function.

### The *Tetrahymena* Scc3 homolog associates with Rec8, Smc1, and Smc3

Similar to Smc1 and Rec8, Scc3 localizes only in the germline nucleus during both vegetative growth and mating of *Tetrahymena* (Ali et al., 2018; Howard-Till et al., 2013). Likewise, the expression profile of SCC3 shows a pattern similar to the other cohesin subunits, with a distinct double peak during meiosis and gametogenic mitosis (Miao et al., 2009)(Figure 5). In agreement with the expression profile, western blots of mCherry tagged Scc3 show the protein level of Scc3 is higher in mating than in growing or starved cells (Figure 5). It is likely that the expression of SCC3 gene is also high during mitosis, but in unsynchronized growing cells, only about 13% of the cells are undergoing mitosis (Ali et al., 2018).

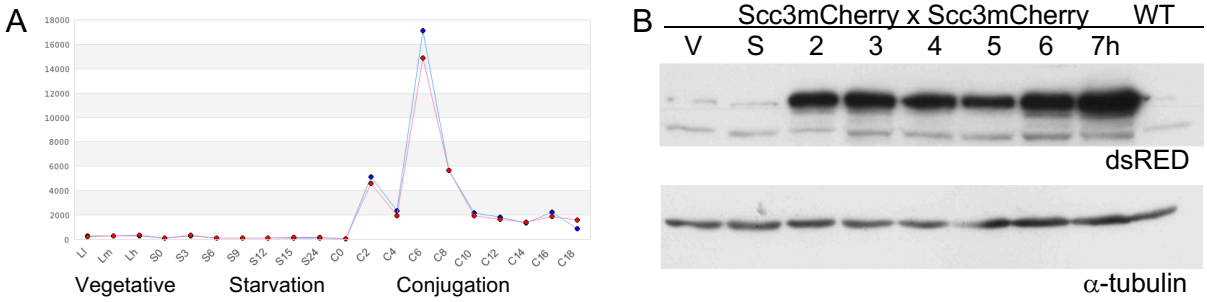


**Figure 5. The expression and protein level of Scc3 increases during mating.**
A. The expression profile of SCC3 (TTHERM_00225630) shows elevated expression in mating *Tetrahymena*. L: vegetative cells, S: starvation, C: conjugation. The expression data was obtained from http://tfgd.ihb.ac.cn/ (Miao et al., 2009; Xiong et al., 2013). B. Similar to the expression profile, the protein level of Scc3 increases during mating. Cells expressing Scc3-mCherry were used for whole protein extracts at the indicated time points. (V: vegetative, S: starvation, 2-7: hours after initiating mating, WT: wild-type vegetative) (Ali et al., 2018).

To test whether *Tetrahymena* Scc3 associates with Smc1, Smc3, and Rec8, strains expressing HA tagged Smc1 or Scc3 from the endogenous loci were created. Because the protein level of cohesin subunits is abundant during mating, immunoprecipitations (IPs) were performed at 4h and 6h after initiation of mating. The 4h time point corresponds to meiotic prophase whereas the 6h time point corresponds to anaphase II of meiosis and gametogenic mitosis. We hoped to differentiate between protein interactions important for meiotic pairing and meiotic DSB repair at the early timepoint, and cohesin loading during replication and a mitosis-like division at the late timepoint. Mass spectrometry (MS) analysis of Smc1-HA IP samples identified Scc3 together with Smc3 and Rec8 as Smc1 associated proteins (Ali et al., 2018). As a reciprocal experiment, IPs were performed on Scc3-HA in 4h mating cells (Table 1). MS of this sample confirmed that all cohesin subunits coprecipitated with Scc3, indicating that Scc3 is a stable part of the cohesin complex. Unfortunately, neither experiment revealed any new potential cohesin interactors (Ali et al., 2018).

**Table 1. Mass Spectrometry of IPs shows the interaction of Scc3 with other cohesin subunits.** (Ali et al., 2018)

| Bait protein | Proteins Identified | Unique peptides | Sequence coverage (%) |
|---|---|---|---|
| Smc1-HA | | | |
| | Smc1 | 116 | 71,1 |
| | Smc3 | 93 | 55,8 |
| | Scc3 | 80 | 54 |
| | Rec8 | 36 | 59,5 |
| Scc3-HA | | | |
| | Scc3 | 74 | 48,2 |
| | Smc1 | 79 | 55,4 |
| | Smc3 | 64 | 43,5 |
| | Rec8 | 27 | 41,5 |

## Scc3 is required for proper chromosome segregation in mitosis and DSB repair in meiosis

In order to study the function of Scc3, inducible RNA interference (RNAi) was used to deplete Scc3 (Howard-Till and Yao, 2006). When Scc3-mCherry strains were induced for Scc3 RNAi (*scc3*i) for 24h, Scc3 was not detectable either by cytology or western blotting (Figure 6A). Vegetative cells depleted of Scc3 had chromosome segregation defects. 23% of the cells had lagging chromosomes during mitotic anaphase, whereas none was detected in WT cells (Ali et al., 2018) (Figure 6B). To allow direct comparison of Scc3 depletion and WT cells in meiosis, WT cells were mated with Scc3 depleted cells. In each mating pair, elongation of the germline nucleus during prophase was observed in both cells. However, the scc3i partner arrested at a metaphase-like stage, while the WT cells were able to complete anaphase II (Ali et al., 2018). To test the formation and processing of meiotic DSBs in the absence of Scc3, slides prepared from the same mating were stained with antibodies recognizing Dmc1/Rad51 and γ-H2A.X. Both Dmc1/Rad51 and γ-H2A.X foci mark the formation of DSBs during early prophase until their repair during late prophase (Howard-Till et al., 2011; Mochizuki et al., 2008). In the WT partner cell, the DSB foci were visible at prophase and they disappeared at metaphase. In the *scc3*i cell, however, the DSB signals were formed

during prophase and were still present in the arrested metaphase-like stage indicating delayed or aborted DSB repair (Ali et al., 2018). These results indicate that Scc3 is not required for meiotic DSB formation, but it is essential for DSB repair. This *scc3*i defect resembles the phenotype observed for Rec8 and Smc1 depletion, suggesting that the phenotype might be due to the absence or lack of function of the entire cohesin complex (Howard-Till et al., 2013).

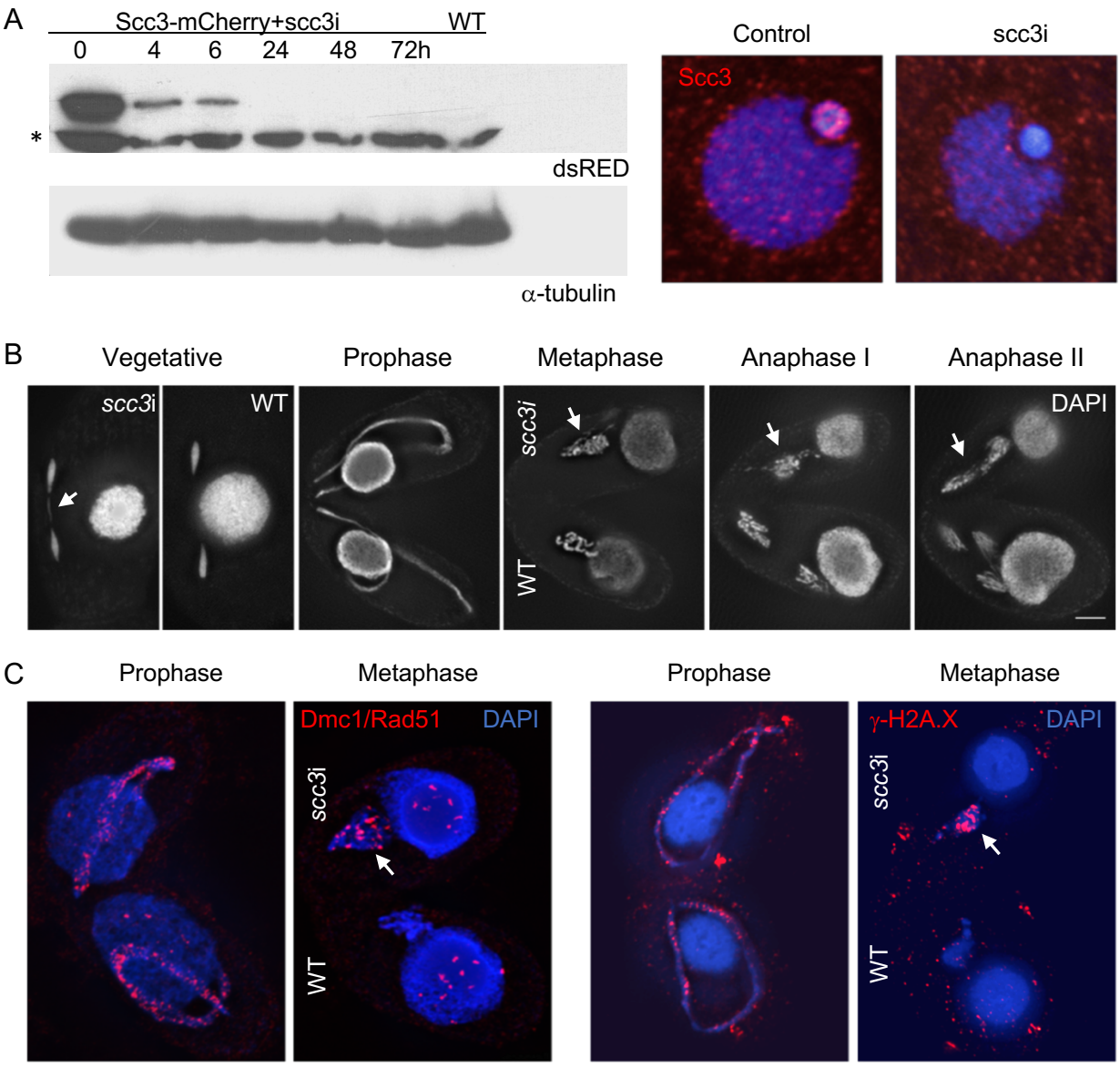


**Figure 6. Scc3 is required for chromosome segregation and DSB repair.**
A. Protein extracts of vegetative Scc3-mCherry + *scc3*i cells were collected at indicated time points after RNAi induction. α-tubulin was used as a loading control in the western blot, and * indicates a non-specific band recognized by the dsRED antibody. For cytology, cells were fixed at 0h (control) and 24h (*scc3*i). Both the western blot and IF show that induction of *scc3*i for 24h is sufficient for complete

depletion of Scc3. B. Vegetative cells were collected 24h after induction of scc3i. Lagging chromosomes during mitotic divisions were observed in *scc3*i cells, but not in the WT cells. Matings of WT cells with *scc3*i cells show a metaphase-like arrest only in the *scc3*i partner, whereas WT cells proceed through meiosis. C. DSB repair is defective in the absence of Scc3. Mating cells from B were fixed in high detergent and stained with the Dmc1/Rad51 antibody, or fixed with the modified Schaudinn method and stained for γ-H2A.X. Scale bars equal 5μm (Ali et al., 2018).

## The germline localization of Rec8 and Smc1 is Scc3 dependent

It has been shown that Scc3 is required for the association of cohesin with chromatin in mice and budding yeast (Fukuda et al., 2014; Roig et al., 2014). Therefore, the observed meiotic phenotype of *scc3*i might be due to the inability of cohesin to associate with chromatin. In order to test this possibility, Scc3 was depleted in strains expressing either Smc1-HA or Rec8-HA3His6. Cytological analysis showed that neither Smc1 nor Rec8 was able to localize to the germline nucleus in the absence of Scc3. However, depletion of Scc3 did not have any effect on the protein level of Smc1 and the overall protein level of Rec8, although one form of Rec8, which was possibly phosphorylated, was absent after depletion of Scc3 (Figure 7, A+B)(Ali et al., 2018).
Previous studies have shown that chromatin association of Scc3 is α-kleisin dependent (Roig et al., 2014). To determine whether this is also the case in *Tetrahymena*, Rec8 was depleted in cells expressing Scc3-HA. Similar to Scc3, complete depletion of Rec8 protein level could be obtained by inducing RNAi for 24h (Ali et al., 2018; Howard-Till et al., 2013). While Rec8 depletion did not have any effect on the protein level of Scc3, Rec8 was required for the Scc3 localization in the germline nucleus (Figure 7C) (Ali et al., 2018). This supports the idea that Scc3 is an essential part of the cohesin complex, and does not function independently or associate with chromatin without the other cohesin subunits.

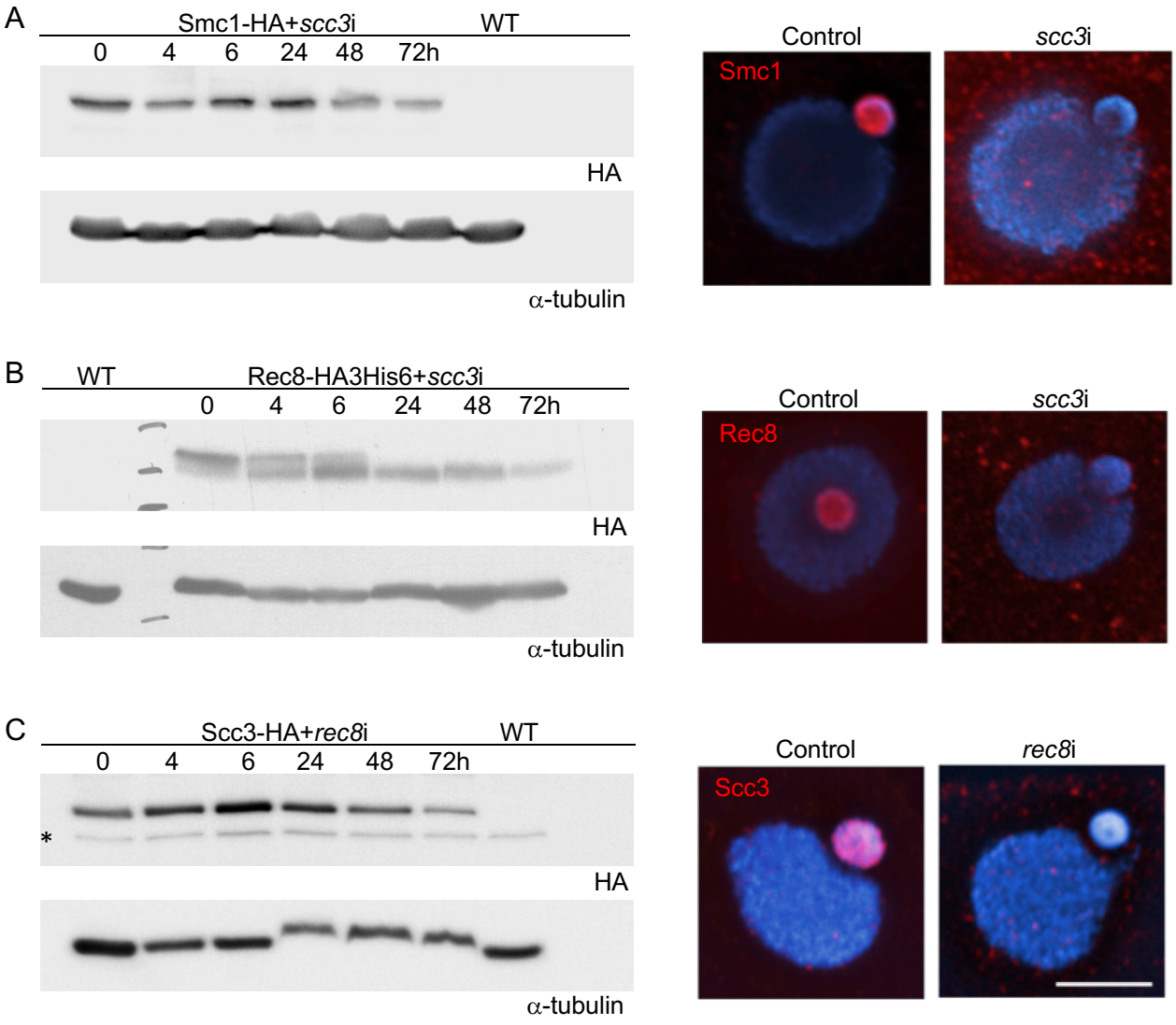


**Figure 7. The germline localizations of Rec8, Smc1, and Scc3 are inter-dependent.**

Protein extracts of vegetative cells expressing different tagged cohesin subunits were prepared at the indicated time points after induction of either *scc3*i or *rec8*i. For immunofluorescence, cells were fixed at 0h (control) and 24h (*scc3*i / *rec8*i) and stained with anti-HA. A. In Smc1-HA + *scc3*i cells, depletion of Scc3 does not affect the protein level of Smc1, but it does abolish its nuclear localization. B. Rec8-HA3His6 + *scc3*i cells show that one form of Rec8 and its localization is dependent on the presence of Scc3. C. In Scc3-HA + *rec8*i cells, the germline localization of Scc3 is Rec8 dependent, but the protein level of Scc3 does not change. * indicates a non-specific band recognized by the HA antibody. Scale bars equal 5μm (Ali et al., 2018).

## Scc3 is required for the phosphorylation of Rec8

A western blot of Rec8-HA3His6 from vegetative cells shows a double band pattern for Rec8, with the upper band being the predominant form (0h in Figure 7B). To test whether the slower migrating form represents phosphorylated Rec8, Rec8 was immunoprecipitated from starved cells and subjected to phosphatase treatment (in collaboration with Rachel Howard-Till). The slower migrating form of Rec8 was lost after lambda protein phosphatase treatment, indicating that Rec8 is phosphorylated (Figure 8A). As mentioned above, the phosphorylated form of Rec8 (pRec8) disappeared gradually after induction of *scc3*i, disappearing altogether by 24 hours of induction. Concurrently, the germline localization of Rec8 was also lost. To investigate the link between Rec8 phosphorylation and chromatin association, cellular fractionation was performed in Rec8-HA3His6 expressing cells to separate soluble vs. chromatin bound proteins. In starved cells, pRec8 was found primarily in the chromatin fraction, and only a small amount of unphosphorylated Rec8 was present in the soluble fraction (Figure 8B). Vegetatively growing cells had higher levels of unphosphorylated Rec8 in the soluble fraction. In the absence of Scc3, only the soluble, unphosphorylated form of Rec8 was detected, in agreement with previous western blots and cytology (Figures 7B and 8B). Therefore, these results show that chromatin-bound Rec8 is phosphorylated. Immunoprecipitated Rec8 from chromatin and soluble fractions was also subjected to mass spectrometry analysis to identify modified residues. Six serine residues: 162, 164, 208, 354, 355, and 529, showed enriched phosphorylation in chromatin bound Rec8 compared to soluble Rec8 (Figure 8C) (Ali et al., 2018).

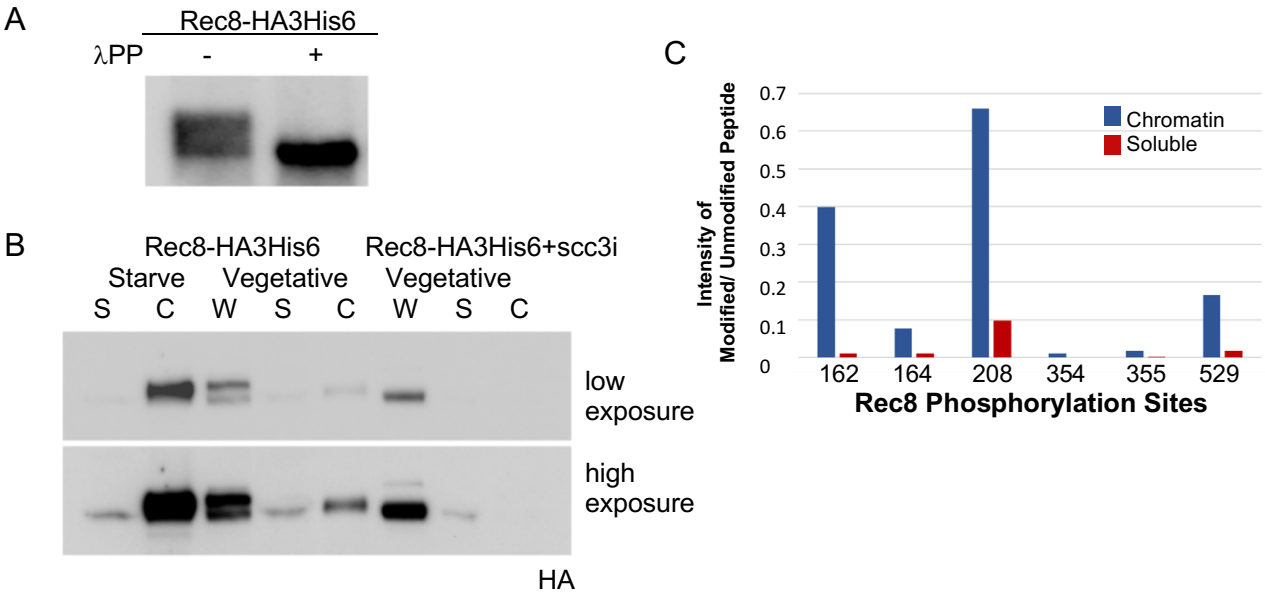


**Figure 8. Chromatin bound Rec8 is phosphorylated.**
A. Rec8-HA3His6 was immunoprecipitated and treated with lambda phosphatase (λPP). The upper band representing phosphorylated Rec8 was lost after the treatment (courtesy of Rachel Howard-Till). B. Scc3 is required for the chromatin association of phosphorylated Rec8. Cellular fractionation was performed on Rec8-HA3His6 or Rec8-HA3His6 + *scc3*i cells after 24h of RNAi induction. In the absence of Scc3, Rec8-HA3His6 is only detected in the soluble fraction. (S: soluble, C: chromatin bound, W: whole cell lysate). C. Phosphorylation sites of chromatin bound Rec8 were identified by MS. Rec8-HA3His6 was immunoprecipitated from soluble and chromatin fractions. Six residues were found to be more phosphorylated in the chromatin fraction compared to the soluble fraction, as shown by the ratio of the intensity of phospho-peptide to the intensity of unmodified peptide. Blue bars represent the chromatin fraction and red bars represent the soluble fraction (Ali et al., 2018).

## *de novo* loading of Rec8 in meiotic prophase is Scc3 dependent

The loading of cohesin occurs during telophase in higher vertebrates and during S phase in yeast (Darwiche et al., 1999; Michaelis et al., 1997; Sumara et al., 2000; Uhlmann et al., 1999). Immunofluorescence of *Tetrahymena* cohesin subunits shows that cohesin is present on germline chromatin at all stages of the life cycle, which makes it difficult to determine at which stage new cohesin loading occurs (Howard-Till et al., 2013). However, a feature of mating *Tetrahymena* is that proteins can be

exchanged between paired cells (McDonald, 1966), which can allow for detection of *de novo* loading of tagged cohesin expressed in only one partner. At late meiotic prophase, Rec8-mCherry is detected in the germline nucleus of WT (untagged) cells mated with cells expressing tagged Rec8, suggesting that cohesin loading is occurring at this time (Figure 9). *scc3*i was induced in starved Rec8-mCherry cells prior to mating in order to suppress new Scc3 protein translation during mating. In this case, germline Rec8 was still observed in the *scc3*i cells, suggesting that only new cohesin loading is affected, and cohesin already loaded prior to mating remains unchanged. However, loading of new cohesin was disrupted in absence of Scc3, as no Rec8 signal is detected in the germline of the WT partner (Figure 9). These experiments were performed at late prophase stage where DSB repair occurs (Howard-Till et al., 2011; Loidl and Lorenz, 2016). Loading of new cohesin and establishment of cohesion occurs in the presence of DNA breaks in other model systems (Heidinger-Pauli et al., 2008, 2009; Unal et al., 2007). To test if meiotic cohesin loading in *Tetrahymena* occurs in response to meiotic DSB formation, RNAi was used to deplete Spo11, the Topo II-like protein that is responsible for creating meiotic DSBs (Howard-Till et al., 2013). Rec8-mCherry cells were mated with either WT cells or *spo11*i cells and fixed using a high concentration of detergent, which removes unbound proteins from the germline (Howard-Till et al., 2011) Rec8 was detected in WT cells as well as in the Spo11 depleted cells. These results indicate that the loading of cohesin is not DSB dependent (Ali et al., 2018).

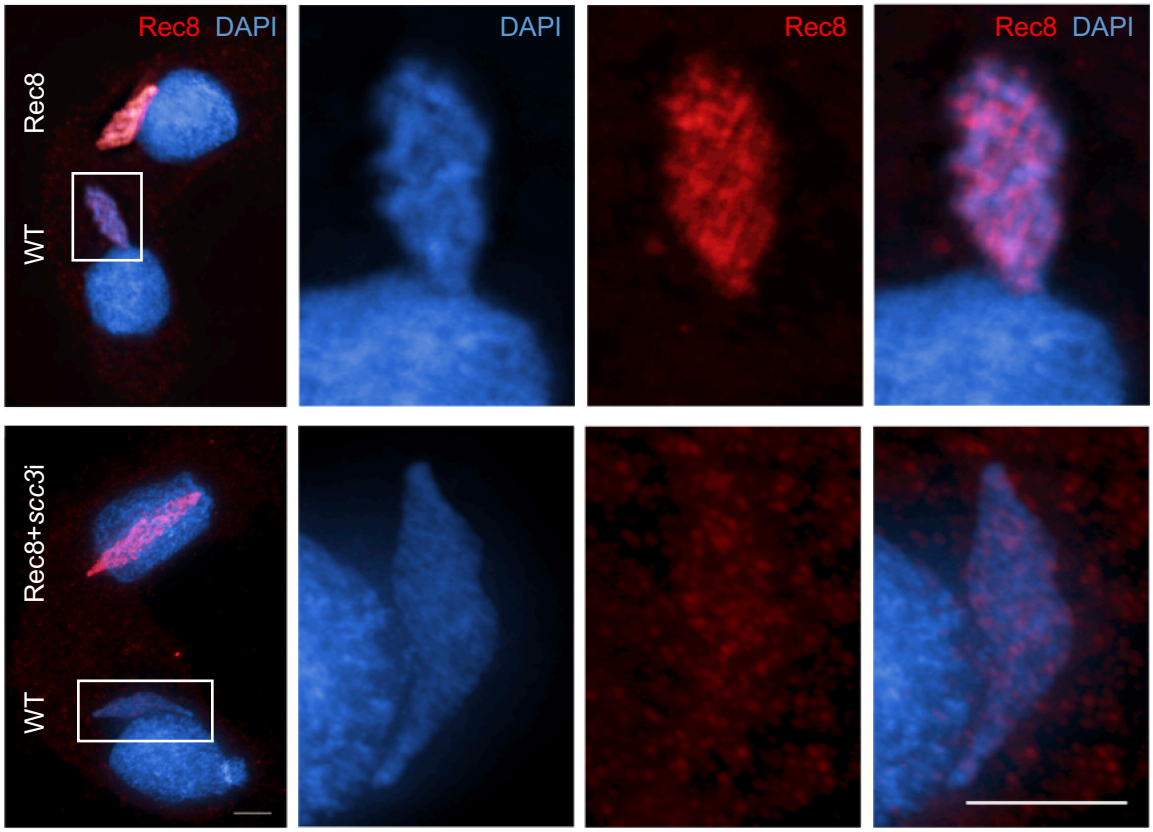


**Figure 9. Scc3 is required for the *de novo* association of Rec8 with chromatin in meiotic prophase.**

Mating was induced between WT cells and cells expressing Rec8-mCherry in the presence (bottom panel) or absence of *scc3*i (top panel). The cells were fixed with a high detergent method 4h after initiation of mating. The enlarged images show the germline nucleus of the WT partner. Chromatin association of Rec8 was detected in the control matings but not in *scc3*i matings. Scale bars equal 5μm (Ali et al., 2018)

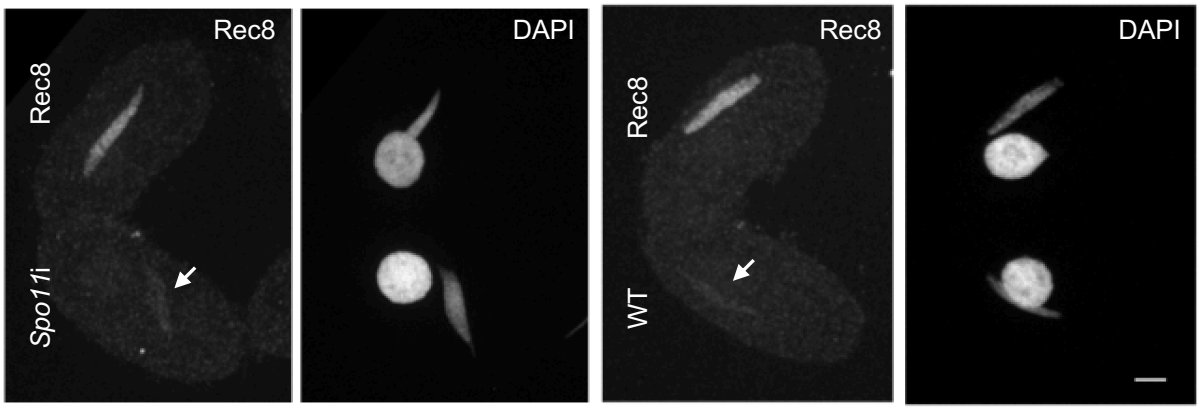


**Figure 10. Loading of Rec8 is not Spo11 induced DSB dependent.**

Cells expressing Rec8-HA3His6 were mated with WT cells or *spo11*i cells. Rec8 localization in the germline was still detected in the absence of Spo11. Scale bar equals 5μm (Ali et al., 2018)

# Chapter 2. Characterization of a *Tetrahymena* Scc2 homolog

## TTHERM_00678460 gene encodes for a homolog of Scc2, a cohesin loader complex subunit

TTHERM_00678460 was identified as a meiosis specific gene in a screen for meiotically upregulated genes (Loidl J. personal communication). To identify the protein encoded by this gene, the predicted protein sequence was used to search publicly available protein sequence databases (States and Gish, 1994). A BLAST search revealed homology to the Scc2/Nipbl subunit of the cohesin loader complex. To search for conserved residues, the predicted protein sequence of TTHERM_00678460 was aligned with Scc2 homologs from different organisms (Edgar, 2004; Kearse et al., 2012). The three most homologous regions are shown in Figure 11A. Two of these regions include residues that have been identified as important for the interaction of Scc2 with the cohesin kleisin subunit Scc1, which are conserved in *Tetrahymena* (Ali et al., 2018; Kikuchi et al., 2016). Therefore, based on the protein's homology to Scc2, we named TTHERM_00678460 gene as SCC2.

The expression profile of the SCC2 gene shows high peak of expression at 2-4h during mating (http://tfgd.ihb.ac.cn) (Miao et al., 2009; Xiong et al., 2013)(Figure 11B). To determine protein levels of Scc2 at different stages, the C-terminal end of the SCC2 gene was fused with the HA3His6 tag at the endogenous locus (Ali et al., 2018). Western blotting of samples collected from different stages of *Tetrahymena* life cycle show that Scc2 is present in both vegetative and sexually reproducing cells (Figure 11C). Similar to the RNA expression profile, the protein levels peak between 2h and 4h of mating. This time interval corresponds to meiotic prophase, where programmed DSBs are formed and repaired, homologous chromosomes are paired, and meiotic recombination occurs (Howard-Till et al., 2011; Lukaszewicz et al., 2010; Mochizuki et al., 2008).

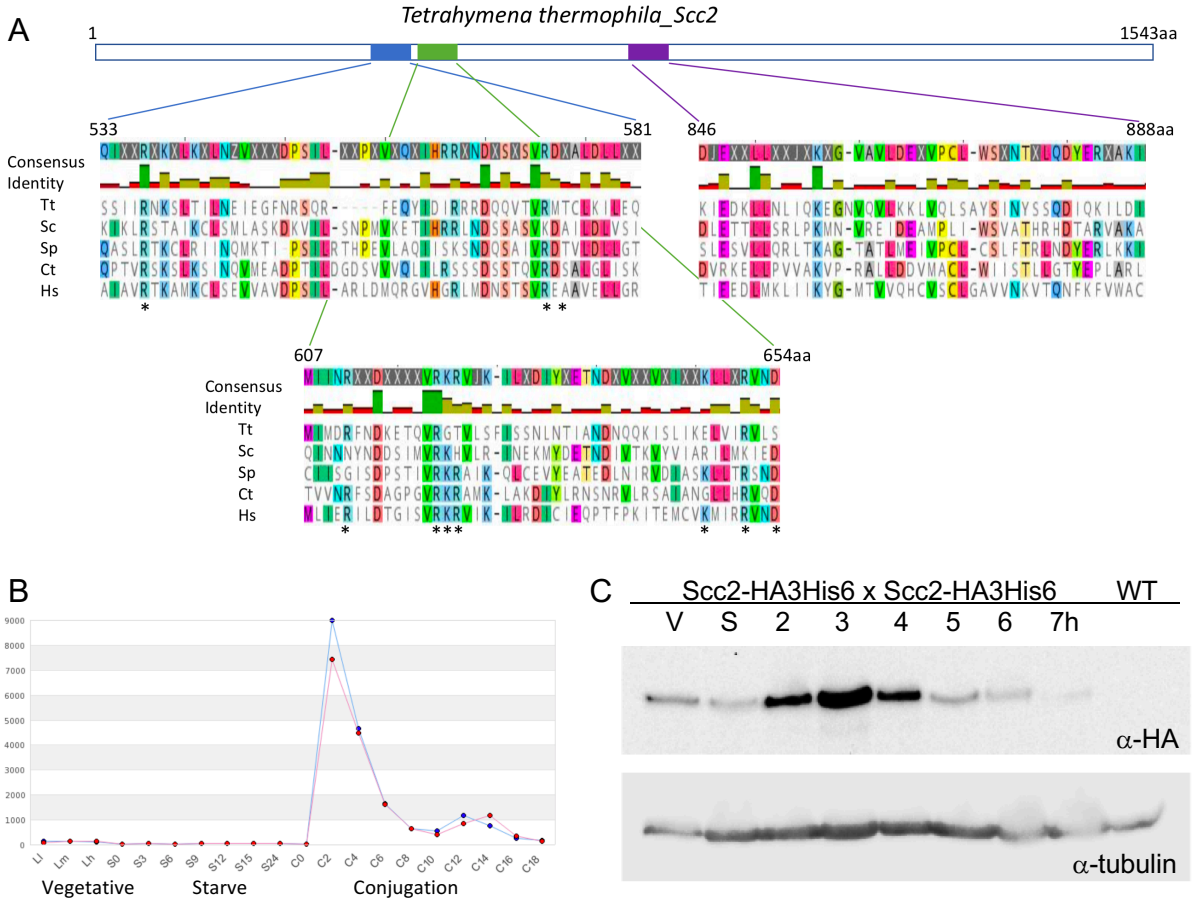


**Figure 11. *Tetrahymena* TTHERM_00678460 is a homolog of Scc2 with enriched protein level during prophase.**

A. *Tetrahymena* TTHERM_00678460 protein shows homology to the cohesin loader subunit Scc2/Nipbl of different species. Protein sequences of Scc2 homologs from *Tetrahymena thermophila* (Tt), *Saccharomyces cerevisiae* (Sc), *Schizosaccharomyces pombe* (Sp), *Chaetomium thermophilum* (Ct), and *Homo sapiens* (Hs) were used to create the alignment in Geneious software (version 11.0.4) using the Muscle algorithm 3.8.425 (Edgar, 2004; Kearse et al., 2012). The selected regions show homology at some of the residues (labeled with *) that interact with the Scc1 kleisin (Kikuchi et al., 2016). B. The expression profile of TTHERM_00678460 shows a peak during early time points of mating. L: vegetative cells, S: starvation, C: conjugation. Data was obtained from http://tfgd.ihb.ac.cn/ (Miao et al., 2009; Xiong et al., 2013). C. Western blot of Scc2-HA3His6 shows high protein levels during early meiosis (2-4h after initiating mating). Samples were collected at different time points of *Tetrahymena* cell cycle; V: vegetative growth, S: starvation, 2-7h after initiating mating. WT: untagged vegetative wild-type. α-tubulin was used as the loading control (Ali et al., 2018).

If the function of *Tetrahymena* Scc2 as a cohesin loader is conserved, the protein should be localized in the germline nucleus, like other cohesin subunits (Howard-Till et al., 2013). To assess the localization of Scc2, Scc2-HA3His6 cells were fixed during vegetative growth and different stages of mating and stained against HA. Scc2 is present in both vegetative and mating cells, and, similar to the cohesin subunits, Scc2 is localized only in the germline nucleus (Figure 12). The Scc2 signal is strongest in early prophase, in the elongating germline nuclei up to the full crescent stage, decreasing at the later stages of mating (Figure 12A). To determine if Scc2 was bound to chromatin, Scc2-HA3His6 cells mated with cells co-expressing Scc2-HA3His6 and Rec8-mCherry were fixed under high-detergent conditions (Figure 12B). As previously shown, chromatin-bound Rec8 can be detected at all stages of mitosis and meiosis (Howard-Till et al., 2013). Scc2 also appears to be chromatin bound, and shows the strongest signal in the germline during early meiotic prophase.

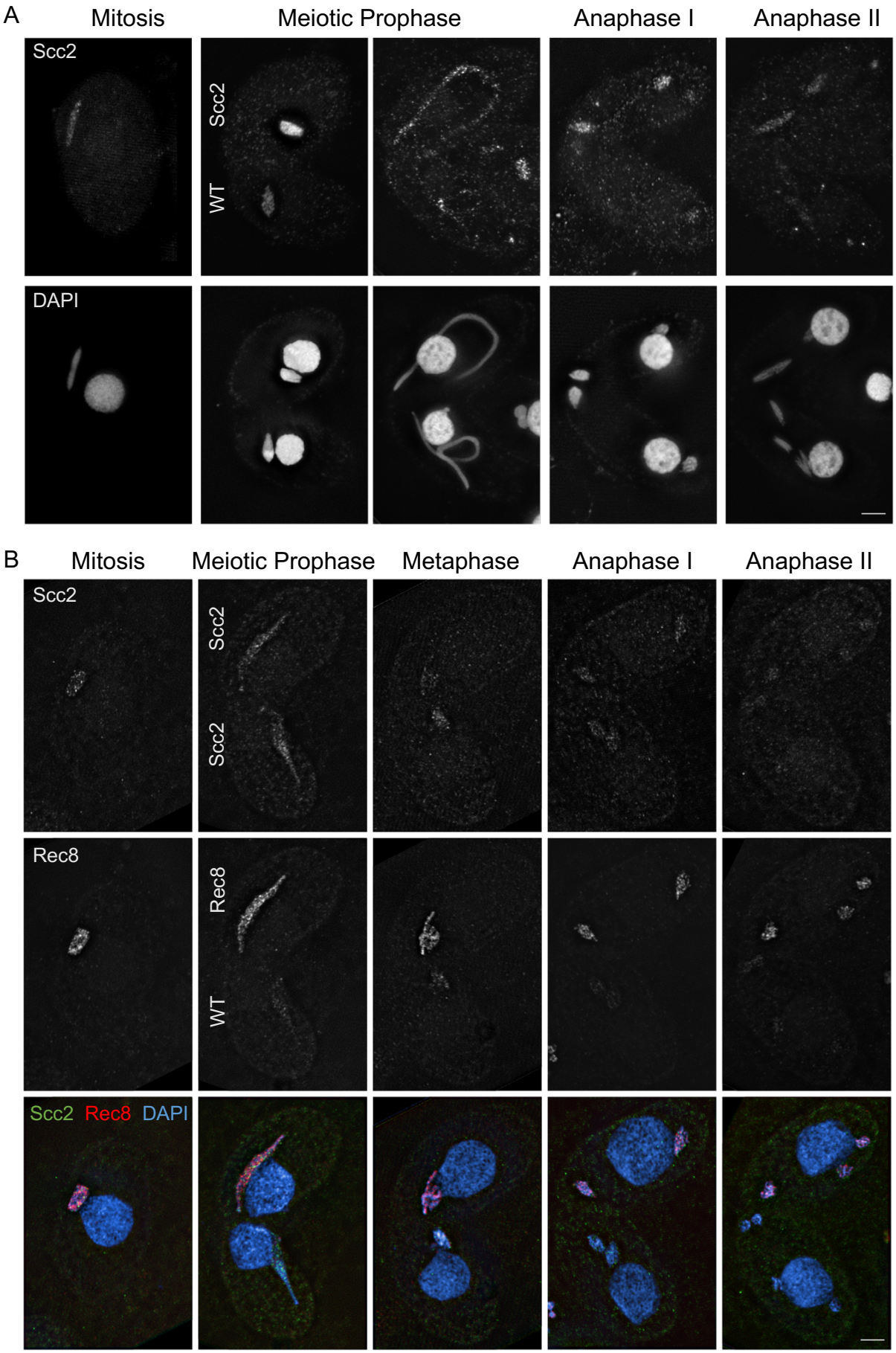
A
Mitosis
Meiotic Prophase
Anaphase I
Anaphase II
Scc2
Scc2
WT
DAPI
B
Mitosis
Meiotic Prophase
Metaphase
Anaphase I
Anaphase II
Scc2
Scc2
Scc2
Rec8
Rec8
WT
Scc2 Rec8 DAPI

**Figure 12. Scc2 localization in the germline nucleus during vegetative and sexual reproduction.**
A. Scc2 localizes to the germline nucleus in mitosis and meiosis. Vegetative Scc2-HA3His6 cells or cells mated with WT cells were fixed with the standard formaldehyde method for IF. B. Scc2 is chromatin associated and shows strongest localization at meiotic prophase. Cells expressing both Scc2-HA3His6 and Rec8-mCherry were fixed during vegetative growth or while mating with Scc2-HA3His6 cells. Fixations were performed in high detergent to remove soluble protein. Chromatin association of Rec8 could also be detected at different stages. Scale bars equals 5 μm (Ali et al., 2018).

## The abundant meiotic prophase localization of Scc2 is not dependent on Spo11 induced DSBs

Localization and protein levels of Scc2 suggest that it is most active during early prophase. In many organisms, the pairing of homologous chromosomes and the formation of crossovers during meiotic prophase depend on the assembly of the SC and the induction and repair of programmed DSBs (Hunter, 2015; Subramanian and Hochwagen, 2014). The Scc2/Scc4 loader and meiosis specific cohesin complexes contribute to these processes in other models (Gyuricza et al., 2016; Visnes et al., 2014; Agostinho et al., 2016; Rong et al., 2016). To test whether Scc2 accumulation is dependent on the presence of Spo11 induced DSBs, Scc2-HA3His6 cells were mated with *spo11*i cells to prevent the induction of DSBs. As a control, WT cells were mated with Scc2-HA3His6 expressing cells. Scc2 is present in the germline nucleus in both the control samples and the Spo11 depleted cells, suggesting that the localization of Scc2 during early prophase is not a downstream step of meiotic DSB induction or repair (Figure 13) (Ali et al., 2018).

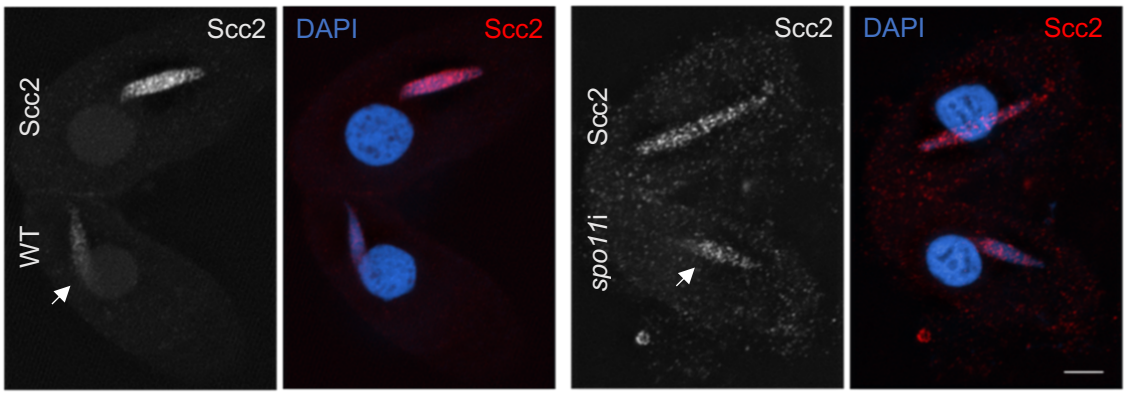

**Figure 13. The meiotic prophase localization of Scc2 is not DSBs dependent.**
Cells expressing Scc2-HA3His6 were mated with wild-type cells or spo11i cells. Samples were fixed 4h after initiating mating and immunostained for HA. Scc2 is present in the germline nucleus of wild-type cells as well as in Spo11 depleted cells (arrows). Scale bar equals 5 μm (Ali et al., 2018).

## *Tetrahymena* Scc2 interacts with Rec8 and Scc3

Scc2 is able to interact with different cohesin subunits, either alone or as part of the Scc2/Scc4 loader complex (Bermudez et al., 2012; Murayama and Uhlmann, 2014; Kikuchi et al., 2016). To study the interaction of *Tetrahymena* Scc2 with other cohesin subunits, cells co-expressing Scc2-HA3His6 and Rec8-mCherry or Scc2-HA3His6 and Scc3-mCherry were generated and mated with WT cells. Cells expressing only Rec8-mCherry or Scc3-mCherry were used as negative controls. Scc2-HA3His6 was immunoprecipitated from protein extracts prepared 4 h after initiating mating, when protein levels of Scc2 are highest. Western blot analysis of the IPs shows that both Scc3 and Rec8 were pulled down with Scc2, confirming that *Tetrahymena* Scc2 is able to interact with different cohesin subunits (Figure 14)(Ali et al., 2018).

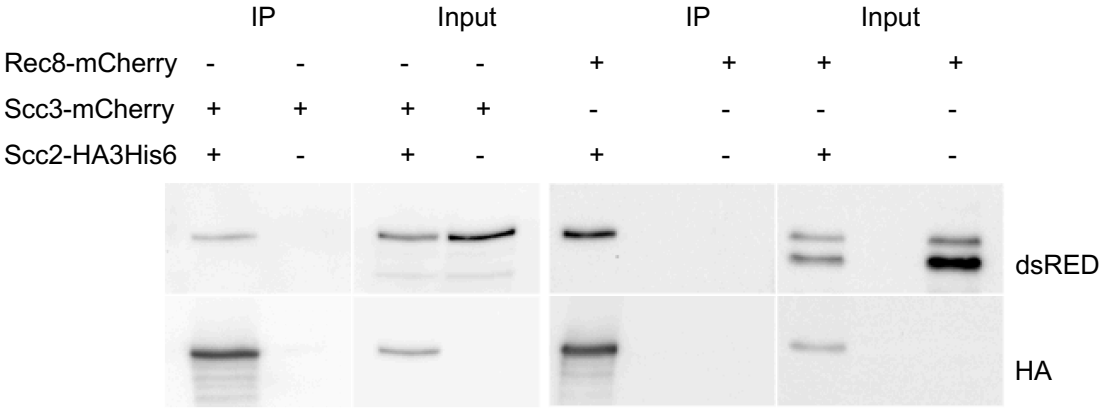


**Figure 14. Scc3 and Rec8 interact with Scc2.**
Cells expressing Scc2-HA3His6 + Scc3-mCherry, Scc3-mCherry, Scc2-HA3His6 + Rec8-mCherry, or Rec8-mCherry were mated to WT cells. 4h after initiation of mating, cell lysates were prepared and used for immunoprecipitation of Scc2. Western blots of IP and input samples were probed with antibodies against dsRED and HA. Scc3 and Rec8 co-precipitated with Scc2 (Ali et al., 2018).

## Scc2 is essential for proper chromosome segregation and meiotic DSB repair

To study the function of Scc2 in *Tetrahymena*, knock-out strains of Scc2 (*scc2Δ*) were generated (in collaboration with Josef Loidl). During vegetative growth, cells show anaphase bridges and lagging chromosomes in mitotically dividing germline nuclei (Ali et al., 2018). In mating *scc2Δ* cells, the germline nuclei form a disrupted elongated structure with regions devoid of DNA, for which we do not have an explanation. Moreover, meiotic progression was blocked without formation of distinct bivalents. To avoid the confounding effects of accumulated mitotic defects on meiosis, Scc2 was depleted just prior to mating using RNAi (*scc2*i). In matings between *scc2*i and WT cells, the WT partners were able to complete meiosis, whereas the *scc2*i cell arrested with uncondensed chromosomes. This phenotype is similar to that of cells depleted of cohesin subunits, which arrest with unrepaired meiotic DSBs. To investigate whether meiotically arrested *scc2*i cells have DSB repair problems, *scc2*i cells were mated with WT and stained for the DSB markers Dmc1/Rad51 and γ-H2A.X. Foci for both markers were detected in the germline nuclei at prophase stage of WT and Scc2 depleted cells, indicating that DSB formation is not dependent on Scc2. While both Dmc1/Rad51 and γ-H2A.X foci disappear at metaphase in WT cells, the *scc2*i cells show multiple foci (Figure 15C)(Ali et al., 2018). Consistent with observations in *C.elegans* and budding yeast (Brar et al., 2009; Klein et al., 1999; Lightfoot et al., 2011), these results imply that Scc2 is required for the repair of meiotic DSBs in *Tetrahymena*.

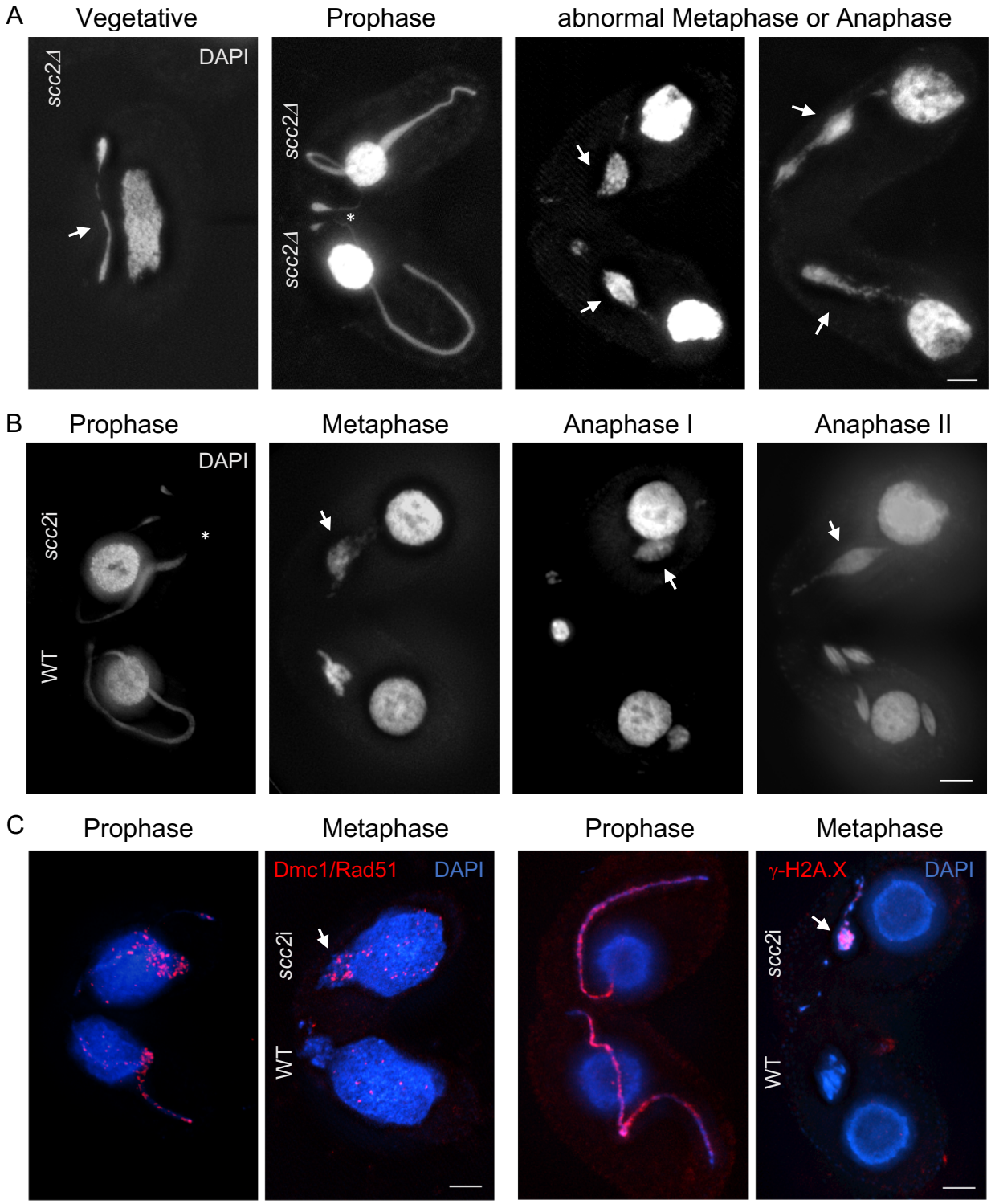


**Figure 15. Chromosome segregation, meiotic progression, and meiotic DSB repair are dependent on Scc2.**

A. *scc2Δ* cells were fixed at different stages and stained with DAPI. In the absence of Scc2, vegetative cells show defective mitotic divisions of the germline nucleus (arrow) (courtesy of Josef Loidl). B. WT cells were mated with *scc2*i cells induced for 24h. WT cells complete meiosis whereas Scc2 depleted cells arrest prior to metaphase. * indicate disrupted germline nuclei. C. Mating cells in (B) were stained for Dmc1/Rad51 or γ-H2A.X. Scale bars equal 5 μm (Ali et al., 2018).

## Scc2 is not required for the chromatin association of Rec8 and Scc3

In other systems, Scc2 is a subunit of the cohesin loader complex which is required for cohesin loading during mitosis and meiosis (Ciosk et al., 2000; Lightfoot et al., 2011; Watrin et al., 2006). To investigate the role of *Tetrahymena* Scc2 in cohesin loading, the chromatin association of Rec8 and Scc3 was tested in Scc2 depleted cells. *scc2*i was induced in cells co-expressing either Scc2-HA3His6 and Scc3-mCherry or Scc2-HA3His6 and Rec8-mCherry. Similar to the depletion of cohesin subunits, complete depletion of Scc2 was achieved 24h after RNAi induction. IF was performed on high-detergent fixations of uninduced controls and *scc2*i cells induced for 24h, which showed that Scc3 and Rec8 are chromatin bound in the germline nucleus both in the presence and absence of Scc2 (Figure 16). In addition, protein samples at different time points after the RNAi induction were collected and analyzed by western blotting. Consistent with the IF, the protein level of Scc3 does not change after Scc2 depletion (24h). Although Rec8 is present after complete depletion of Scc2, the slower migrating phosphorylated form of Rec8 is lost. In the case of Scc3 depletion, hypo-phosphorylated Rec8 is not able to associate with chromatin (Figure 8A+B). To test whether this is also the case after Scc2 depletion, soluble and chromatin fractions were collected from Rec8-HA3His6 or Rec8-HA3His6 + *scc2*i vegetative cells. In contrast to the Scc3 depletion, some unphosphorylated Rec8 is present in the chromatin fraction.

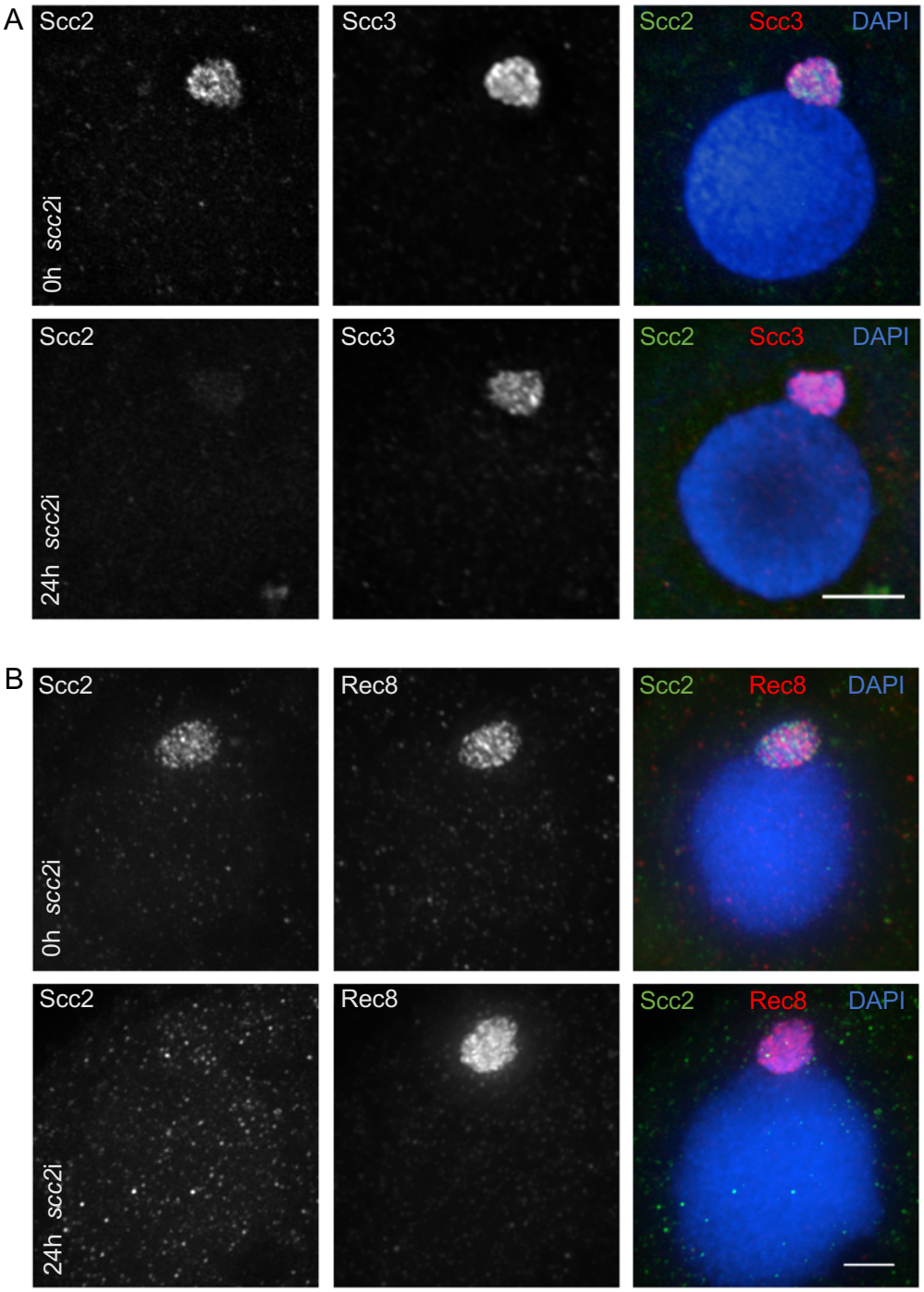


**Figure 16. The chromatin association of Scc3 and Rec8 is not Scc2 dependent.** IF was performed on high-detergent fixations of Scc3 or Rec8 at 0h or 24 h after induction of *scc2*i. Scc2 localization is absent in the germline nuclei 24h after RNAi induction whereas the localization of Scc3 and Rec8 is not affected by Scc2 depletion. A. Scc2-HA3His6 and Scc3-mCherry + *scc2*i B. Scc2-HA3His6 and Rec8-mCherry + *scc2*i. Scale bar equals 5 μm. (Ali et al., 2018)

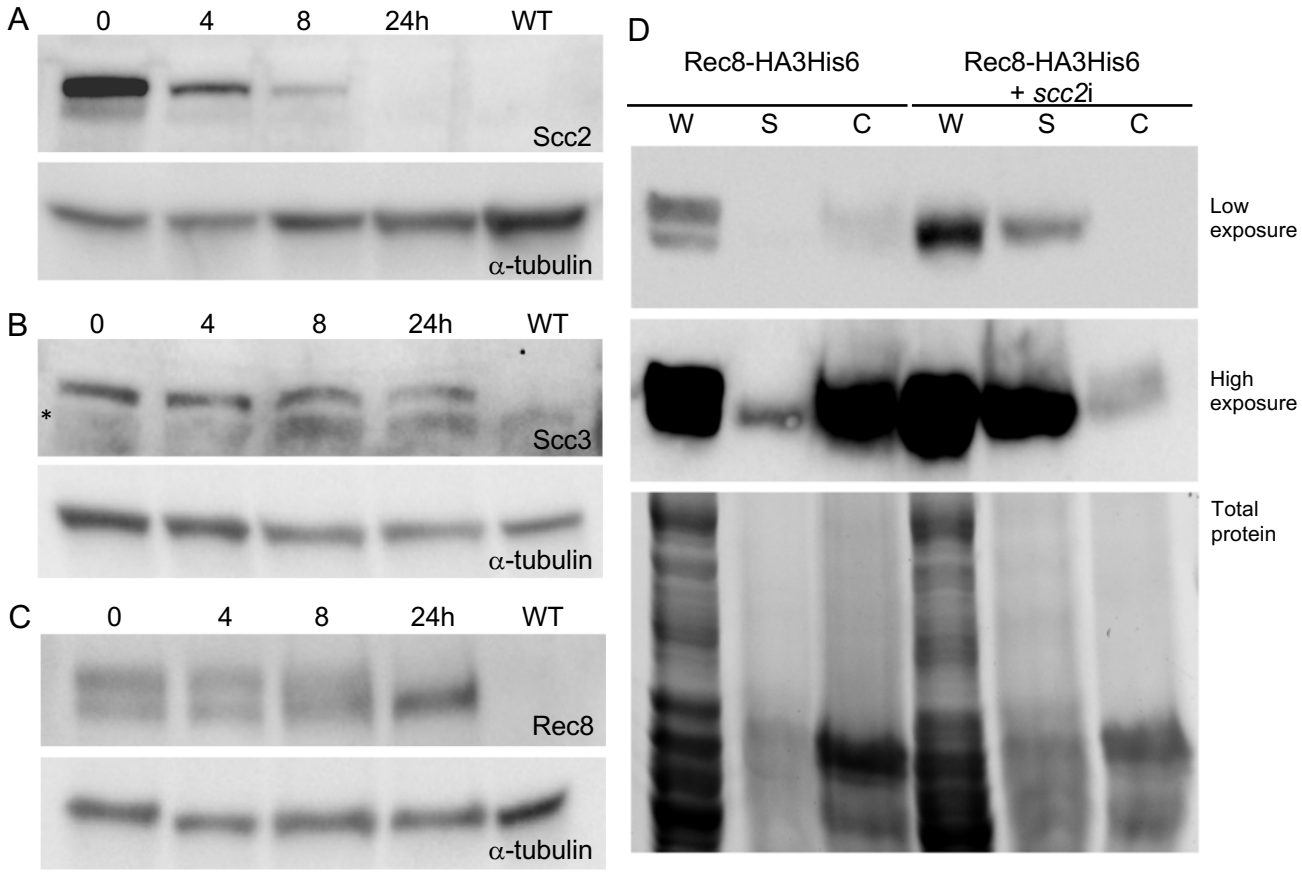


**Figure 17. The overall protein level of Scc3 and Rec8 is not dependent on Scc2 but Rec8 phosphorylation requires Scc2.**

A-C Total cell extracts for each sample were collected at the indicated time points after RNAi induction. α-tubulin was used as loading control. A. Vegetative cells of Scc2-HA3His6 + *scc2*i show complete depletion of Scc2 at the 24h time point. B. Scc2 depletion in Scc3-mCherry cells does not change the protein level of Scc3.

* indicates a non-specific band. C. Scc2 depletion results in the loss of the phosphorylated form of Rec8. D. Vegetative cells of Rec8-HA3His6 or Rec8-HA3His6+*scc2*i with RNAi induction for 24h were used for cellular fractionation. After Scc2 depletion, Rec8 is detected in both the soluble and chromatin fractions. W: whole cell lysate, S: soluble fraction, C: chromatin fraction (Ali et al., 2018).

## The chromatin association of Scc2 depends on cohesin

Although cohesin association with chromatin persists in the absence of Scc2, the physical association of Scc2 with cohesin suggests some functional connection. In budding yeast, it has been shown that cohesin is required for the centromeric association of the Scc2/Scc4 loader complex (Fernius et al., 2013). In addition, the interaction of Scc2 with chromatin-bound cohesin has been suggested based on FRAP and single-molecule tracking experiments (Rhodes et al., 2017a). To investigate the dependence of Scc2 chromatin localization on cohesin, cells co-expressing both Scc2-HA3His6 and Rec8-mCherry were transformed with Scc3 RNAi. Since complete depletion of Scc3 can be achieved 24h after RNAi induction, RNAi was induced for 24h before mating with WT cells, which also results in loss of cohesin in the germline. In the control experiment, WT cells were mated with cells co-expressing Scc2-HA3His6 and Rec8-mCherry. As shown in the lower panel of Figure 18, both Scc2 and Rec8 are localized in the germline nucleus of the control sample. As shown previously in Figure 7B, the chromatin association of Rec8 depends on Scc3. Depletion of Scc3 eliminated the germline localization of both Rec8 and Scc2, indicating that Scc2 localization depends on the presence of chromatin bound cohesin (Ali et al., 2018).

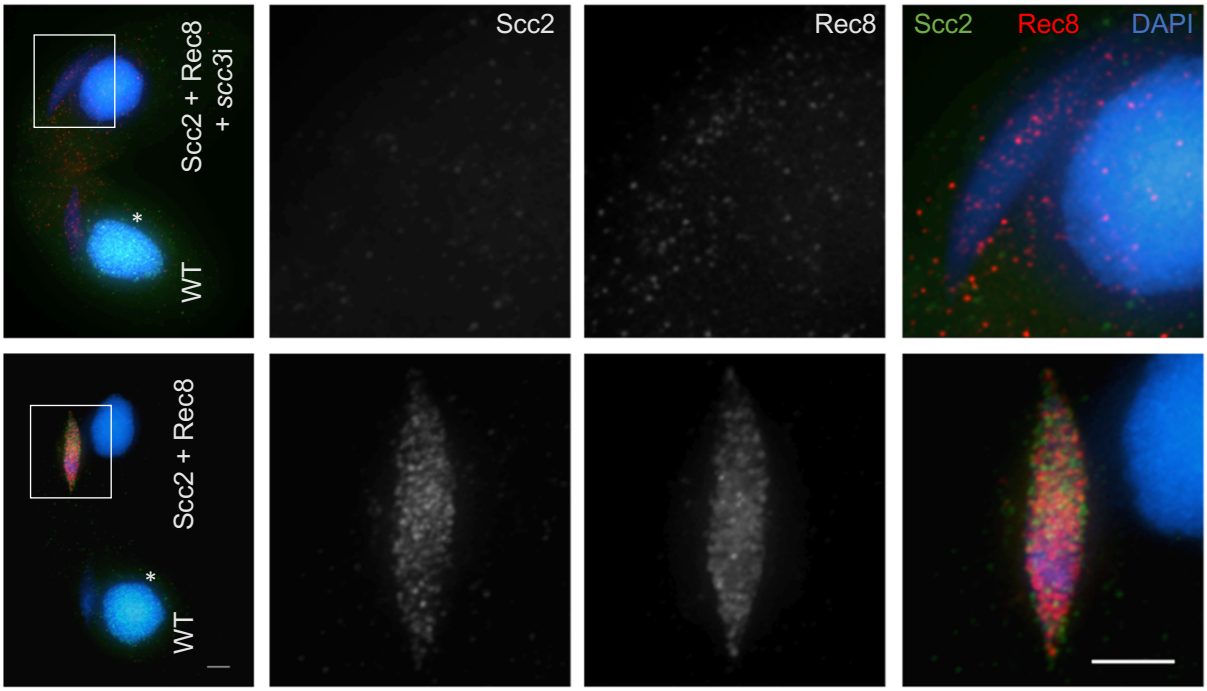

**Figure 18. Rec8 and Scc2 are absent from the germline nucleus after Scc3 depletion.**
Cells expressing Scc2-HA3His6 and Rec8-mCherry induced 24h for *scc3*i (upper panel) or without RNAi (lower panel) were mated with WT cells and immunostained for Scc2 (green), Rec8 (red) and DAPI. The germline localization of both Scc2 and Rec8 is observed in control cells but not in the *scc3*i cells. Boxes designate the enlarged areas, * marks the somatic nucleus of WT cells expressing an HA tagged protein specific to somatic nucleus (Cpdt2-HA), which were used to enable distinction of WT and scc3i cells (Howard-Till and Loidl, 2018). Scale bar equals 5 μm. (Ali et al., 2018)

## Cohesion is slightly reduced in the absence of Scc2

Vegetatively growing cells lacking Scc2 show chromosome segregation problems, which suggests that although Scc2 is not apparently required for the chromatin association of cohesin, it might still be important for cohesion. Cohesion is difficult to assess in vegetative cells due to the small size and highly condensed chromatin of the germline nucleus. However, meiotic cohesion can be determined by counting FISH (Fluorescence in situ hybridization) signals of fully elongated germline nuclei (Howard-Till et al., 2013). FISH signals that appear as 1 dot represents paired homologs, whereas 2 dots represent the unpaired homologous loci, with cohesed sister chromatids. The presence of 3 or 4 dots represents the separation of sister chromatids (Howard-Till et al., 2013; Loidl, 2004). Four independent experiments were used to evaluate cohesion in matings of WT cells, uninduced and induced *scc2*i cells. Western blot analysis indicated that Scc2 was completely depleted in RNAi induced cells. 10% of WT cells have 3 or 4 dots; 16% of uninduced scc2i cells, and 26% of induced *scc2*i cells show loss of cohesion. A Mann-Whitney test shows a statistically significant difference ($p = .0286$) between WT and RNAi induced cells, whereas the difference between induced and uninduced RNAi cells is not significant (Ali et al., 2018). Although the depletion of Scc2 appears complete by western blotting, the cells might retain a small amount of the protein that allows some cohesion, and uninduced RNAi can be slightly leaky, causing a minor phenotype and thus reducing the difference between uninduced and induced cells.

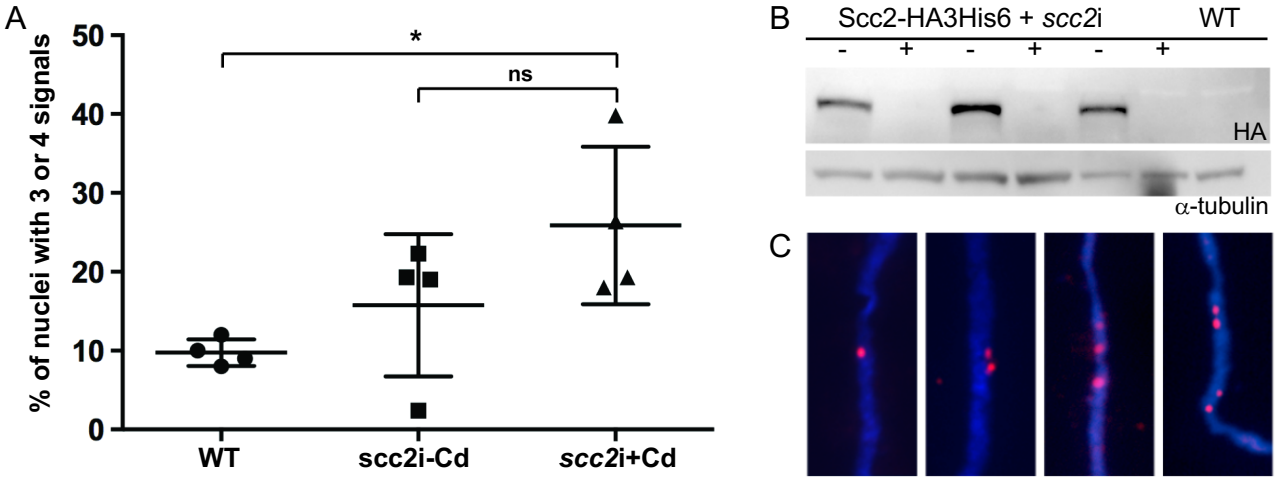


**Figure 19. Cohesion defects can be observed after Scc2 depletion.**
A. FISH signals were counted in the elongated germline nuclei of different mating strains; WT cells, uninduced or induced Scc2 RNAi cells. The graph shows the percentage of nuclei with 3 or 4 signals; data is from four independent experiments, with 100 cells counted for each. B. Western blot analysis of the protein level of Scc2 in three different experiments used in the graph. C. Examples of FISH spots used for the evaluation. (Ali et al., 2018)

# Chapter 3. Post-translational modifications of the *Tetrahymena* cohesin complex

MS analysis of IPs conducted with various cohesin subunits did not reveal any conserved or *Tetrahymena*-specific interacting proteins involved in cohesin function, such as Wapl, Eco1, and Pds5 (Howard-Till et al., 2013; Ali et al., 2018). The intriguing question, then, is how a single complex is able to perform in different nuclear processes. The distinct regulation of cohesion in meiotic chromosome segregation was of particular interest, as most organisms employ a meiosis specific complex for this specialized cell division. In the absence of such a specialized complex, we reasoned that unique post-translational modifications might be employed to differentially regulate a single cohesin complex.

## Mass spectrometry analysis revealed multiple post-translational modification sites in cohesin subunits

To identify specific post-translational modifications on the cohesin complex at particular stages of *Tetrahymena*'s life cycle, MS analysis was performed for IP samples of Rec8-HA3His6. The samples were collected from four different stages (two biological replicates each): vegetative growth, starvation, and 4h and 6h after the initiation of mating. Vegetative growing cells are unsynchronized, but in two repeats of the experiments 17% and 20% of cells in the vegetative sample were undergoing mitosis, whereas starved cells were arrested in G2. Therefore, any differences in post-translational modifications found between these samples would identify mitosis specific vs G2 stage-specific cohesin modifications. In addition, two timepoints were selected from mating cells. At 4h, 82% and 70% of cells in two repeats of the experiments were in meiotic prophase, where centromere and telomere clustering, chromosome pairing, DSB induction and repair occur (Mochizuki et al., 2008; Lukaszewicz et al., 2010; Howard-Till et al., 2011; Loidl et al., 2012). At 6h, 66% and 78% of cells in two experiments were at the post-meiotic stage in which selected germline nuclei undergo mitosis (Cole and Sugai, 2012). Therefore, any difference between 4h and 6h timepoints should differentiate meiosis from mitosis specific cohesin modifications.

The post-translational modifications were identified in Rec8, Smc1, Smc3, and Scc3. The localization of PTMs in Rec8 were distributed throughout the entire protein sequence with some clustering in the central non-conserved region. Multiple alignments of Smc1 and Smc3 show the presence of more conserved residues at the hinge and NBD containing head domains than the regions forming coiled-coils (Appendix 1+2). Most of the identified modifications in Smc1 and Smc3 were detected at the coiled-coil regions and the head domains. The homology of the Scc3 subunit to that of other species is restricted to the conserved STAG domain (Howard-Till et al., 2013). All modifications detected in Scc3 are located in non-conserved parts of the protein (Figure 20).

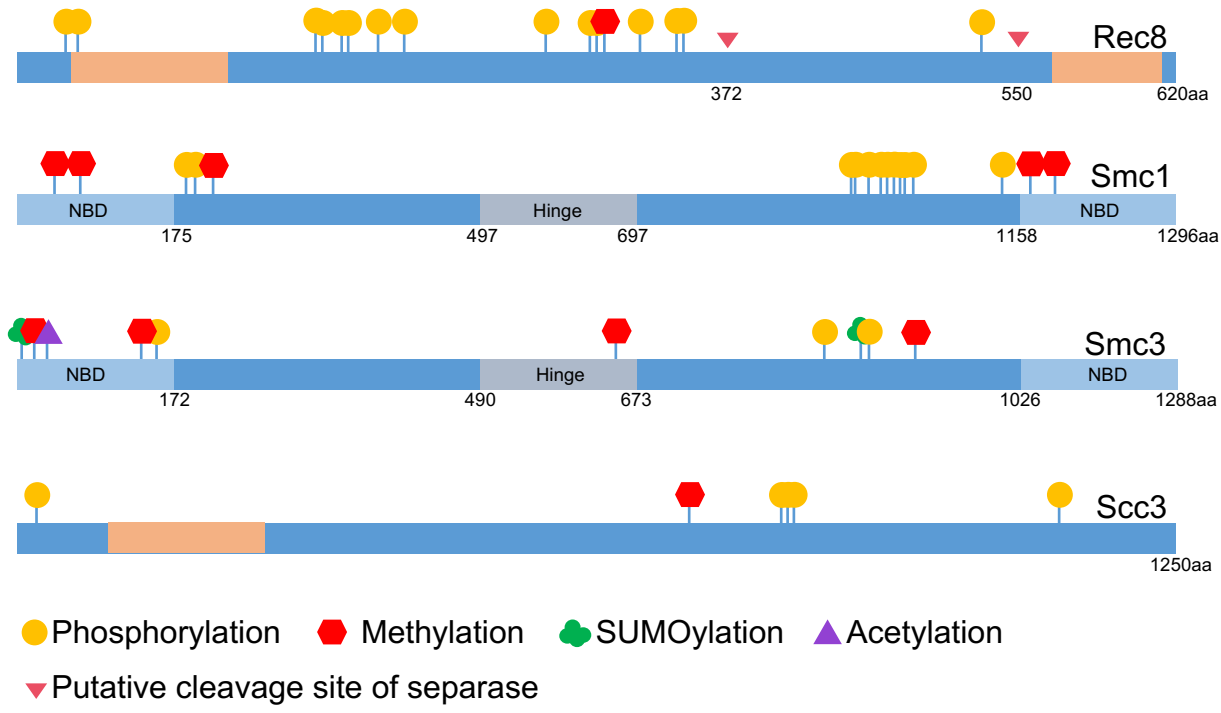


**Figure 20. Schematic representation of post-translational modifications of cohesin subunits.**
Post-translationally modified sites identified by MS of different IP samples are shown for all cohesin subunits. The orange boxes indicate conserved regions in Scc3 and Rec8 (30-130aa and 579-607aa) (Howard-Till et al., 2013). The separase recognition sites were predicted by the presence of D/EXXR consensus motif where X is any residue (Winter et al., 2015). The positions of the nucleotide binding domain (NBD) and hinge domains were estimated based on their location in the human Smc1α and Smc3 (Hons et al., 2016).

All cohesin subunits are known to be phosphorylated and the modification of specific residues could be important for the function of the complex in distinct cellular processes. Mass spectrometry analysis (MS) revealed 15 sites in Rec8, 12 sites in Smc1, 3 sites in Smc3, and 5 sites in Scc3 to be phosphorylated (Table 2). Although the alignment of the protein sequences showed that some of the identified residues are present in the corresponding subunits of the other organisms, the phosphorylation of these residues in these species has not been reported (Appendix 1-5). Most of the sites identified in this study are *Tetrahymena* specific.

Among the modified sites, only few were detected at a particular cell stage in both biological repeats. For instance, S162 in Rec8 and S960 and S974 in Smc1 were modified at all stages in both experiments whereas the other residues were detected either only by one experiment or by both experiments but at different stages. This makes it difficult to assign a particular modification to a distinct cell stage. A time course with more time points and several replicates can increase the confidence of the identified modifications and their significance at particular stage.

The phosphorylation of budding yeast Mcd1 (the mitosis specific $\alpha$-kleisin) at serine 83 has been shown to be essential for DNA damage induced cohesion in G2/M stage cells (Heidinger-Pauli et al., 2008). Although this serine residue is conserved in *Tetrahymena* Rec8, its phosphorylation was not detected in current experiments. In addition to the $\alpha$-kleisin phosphorylation, DNA damage dependent phosphorylation has been observed to occur at S957 and S966 in mammalian Smc1 and S1083 in mammalian Smc3 (Kim et al., 2002; Yazdi et al., 2002). Although the multiple alignments of Smc1 and Smc3 show that these residues are not conserved, the location of S957 and S966 of Smc1 matches with the region containing multiple phosphorylated sites in *Tetrahymena* Smc1 (Figure 21).

Previous to this work, a preliminary quantitative phosphoproteomic study performed by a collaborator identified a decrease in phosphorylation of Rec8 S164 in spo11 knockout cells compared to WT *Tetrahymena* cells (unpublished data, Miao Tian). This result was intriguing, as it presented the possibility that S164p was a stage specific modification made in response to DSBs. However, the present combined MS data of both replicates show similar intensity but low percentage of modified/unmodified peptides at vegetative, meiotic prophase, and post-meiotic stages. In addition, the phosphorylation of S162 was also identified at all stages. We

attempted to generate a phospho-specific antibody recognizing phosphorylated S162 and S164. However, the antibody was not specific.

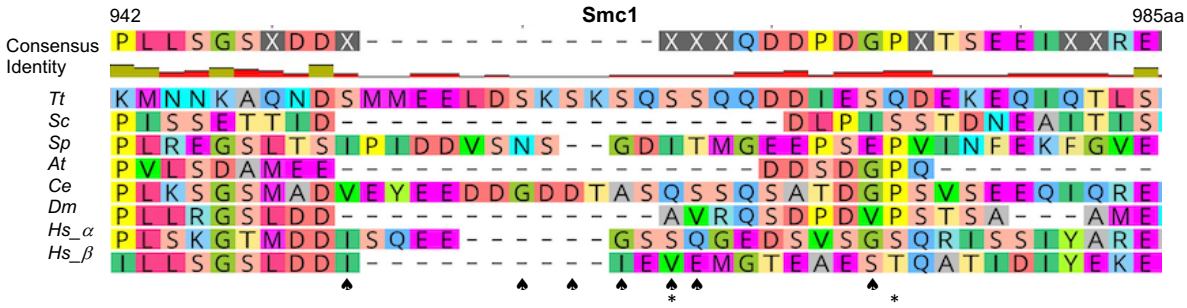


**Figure 21. Multiple alignment of Smc1**
The alignment was generated with Geneious software (Ali et al., 2018; Edgar, 2004; Kearse et al., 2012). '*' indicates the location of S957 and S966 in human Smc1α, whereas '♠' indicates phosphorylated *Tetrahymena* residues of Smc1. Tt: *Tetrahymena thermophila*, Sc: *Saccharomyces cerevisiae*, Sp: *Schizosaccharomyces pombe*, At: *Arabidopsis thaliana*, Ce: *Caenorhabditis elegans*, Dm: *Drosophila melanogaster*, Hs: *Homo sapiens*.

**Table 2. Identified phosphorylation sites in cohesin subunits**.
MS analysis was performed for immunoprecipitated Rec8-HA3His6. V: vegetative, S: starved, 4h and 6h post-mixing. Percentage of modified over unmodified peptides, intensity of peptides (+ < 20, ++ 20-25, +++ >25 )

| | 1st replicate | | | | 2nd replicate | | | |
|---|---|---|---|---|---|---|---|---|
| | V | S | 4h | 6h | V | S | 4h | 6h |
| **Rec8** | | | | | | | | |
| $^{29}$S | | 21,+ | 4,++ | 3,++ | | | | 11,++ |
| $^{32}$S | | | | | | | | 5,++ |
| $^{162}$S | 0,+ | 0,+ | 0,++ | 0,++ | 5,++ | NA,+++ | 3,++ | 5,++ |
| $^{164}$S | | 0/+ | | 0,++ | 1,++ | | 1,++ | 2,++ |
| $^{169}$S | | | 0,++ | 1,++ | NA,+++ | | NA,++ | NA,++ |
| $^{171}$T | | 1,++ | 1,++ | 1,++ | | | | |
| $^{194}$S | | | | | 4,++ | | 3,++ | 3,++ |
| $^{208}$S | | | | | 29,++ | 13,++ | 12,++ | 17,++ |
| $^{282}$S | | | | | | | | 2,+ |
| $^{307}$S | 4,++ | | 16,+++ | 0,++ | 1,++ | | | 2,++ |
| $^{308}$S | 1,+ | 0,++ | 3,+++ | 2,+++ | 3,++ | | 7,++ | 7,++ |
| $^{333}$T | | 1,+ | 2,++ | 1,+ | | | 0,++ | 9,++ |
| $^{354}$S | | | | | 1,++ | | | 3,++ |
| $^{355}$S | 4,++ | 5,+++ | 7,+++ | 4,+++ | | | 2,++ | |
| $^{529}$S | | | | | 2,++ | | 7,++ | 17,++ |
| **Smc1** | | | | | | | | |
| $^{191}$S | | | 0,++ | 0,++ | | | | |
| $^{193}$S | 0,+ | 0,+ | 0,++ | 0,++ | | | | |
| $^{942}$S | | | | | | | | NA,++ |
| $^{943}$S | 11,+ | 16,+ | | 314,+++ | | | NA,++ | NA,++ |
| $^{953}$S | 1,+ | 1,+ | 2,++ | 2,++ | | | | |
| $^{960}$S | 6,++ | 1,++ | 6,++ | 5,+++ | 3,++ | 3,++ | 3,++ | 6,++ |
| $^{962}$S | 67,++ | | | | 88,++ | 38,+ | 146,++ | 116,++ |
| $^{964}$S | | 3,++ | | 2,+++ | | | | 1,++ |
| $^{966}$S | | | 1,++ | 2,+++ | 1,++ | 2,++ | 1,++ | |
| $^{967}$S | 1,++ | | | | | | | 1,++ |
| $^{974}$S | 1,++ | 2,++ | 2,++ | 2,+++ | 16,+++ | 29,+++ | 24,+++ | 15,+++ |
| $^{1000}$S | | 0,+ | 15,+++ | 0,+ | | | 29,+++ | 2,++ |
| **Smc3** | | | | | | | | |
| $^{155}$S | | 0,++ | 0,++ | 0,++ | | | | |
| $^{900}$S | | 0,+ | 1,++ | 0,++ | | | | |
| $^{949}$S | | | | | 0,++ | 0,++ | 0,++ | 0,++ |
| **Scc3** | | | | | | | | |
| $^{21}$S | | | 2,++ | | | | | |
| $^{829}$S | 8,++ | 21,++ | 2,++ | | | | | |
| $^{833}$S | | | 0,++ | 3,++ | | | | |
| $^{837}$S | | | 2,++ | | | | | |
| $^{1128}$S | | | | | | | | |

In addition to phosphorylation sites, methylated residues in various cohesin subunits were also identified (Table 3). One lysine (K309) in Rec8, four lysines (K37, K67, K207, K1182) and one arginine (R1282) in Smc1, and two lysines (K669 and K1002) in Smc3 were detected to be methylated in all different stages. On the other hand, the methylation of lysine (K18) and arginine (R139) in Smc3 was absent in starved cells. Methylation of lysine (K727) in Scc3 was detected only in samples from starved and 6h mating cells with high intensity but low percentage of modified/unmodified peptides. When modified sites were inspected for conservation, lysine 37 in Smc1 and arginine 139 in Smc3 were found to be conserved but not known to be methylated in other species (Figure 22A+B). Both residues are located at the head domains which contain more conserved residues than the coiled coil regions of the Smc proteins (Appendix 1+2). A recent study in fission yeast showed that residues K536 and K1200 of Psm1 (Smc1 homolog), located at the hinge and head domains respectively, are methylated during meiotic prophase, and mutation of these sites leads to sensitivity to DNA damage (Sanyal et al., 2018). The protein alignment of Smc1 shows that these sites are not conserved in *Tetrahymena*. However, methylation of a residue located at the hinge domain of Smc1 (K207) was detected to be present in all samples with high intensity, which makes it a candidate for further studies.

**Table 3. Identified methylation sites in cohesin subunits**.
MS was performed for immunoprecipitated Rec8-HA3His6. V: vegetative, S: starved, 4h and 6h post-mixing. Percentage of modified over unmodified peptides, intensity of peptides (+ < 20, ++ 20-25, +++ >25 )

| | 1st replicate | | | | 2nd replicate | | | |
|---|---|---|---|---|---|---|---|---|
| | V | S | 4h | 6h | V | S | 4h | 6h |
| **Rec8** | | | | | | | | |
| $^{309}$K | 0,++ | 0,++ | 0,++ | 0,+ | | | | |
| **Smc1** | | | | | | | | |
| $^{37}$K | | | | | 47,++ | 22,++ | 36,++ | 36,++ |
| $^{67}$K | | | | | NA,++ | 9,++ | NA,++ | 23,++ |
| $^{207}$K | 17,++ | 41,++ | 262,+++ | 176,+++ | 29,++ | 52,++ | 75,++ | 31,++ |
| $^{1182}$K | 0,++ | 0,++ | 0,++ | 0,++ | 97,++ | 72,++ | 99,+++ | 81,++ |
| $^{1282}$R | | | | | 0,++ | 0,++ | 2,++ | 1,++ |
| **Smc3** | | | | | | | | |
| $^{18}$K | | | | | 50,+ | | NA,+ | 84,++ |
| $^{139}$R | | | | | 8,++ | | 14,++ | 14,++ |
| $^{669}$K | | | | | 46,++ | 28,++ | 47,++ | 45,++ |
| $^{1002}$K | NA,++ | NA,++ | NA,++ | NA,++ | 0,+ | 0,+ | 0,+ | 0,+ |
| **Scc3** | | | | | | | | |
| $^{727}$K | | 5,+++ | | 6,+++ | | | | |

The acetylation of highly conserved lysines (K112 and K113 in yeast, K105 and K106 in human) close to the ATPase domain of Smc3 is known to be essential for the establishment of cohesion during DNA replication (Beckouët et al., 2010; Ben-Shahar et al., 2008; Rowland et al., 2009; Zhang et al., 2008). The alignment of Smc3 protein sequences revealed that these two sites are not conserved in *Tetrahymena*. However, *Tetrahymena* specific acetylation of lysine 32, located at the NBD domain, was identified to be present with same intensity at different cell stages. Mutation of this residue will be important to uncover the role of this modification in cohesin function.

**Table 4. Identified acetylation and SUMOylation sites in Smc3.**
MS analysis was performed for immunoprecipitated Rec8-HA3His6. V: vegetative, S: starved, 4h and 6h post-mixing. Percentage of modified over unmodified peptides, intensity of peptides (+ < 20, ++ 20-25, +++ >25 )

| | 1st replicate | | | | 2nd replicate | | | |
|---|---|---|---|---|---|---|---|---|
| | V | S | 4h | 6h | V | S | 4h | 6h |
| **Acetylation** | | | | | | | | |
| $^{32}$K | | | | | NA,++ | NA,++ | NA,++ | NA,++ |
| **SUMOylation** | | | | | | | | |
| $^{4}$K | NA,++ | NA,++ | NA,++ | NA,++ | | | | |
| $^{943}$K | | | | | | | 1,+ | |

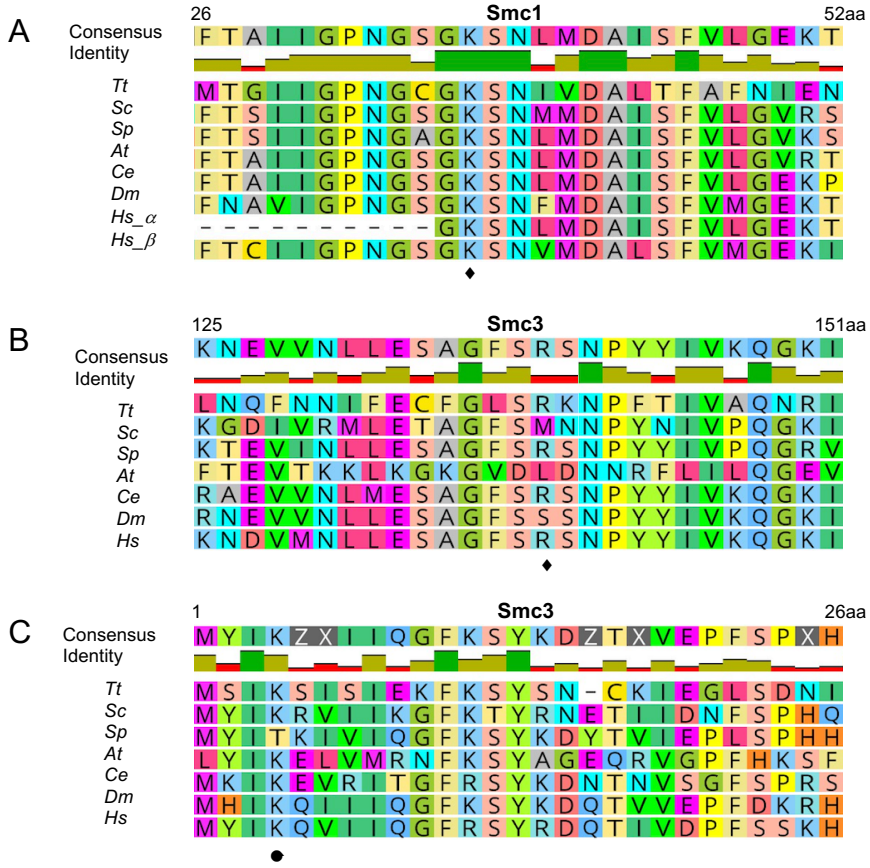


**Figure 22. Conserved methylation and SUMOylation sites in Smc1 and Smc3.** The alignment was generated with Geneious software (Ali et al., 2018; Edgar, 2004; Kearse et al., 2012). '♦' indicates methylation sites and '●' indicates SUMOylation site. Tt: *Tetrahymena thermophila*, Sc: *Saccharomyces cerevisiae*, Sp: *Schizosaccharomyces pombe*, At: *Arabidopsis thaliana*, Ce: *Caenorhabditis elegans*, Dm: *Drosophila melanogaster*, Hs: *Homo sapiens*.

MS analysis revealed SUMO-SUMO branched peptides on two residues, lysine 4 and lysine 943 in Smc3. SUMO of K4 shows same intensity in all different stages. A multiple alignment of the Smc3 protein sequence revealed that this site is conserved (Figure 22C). However, there is no information regarding the modification of this residue in other organisms. In addition, SUMO on K943 was identified only in the 4h sample. Although the alignment of Smc3 shows that this residue is also present in *A.thaliana* and *S. pombe*, there is no data about its SUMOylation in these organisms. The IP protocol used in this experiment was not specifically designed to enrich for or detect SUMOylation, therefore a more optimized protocol may be able to detect additional SUMOylated residues. Additional experiments to address the functional importance of cohesin's SUMOylation in *Tetrahymena* are discussed below.

## Cohesin association with chromatin decreases in the absence of cohesin SUMOylation

In addition to the bulk of Rec8 protein which migrates at about 90 kDa, we occasionally observed additional, slower migrating forms (Figure 23B), which we hypothesized could be SUMOylated. Moreover, immunoblotting Rec8-HA3His6 IP samples with an anti-SUMO antibody revealed a higher molecular weight band that could correspond to either modified Rec8 or another cohesin subunit pulled down with Rec8 (Figure 23A). Based on the MS analysis (see Table 4), this band could represent Smc3 because K4 and K943 of Smc3 were identified to be SUMOylated (Figure 22C). In order to further investigate the role of SUMOylation in cohesin function, we used an approach developed by Almedawar et.al to reduce SUMOylation of cohesin. In short, the method is based on fusing the catalytic domain of the Ulp1 SUMO protease to Rec8 (Almedawar et al., 2012). They showed that the cohesin complex was efficiently deSUMOylated without disrupting the complex formation and its association with chromatin (Almedawar et al., 2012).

The ULP1 gene (TTHERM_00348200) has been annotated in the *Tetrahymena* genome. Multiple alignment of protein sequences from different organisms showed the presence of conserved residues at the C-terminal end of *Tetrahymena* Ulp1 (Appendix 6). Therefore, the last 231 amino acids (301-531aa) of Ulp1 were used as the Ulp1 catalytic domain (UD). In order to obtain a catalytically inactive UD, the

conserved cysteine (483) was mutated to serine. The UD domains were fused to the C-terminal end of the full length Rec8 with the HA3His6 tag as a linker.

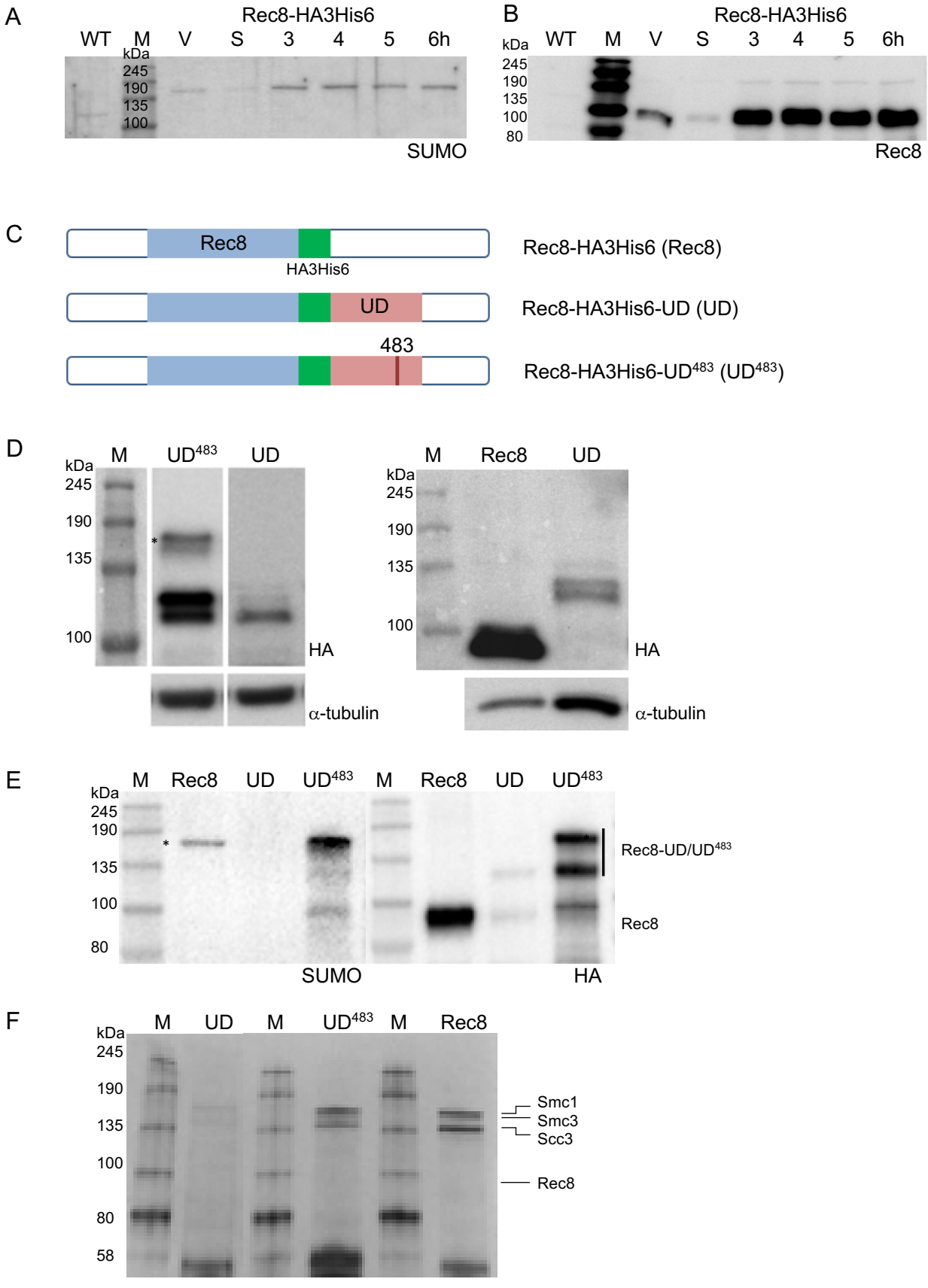

**Figure 23. Rec8 protein level decreases when deSUMOylated**
A-B. Western blotting of Rec8-HA3His6 IPs at different time points. The membrane was probed with anti-SUMO (A) and anti-Rec8 (B) antibodies. V: vegetative, S: starve, WT: wild-type, 3-6 h: time points after initiating mating. C. Schematic representation of constructs used for the SUMOylation experiments. UD: Ulp1 catalytic domain, UD483: 483 (C) was replaced with (S) to eliminate the catalytic activity. D. The protein level of Rec8 is lower in the presence of an active Ulp1 catalytic domain. Whole cell lysates were collected from vegetative cells expressing corresponding constructs and probed with anti-HA and anti-tubulin antibodies. E. SUMOylation was not detected in Rec8-HA3His6-UD and was restored in the Rec8-HA3His6-UD$^{483}$. All samples were collected at 4h after initiating mating and immunoprecipitation was performed with HA magnetic beads. The membrane was probed with anti-SUMO antibody followed by stripping and probing with anti-HA antibody. F. Silver staining of IP samples from cells expressing Rec8-HA3His6, Rec8-HA3His6-UD, Rec8-HA3His6-UD$^{483}$ shows the cohesin complex was pulled down with all Rec8 constructs. M indicates Protein Standard, * indicates SUMOylated proteins.

Total cell lysates were collected from cells expressing Rec8-HA3His6, Rec8-HA3His6-UD, or Rec8-HA3His6-UD$^{483}$ (Figure 23D). The amount of Rec8-HA3His6-UD was less than the amount of Rec8-HA3His6 and Rec8-HA3His6-UD$^{483}$. The presence of abundant Rec8 in the Rec8-HA3His6-UD$^{483}$ suggests that the mere fusion of an additional domain to Rec8 is not the cause of the decrease in Rec8 abundance. On the contrary, these results imply the protein level of Rec8 decreases as a result of its deSUMOylation. Since the immunoblots probed with SUMO antibody had multiple unspecific bands (data not shown), IPs were performed from equal amounts of starting cultures of cells. The IP sample from Rec8-HA3His6-UD$^{483}$ shows additional bands on the HA probed blot, and an increase in the abundance of the SUMOylated form (Figure 23E). It was previously suggested that hyperSUMOylation might be due to the binding of the inactive UD to the SUMO substrate, preventing its deSUMOylation by the endogenous Ulp1 enzymes (Almedawar et al., 2012). SUMO signal could not be detected for Rec8-HA3His6-UD. This could be due to a combination of the low amount of Rec8 as well as deSUMOylation. Silver staining of the same IP samples revealed similar band pattern at 135-190kDa for all samples. The weak band pattern for Rec8-HA3His6-UD suggests that it was able to pull down the rest of the cohesin complex and the cohesin complex was formed in the presence of UD domain (Figure 23F).
Rec8 is normally localized in the germline nucleus both during vegetative growth and conjugation (Ali et al., 2018; Howard-Till et al., 2013). Rec8-HA3His6-UD was detected in the germline nuclei of vegetative cells, but was barely detectable in

prophase cells and was completely absent at metaphase (Figure 24C,D). A similar meiotic pattern was seen in samples fixed with a high-detergent method, which suggested that Rec8-HA3His6-UD was able to bind to chromosomes during early stages of conjugation but could not be maintained or loaded at later stages. Moreover, the cells were not able to proceed through metaphase stage and the chromosomes were not condensed. Cells expressing catalytically inactive UD had Rec8 localized in the germline nuclei, and they were able to complete meiosis (Figure 24E). Immunofluorescence with an antibody against Dmc1/Rad51 suggested the presence of unrepaired DSBs only in Rec8-HA3His6-UD cells. This observation is similar to the phenotype detected in the cells depleted of Rec8 and Scc3, in which DSB repair is defective (Ali et al., 2018; Howard-Till et al., 2013). Therefore, the phenotype of Rec8-HA3His6-UD might be due to the reduced amount of cohesin bound to chromosomes, as DSB repair is extremely sensitive to the levels of cohesin (Heidinger-Pauli et al., 2010). It seems likely that de-SUMOylation reduces the stability of the Rec8 protein or the cohesin complex in general, thus reducing overall levels of cohesin on the chromosomes.

To test the cytological localization of SUMO at different stages of *Tetrahymena* life cycle, cells were fixed and stained with anti-SUMO antibody. Consistent with the previous observations, SUMO signal could be detected in the somatic nucleus (Nasir et al., 2015). In addition, a strong signal for SUMO was observed at one end of the crescent shaped germline nucleus during meiotic prophase. In this stage, centromeres are clustered at the one end and telomeres at the other end of the elongated germline nucleus (Loidl et al., 2012). To test which end shows the SUMOylation signal, mating cells expressing Ndc80-HA, a component of the kinetochore complex, were fixed and stained with antibodies against HA and SUMO. The signals for Ndc80 and SUMO were detected at opposite ends of the elongated nucleus, suggesting that the SUMO signal is corresponding to the telomere end of the crescent. The signal was reduced in cells expressing UD fused Rec8 (Figure 26B). However, the signal was restored in cells expressing the mutant form of UD (Figure 26C). In addition, cells expressing the catalytically dead UD fusion appear to have an increased amount of Rec8 at the telomeres (Figure 24E). These results suggest that SUMOylated cohesin accumulates preferentially at telomeres, and that hyperSUMOylation of cohesin, as occurs in the Rec8-UD$^{483}$ cells, may drive additional binding.

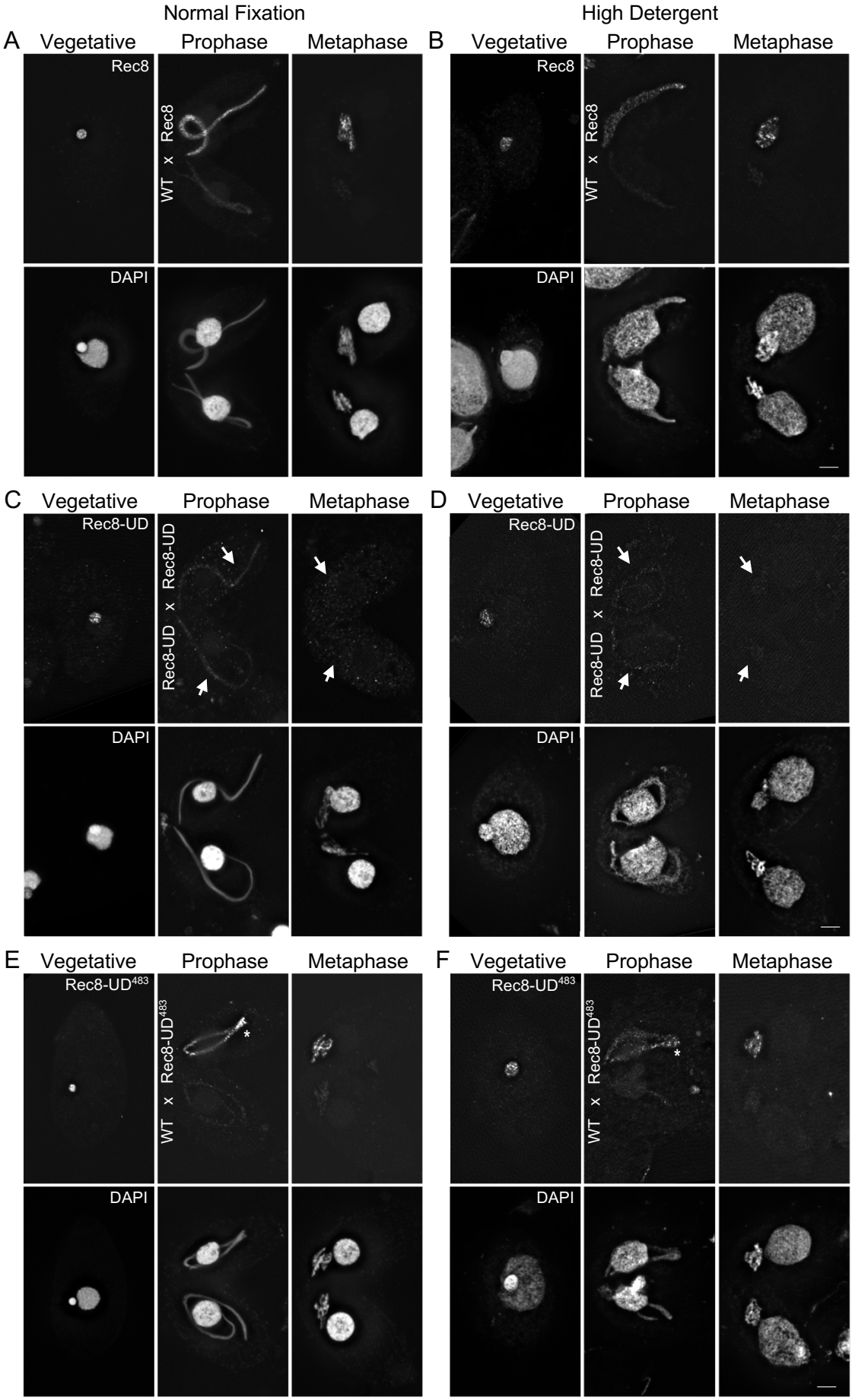
Normal Fixation
High Detergent
A
Vegetative
Prophase
Metaphase
B
Vegetative
Prophase
Metaphase
Rec8
WT x Rec8
DAPI
C
Vegetative
Prophase
Metaphase
D
Vegetative
Prophase
Metaphase
Rec8-UD
Rec8-UD x Rec8-UD
DAPI
E
Vegetative
Prophase
Metaphase
F
Vegetative
Prophase
Metaphase
Rec8-UD483
WT x Rec8-UD483
DAPI

**Figure 24. DeSUMOylation of cohesin reduces Rec8 localization in the germline nucleus.**

A,B. Rec8-HA3His6 shows germline localization at different stages of *Tetrahymena*'s life cycle. C,D. Rec8-HA3His6-UD localization is detected in vegetative cells. Once cells enter meiosis the Rec8 signal is almost absent (arrows) and cells arrest in metaphase. E,F. Rec8-HA3His6-UD localization in the germline can be detected both during vegetative growth and mating. Mating cells were fixed with either formaldehyde (A,C,E) or high detergent method (B,D,F). * indicates the abundant Rec8 at the end of elongated nucleus. Scale bars equal 5 μm.

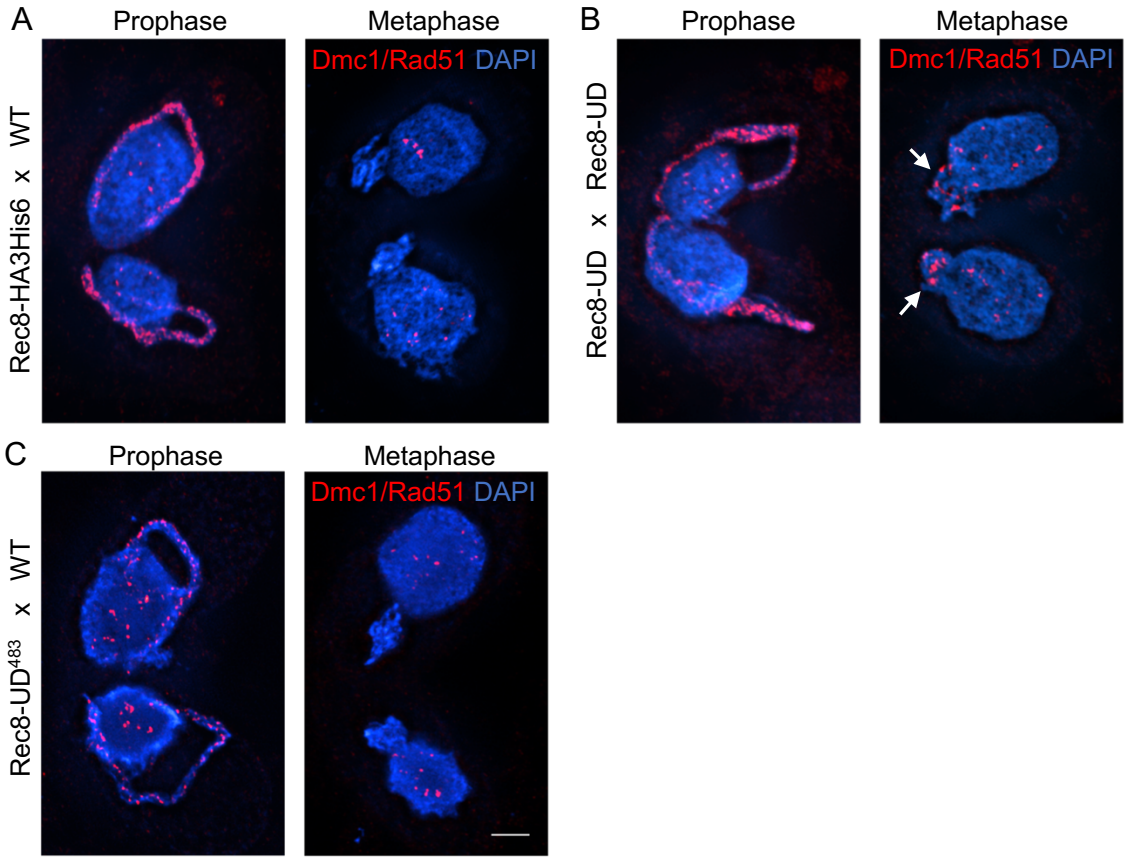


**Figure 25. Cells expressing Rec8-UD show increased Dmc1/Rad51 foci at metaphase.**

Mating of wild-type cells with A. Rec8-HA3His6 B. Rec8-HA3His6-UD, C. Rec8-HA3His6-UD$^{483}$. All matings were fixed with high detergent method and stained with anti-Dmc1/Rad51 antibody. A. In the presence of WT Rec8, signal is detected during prophase and disappears once cells enter the metaphase stage. B. Dmc1/Rad51 foci persist in the absence of cohesin SUMOylation, suggesting the presence of unrepaired DSBs. C. Abolishing the Ulp1 catalytic activity is sufficient to restore DSB repair. Scale bar equals 5 μm.

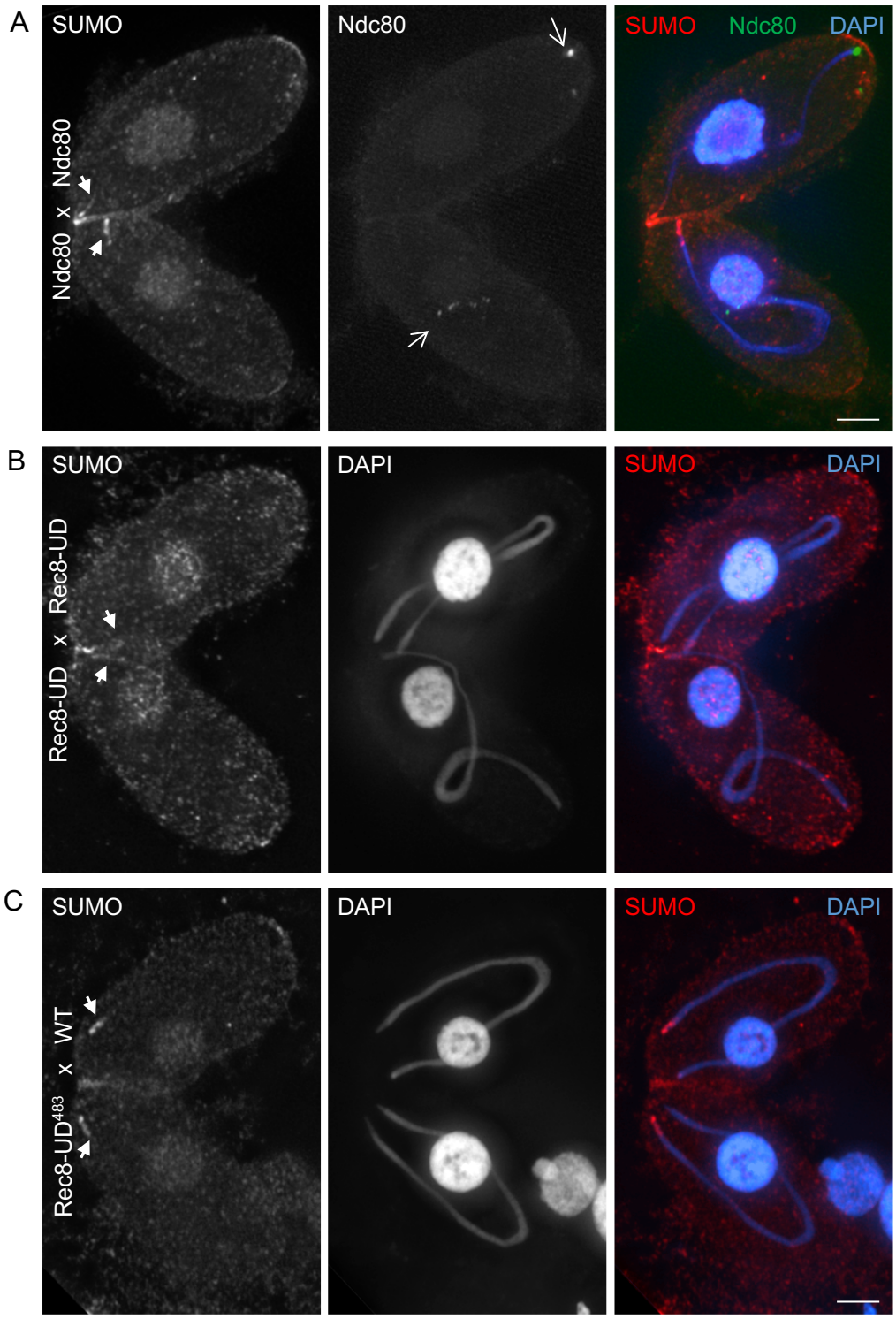


**Figure 26. Strong SUMO signal is detected at the telomere end of the elongated germline nucleus**

A. Mating Ndc80-HA cells were stained with both anti-HA and anti-SUMO antibody. Ndc80 signal is present at one end whereas the SUMO signal is present at the other end of elongated germline nucleus. B-C. Mating cells expressing Rec8-HA3His6-UD, Rec8-HA3His6-UD$^{483}$ were stained with anti-SUMO antibody. The decreased SUMO signal in Rec8-UD was restored in Rec8-HA3His6-UD$^{483}$ cells. All samples were

collected 4h after the initiation of mating. Filled arrowheads point to the SUMO signal and line arrows point to the Ndc80 signal. Scale bars equal 5 μm.

# Discussion

### *Tetrahymena* uses a minimal cohesin apparatus

The ability of cohesin to function in different contexts depends largely on proteins such as Wapl, Eco1, and Pds5. Additionally, many organisms encode for multiple forms of cohesin subunits. Mammals, for instance, have mitosis-specific SMC1$\alpha$, RAD21, SA1/STAG1, SA2/STAG2, and meiosis-specific SMC1$\beta$, SA3/STAG3, RAD21L and REC8 subunits (Rankin, 2015). The combination of different subunits increases the number of complexes which could be involved in specific functions of cohesin.

Just a single homolog of each cohesin subunit has been previously identified in *Tetrahymena* and the only additional protein known to be involved in cohesin function was separase, which was shown to be required for chromosome segregation (Howard-Till et al., 2013; Ali et al., 2018). In an attempt to identify additional proteins implicated in cohesin function, such as Wapl, Eco1, Pds5, and Scc4, multiple IP experiments of different cohesin subunits were analyzed with MS. Unfortunately, this approach did not reveal any other interactions with conserved or *Tetrahymena* specific proteins, further confirming the existence of a minimal cohesin complex which is sufficient for functions in both mitosis and meiosis. The intriguing question is why *Tetrahymena* uses such a minimal cohesin apparatus. Several features of *Tetrahymena* biology may suggest some answers.

One feature of *Tetrahymena* is its nuclear dualism. The transmission of genetic information and gene transcription take place in separate germline and somatic nuclei, respectively. Cohesin localizes only in the germline nucleus, but not in the transcriptionally active somatic nucleus (Howard-Till et al., 2013; Ali et al., 2018). Although the namesake activity of cohesin is to cohese, or hold together sister chromatids, another function of the complex in interphase nuclei has proven to be no less important for the viability of an organism: Numerous studies of various developmental disorders have identified mutations that interfere with the proper function of cohesin in gene expression and genome organization (Mazumdar and Majeti, 2017). The role of cohesin in gene transcription has been shown to be through mediating long-range interactions between gene regulatory elements (Faure et al., 2012; Kagey et al., 2010; Seitan et al., 2011). In addition, Hi-C studies have revealed the organization of interphase chromosomes into topologically associating domains

(TADs), which also affect gene expression by constraining the interaction of enhancers and promoters within the TADs (Dixon et al., 2015; Dowen et al., 2014). TADs are chromosomal units in which loci within the domain are more likely to interact with each other than with loci outside the domain. At the boundaries of TADs, both cohesin and insulator CTCF (CCCTC-binding factor) are enriched (Dixon et al., 2016; Rao et al., 2017) and TAD structures are lost in cohesin depleted cells (Gassler et al., 2017; Schwarzer et al., 2017). TAD lengths range from a few to several hundred kilobases (Van Bortle et al., 2014; Zhan et al., 2017). Given the fact that the size of chromosomes in the somatic nucleus of *Tetrahymena* range from 20 kb to 3 Mb with average size of 385 kb (Altschuler and Yao, 1985; Conover and Brunk, 1986; Hamilton et al., 2016), the regulation of intra-chromosomal long-range interactions may not be as critical as for other organisms.

Another peculiarity of *Tetrahymena* resides in its cell cycle, and how it transits between mitotic and meiotic divisions. During the mitotic cell cycle, there is a very quick transition from chromosome segregation to DNA replication, which occurs in telophase of mitosis (Doerder and Debault, 1975; Cole and Sugai, 2012). Therefore, the germline nuclei of vegetative cells are mostly at G2. In the absence of nutrients, the cells will enter the sexual reproduction program and the G2 nuclei can undergo meiosis. In this case, the DNA is already replicated, and since cohesin is generally loaded during replication, there may be little opportunity to replace a mitotic cohesin with a meiotic cohesin. It is tempting to speculate that instead loading of new cohesins with different subunit compositions, unique combinations of PTMs on chromatin bound cohesin may provide a faster way to regulate the function of the complex in different contexts.

**Conservation of cohesin functions in *Tetrahymena***

Cohesin is primarily known for its essential role in chromosome segregation. Errors in the segregation can result in aneuploidy, which is a predisposition of cancer and maternal age related birth defects. The reduction of cohesin in aged oocytes results in weak centromere cohesion and incorrect attachment of sister chromatids (merotelic attachment) which leads to lagging chromosomes during meiosis I (Chiang et al., 2010; Lister et al., 2010). In addition, it has been observed that separase overexpression in mouse mammary epithelial cells leads to tumor formation and aneuploidy with premature sister chromatid separation, lagging chromosomes, and

anaphase bridges (Zhang et al., 2008). In *Tetrahymena*, anaphase segregation defects occur in Smc1 and Scc3 depleted germline nuclei of vegetative cells (Howard-Till et al., 2013; Ali et al., 2018). The segregation defect is even stronger in Scc2 depleted cells, and is manifested by lagging chromosomes and anaphase bridges. Lagging chromosomes might be formed as a result of loss of centromeric cohesin and merotelic attachment of the chromatids. The anaphase bridges, on the other hand, may result from incorrect DNA damage repair between different chromosomes and telomere end fusion (Lo et al., 2002; Tusell et al., 2008). In mammalian cells, anaphase bridges form either a micronucleus or a protrusion next to the chromosome mass after the completion of the mitotic division (Pampalona et al., 2016). Since centromere staining by Cna1 was weak, it was not possible to distinguish between these segregation errors. The germline nuclei appear to have roughly equal size after the mitotic division in Smc1, Scc3, and Scc2 RNAi cells suggesting that the incidence of nondisjunction is low. The mild phenotype might be due to incomplete RNAi depletion which results in the retention of a small amount of protein sufficient for the division. Alternatively, the catenation between sister chromatids might provide some cohesion and allow normal chromosome segregation (Farcas et al., 2011; Guacci and Koshland, 2012).

Another function of cohesin that is likely conserved in *Tetrahymena* is its activity in DNA damage repair. However, because this function has not been explored in vegetative cells, it will be discussed below in the context of meiotic DSB repair.

**The role of cohesin in DSB repair during meiotic prophase**

Depletion of Rec8 and Smc1 in *Tetrahymena* results in a failure to repair meiotic DSBs, and similar phenotypes are observed after the knockdown of Scc3 and Scc2 (Howard-Till et al., 2013; Ali et al., 2018). In mitosis, *de novo* cohesin loading provides close connection between sister chromatids in the post-replicative damage repair (Covo et al., 2010; Sjögren and Nasmyth, 2001; Ström et al., 2004; Unal et al., 2007). In meiotic prophase, the repair of programmed DSBs occurs in the context of the chromosome axis structure. The chromosome axis is composed of various proteins, including meiosis specific cohesin, which form a base that connects the linear arrays of chromatin loops (Kleckner, 2006; Klein et al., 1999). The proteins involved in recombination associate with the chromosome axis and the DNA in the loops destined for recombination is tethered to the axis (Blat et al., 2002; Kleckner, 2006; Panizza et

al., 2011). Recombination between homologous chromosomes rather than between sister chromatids is promoted by the loss of cohesion and local separation at CO sites (Eijpe et al., 2003; Kim et al., 2010; Storlazzi et al., 2008). The canonical axial elements and formation of SC have not been identified in *Tetrahymena* (Loidl, 2006; Lorenz, 2004). However, thread-like structures have been observed for proteins involved in recombination suggesting the existence of a meiotic chromosome axis structure (Shodhan et al., 2017).

Recombination and the formation of axial elements are defective in yeast cells depleted of Rec8 (Brar et al., 2009; Klein et al., 1999). Similarly, DSBs are formed but not repaired in *scc3*i and *scc2*i cells. Although the observed phenotype in *scc3*i cells might be due to the lack of chromatin-associated cohesin, this is unlikely to be the case for *scc2*i cells, in which cohesin still interacts with chromatin. Moreover, the *de novo* loading of Rec8 and Scc2 during meiotic prophase is not DSB dependent (Spo11), therefore it is unlikely that cohesin is loaded in response to DSB formation. In mammalian cells, the loading of meiosis specific cohesin complexes during meiotic prophase regulates both the formation and organization of the loop/axis structure (Eijpe et al., 2003; Novak et al., 2008). In fission yeast, which does not assemble an SC, the formation of LinEs (linear elements) and meiotic recombination are dependent on Rec8 and the phosphorylation of Rec11/SA3 (Lorenz, 2004; Ding et al., 2016; Sakuno and Watanabe, 2015). Similarly, cohesin might be involved in chromosome axis formation or similar chromosome organization that is crucial for chromosome pairing and recombination in *Tetrahymena*.

The loop formation during interphase depends on cohesin (Gassler et al., 2017; Wutz et al., 2017). The loop extrusion model has been proposed to explain how cohesin is involved in TAD formation (Merkenschlager and Nora, 2016; Parelho et al., 2008; Wendt et al., 2008). The model proposes that cohesin extrudes DNA until it encounters a CTCF barrier (Fudenberg et al., 2016; Rao et al., 2014). The formation of larger chromatin loops has been suggested to occur as a result of a longer chromatin association time of cohesin in Wapl depleted cells (Haarhuis et al., 2017; Tedeschi et al., 2013; Wutz et al., 2017). The chromatin localization of Scc2 is cohesin dependent and highest during early prophase. It is tempting to speculate that Scc2 might interact with chromatin bound cohesin and stimulate its ATPase activity. Multiple rounds of binding and ATPase stimulation might induce DNA extrusion and loop formation (Rhodes et al., 2017). In this way, the chromosomes may be remodeled to

support homologous recombination. This model would predict that chromatin bound cohesin would be inactive without Scc2, which would inhibit axis formation and DSB repair, and this appears to be the case in *Tetrahymena*.

**The chromatin association of cohesin**

Immunostaining and in vitro studies in other model systems have shown that Scc3 is necessary for the association of cohesin with chromatin (Fukuda et al., 2014; Murayama and Uhlmann, 2014; Pasierbek et al., 2003; Wang et al., 2003). In line with these studies, knockdown of *Tetrahymena* Scc3 resulted in the loss of the germline localization of Rec8 and Smc1 as well as the absence of Rec8 in the chromatin fraction of protein extracts (Ali et al., 2018). In contrast, the overall protein levels of both Smc1 and Rec8 do not change in *scc3*i cells. Similarly the localization but not the expression of Scc3 depends on Rec8. These results suggest that all subunits are interdependent and essential for the chromatin association of cohesin. In many organisms, the loading of cohesin on chromatin depends on its interaction with Scc2, which forms the loader complex together with Scc4 (Ciosk et al., 2000; Lightfoot et al., 2011). In *Tetrahymena*, however, the chromatin association of Rec8 and Scc3 does not strictly depend on Scc2. Nevertheless, both mitotic and meiotic divisions are impaired in the absence of Scc2. Similar to Scc3 depletion, knockdown of Scc2 does not have any effect on the protein levels of other cohesin subunits, but does result in the loss of Rec8 phosphorylation.

The loss of chromatin association and phosphorylation of Rec8 in the Scc3 knockdown suggests that the phosphorylation is present on chromatin bound Rec8. However, the ability of unphosphorylated Rec8 to bind to chromatin in the absence of Scc2, implies that phosphorylated Rec8 may represent a subset of chromatin bound cohesin pool with a specific function. For instance, similar to the DNA damage dependent modification of the mitotic $\alpha$-kleisin in budding yeast, phosphorylation might represent the cohesive fraction of cohesin (Heidinger-Pauli et al., 2008, 2009). In *Tetrahymena*, the activity of separase is required for sister chromatid separation, implying the need for cleaving cohesin (Howard-Till et al., 2013). However, the chromatin localization of *Tetrahymena* cohesin does not change after the onset of anaphase in mitosis and meiosis. It may be that, similar to yeast, only a subset of

cohesin is involved in cohesion while the bulk of cohesin regulates chromosome structure or is needed for subsequent divisions.

The question remains, how does cohesin bind to the chromatin? It has been proposed that the budding yeast condensin is able to interact with DNA through the interface formed between the kleisin and the HEAT repeat subunits (Kschonsak et al., 2017; Piazza et al., 2014). This interaction is followed by ATP hydrolysis and topological entrapment of DNA (Eeftens et al., 2017). The association of *Tetrahymena* cohesin with DNA might be through its corresponding HEAT repeat Scc3 subunit (Figure 27 a), as cohesin cannot bind DNA in the absence of Scc3. Alternatively, some of the cohesin complexes may have topological but dynamic association by continuously loading and dissociating from chromatin (Figure 27 b - e). Similar to budding yeast, Scc2 may stimulate the ATPase activity and induce topological entrapment and cohesion (Figure 29 f and h)(Petela et al., 2018). Additionally, Scc2 might be involved in the shaping of chromatin into the loops by stabilizing the cohesin and promoting extrusion of chromatin. Although the function of Rec8 phosphorylation is unknown, it may be required for (or a result of) stable topological binding or cohesion (Figure 27).

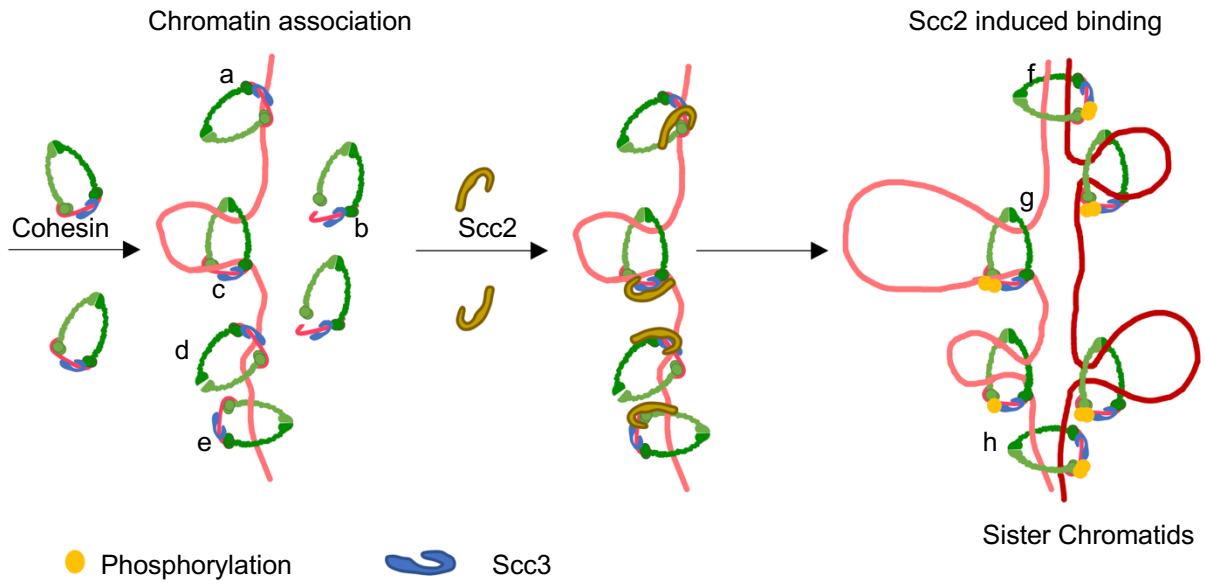


**Figure 27. Model for the role of Scc2 and Rec8 phosphorylation on the chromatin interaction of cohesin.**

Cohesin could have different modes of association with chromatin: it might bind through its HEAT repeat Scc3 (a) or it might topologically entrap a single chromatin strand (e) or it can hold two strands of the same chromatin strand to form a loop (c). Cohesin might have dynamic association by constant loading through hinge opening (d) or release through Smc3-kleisin interface (b). The interaction of Scc2 with chromatin bound cohesin might induce its ATPase activity and convert the complex to cohesive form with both sister chromatids within a single ring (f and h) or it can promote loop extrusion (g). Phosphorylation might stabilize cohesive interaction.

**PTMs of cohesin subunits**

Modification of specific residues on cohesin subunits are known to regulate cohesin function. Since a minimal cohesin complex is sufficient for both mitosis and meiosis in *Tetrahymena*, we hypothesized that differential regulation by PTMs may provide specificity of function for different activities. MS analysis of IPs from different stages in the life cycle resulted in identification of multiple PTMs, including phosphorylation, acetylation, methylation, and SUMOylation on each cohesin subunit.

The post-translationally modified sites on Smc1 and Smc3 were detected not only in the conserved NBD but also in the less conserved coiled coil domains and most of the modified residues on Rec8 and Scc3 are located in non-conserved regions. Most notable are the multiple phosphorylation sites at the coiled coil domain of Smc1. A similar phosphorylation pattern has been previously detected on human Smc1$\alpha$ (Hornbeck et al., 2015). This cluster is within the kinks/break regions that interrupt the coiled coil of Smc1$\alpha$ (Hons et al., 2016). Two of these residues are known to be phosphorylated by ATM in response to DNA damage (Kim et al., 2002; Yazdi et al., 2002; Kitagawa, 2004). ATM has not been identified in *Tetrahymena*, instead ATR has been shown to be involved in DNA damage response (Loidl and Mochizuki, 2009; Yakisich et al., 2006) Considering that the ATM and ATR kinases recognize an SQ/TQ motif (Kim et al., 1999), some of phosphorylation sites within the *Tetrahymena* Smc1 cluster may also be targets of ATR. It would be interesting to investigate the effect of this phospho-cluster on DNA damage repair, or whether phosphorylation of these residues is reduced or abolished upon chemical inhibition of ATR.

Although our initial experimental setup led to the identification of multiple PTMs, further experiments are needed to understand the biological significance of these

modifications and their involvement in cohesin regulation. The time points used in this study represent only certain stages of meiosis and mitosis. Using a full meiotic time-course would give a better view of the modifications at specific stages. Synchronization of mitotic cells by elutriation could also be performed to better understand the cohesin cycle in vegetative cells. In addition, the enrichment of phosphopeptides prior to MS and quantification of relative phosphorylation of given sites would increase the confidence of identified sites, and may provide better insight into stage specific modifications.

**The function of cohesin SUMOylation**

In our MS experiments, we identified SUMOylation on a conserved residue on *Tetrahymena* Smc3. To get a better understanding of the biological significance of cohesin SUMOylation in *Tetrahymena*, we used a method developed by Almedawar et.al in budding yeast (Almedawar et al., 2012). The method is based on the fusion of the catalytic domain of Ulp1 (SUMO protease) to Rec8 (Rec8-UD). In contrast to the results obtained in budding yeast (Almedawar et al., 2012), the protein level and chromatin association of Rec8-UD is much less than for HA tagged Rec8. Mutation of the catalytic cysteine of the UD domain (Rec8-UD$^{483}$) restores both protein level and localization, suggesting that the fusion of the UD domain does not interfere with the stability or function of Rec8. Silver staining of IP samples of Rec8-UD and control constructs showed similar banding patterns between 135-190 kDa, suggesting that some cohesin complex is able to form, therefore reduced stability seems likely. Similar to the knockdown of different cohesin subunits, meiotic progression was arrested at a metaphase-like stage and Rec8-UD cells show signs of unrepaired meiotic DSBs. This phenotype is likely due to the reduced level of chromatin bound cohesin. Future experiments to further identify and mutate the SUMOylated residues of cohesin will give more insight into the function of this modification in *Tetrahymena*.

IF of SUMO at different stages of the *Tetrahymena* life cycle reveals a distinct accumulation of SUMO signal at the telomeric end of the elongated germline nucleus during meiotic prophase. Although we don't have direct proof that the telomeric SUMO signal is SUMOylated cohesin, we did see an increase of this signal in the Rec8-UD483 cells, which show hyper-SUMOylation of Rec8. Conversely, we also see a reduction of this signal in Rec8-UD cells, presumably due to the activity of small amount of protein able to associate with chromatin. Therefore, it seems possible that

this telomeric SUMO signal is either cohesin or a cohesin associated protein. Explaining the significance of telomeric SUMOylation will require further experimental approaches.

**Summary and Outlook**

Studying the function of cohesin in *Tetrahymena thermophila* revealed both conserved and unique features of the complex with many intriguing questions to be further explored. *Tetrahymena* uses a minimal cohesin complex consisting of Smc1, Smc3, Rec8, and Scc3 to perform diverse functions during mitosis and meiosis. It does not require Scc2 for loading to the chromatin. However, Scc2 requires cohesin for its chromatin association. The question is how Scc2 is involved in cohesin function? Does it have ATPase activity like its homologs in other organisms? How does Scc2 contribute to Rec8 phosphorylation? Are there unique PTM combinations on different subunits that distinguish mitotic cohesin from meiotic? What is the importance of telomere SUMOylation during meiotic prophase? The list of the questions can be extended. We are just beginning to understand the role of cohesin in *Tetrahymena*, and there are still many more questions than answers.

# Materials and Methods

*Tetrahymena thermophila* strains and growth conditions

WT strains B2086 (mating type II), CU427 (mating type VI) , and CU428 (mating type VII) were purchased from the Tetrahymena Stock Center, Cornell University (https://tetrahymena.vet.cornell.edu). Cells were grown in Neff's medium at 30°C (Orias et al., 2011). To initiate sexual reproduction, cells from different mating types were starved in 10mM Tris-Cl (pH 7.4) before equal numbers of starved cells were mixed.

Protein alignment

The protein sequences of different species were obtained from NCBI, http://www.ncbi.nlm.nih.gov (NCBI Resource Coordinators, 2012). *Tetrahymena*-specific protein sequences were acquired from TGD, www.ciliate.org (Eisen et al., 2006; Stover, 2006). The alignments were generated by Geneious software (11.0.4) using the Muscle algorithm (3.8.425) (Edgar, 2004; Kearse et al., 2012).

Protein tagging

REC8-mCHERRY-NEO4, REC8-HA3HIS6-NEO4, SCC3-mCHERRY-NEO4, SCC3-HA-NEO5, and SCC2-HA3HIS6-PUR4, REC8-HA3HIS6-UD-NEO5 constructs were created as described previously (Kataoka et al., 2010; Iwamoto et al., 2014; Akematsu et al., 2017; Ali et al., 2018). In short, ~500 bp regions from both the C-terminal end and the downstream UTR of the gene of interest were amplified by PCR. The fragments were combined with NEO4, NEO5 or PUR4 cassettes (gifts from Dr. Kazufumi Mochizuki, CNRS, Montpellier, France and Dr. Takahiko Akematsu, MFPL, Vienna, Austria) by Gibson assembly (NEBuilder HiFiDNA assembly master mix, New England BioLabs). REC8-HA3HIS6-UD$^{483}$-NEO5 construct was created by site-directed mutagenesis (Thermo Scientific, F-541).

All constructs were linearized and transformed into *Tetrahymena* cells by biolistic transformation (Cassidy-Hanley et al., 1997). Selection was performed by gradual increase of the drug concentration and a constant amount of $CuSO_4$ or $CdCl_2$ (Sigma-Aldrich). The initial and final amounts of the drugs used for selection are as following:

| | Initial Selection | Final Selection |
|---|---|---|
| NEO4 | 120 μg/ml paromomycin | 50 mg/ml paromomycin |
| | 0.5 μg/ml $CdCl_2$ | 0.5 μg/ml $CdCl_2$ |
| NEO5 | 120 μg/ml paromomycin | 50 mg/ml paromomycin |
| PUR4 | 400 μg/ml puromycin | 1200 μg/ml puromycin |
| | 0.63 mM $CuSO_4$ | 0.63 mM $CuSO_4$ |

RNAi knockdown and Scc2 knockout

RNAi constructs were created as previously described in (Howard-Till et al., 2013). The selection was initiated by adding 7.5 μg/ml cycloheximide into the transformed cells. The amount of the cycloheximide was gradually increased up to 30 μg/ml. To obtain complete depletion of cohesin subunits, 0.5 μg/ml $CdCl_2$ was added into the growing cultures for 24h followed by addition of 0.05 μg/ml $CdCl_2$ into the starvation media. Scc2 knockout strains were generated by Josef Loidl according to the co-deletion strategy described in (Hayashi and Mochizuki, 2015; Ali et al., 2018).

FISH

The probe spanning a 22.1 kb genomic region was prepared as described in (Loidl and Mochizuki, 2009). The method described by Loidl et.al was followed for slide preparation and probe hybridization (Loidl, 2004).

Protein Sample Preparation

The samples for immunoprecipitation and mass spectrometry analysis were prepared as described in (Ali et al., 2018). The method described at Ali et.al was used for cell fractionation and dephosphorylation experiments. The antibodies used for western blot analysis are listed below.

Immunofluorescence analysis

Different fixation methods described in (Ali et al., 2018) were applied for slide preparation: partial Schaudinn fixation for immunostaining of γH2A.X, high-detergent fixation for visualization of Dmc1/Rad51 and chromatin bound proteins, formaldehyde Triton-X100 fixation for localization of tagged proteins. For immunostaining, slides were washed twice in 1X PBS and once in 1X PBS + 0.05% Triton X-100 and

incubated with primary antibodies for 2 h at room temperature or over night at 4°C. The incubation with secondary antibodies labeled with either Cy3 or FITC was performed for 1 h at room temperature. Unbound antibodies were removed by washing with 1X PBS and 1X PBS + 0.05% Triton X-100, and slides were mounted with Vectashield anti-fading agent supplemented with 0.5 μg/ml DAPI.

Antibodies

The primary antibodies used in this study are as following:

| **Antigene** | **Host** | **Source** | **WB** | **IF** |
|---|---|---|---|---|
| α-tubulin Ab-2 (DM1A) (monoclonal) | mouse | NeoMarkers | 1:10000 | 1:100 |
| Dmc1/Rad51 (monoclonal) | mouse | NeoMarkers | - | 1:100 |
| dsRED (polyclonal) | rabbit | Clontech | 1:1000 | 1:100 |
| GFP JL-8 (monoclonal) | mouse | Takara | 1:1000 | 1:100 |
| HA (monoclonal) | mouse | Sigma | 1:1000 | 1:100 |
| HA (polyclonal) | rabbit | Sigma | 1:1000 | 1:100 |
| γH2A.X (monoclonal) | mouse | BioLegends | - | 1:200 |
| SUMO (polyclonal) | rabbit | James Forney | - | 1:500 |

The secondary antibodies used are as following:

| | **Source** | **IB** | **IF** |
|---|---|---|---|
| Alexa488 anti-mouse | Invitrogen | - | 1:500 |
| Alexa568 anti-rabbit | Invitrogen | - | 1:500 |
| FITC goat anti-mouse | Merck Millipore | - | 1:500 |
| Rhodamine goat anti-rabbit | Merck Millipore | - | 1:2000 |
| HRP goat anti-mouse | Thermo Fisher | 1:5000 | - |
| HRP goat anti-rabbit | Thermo Fisher | 1:10000 | - |

Primers

In addition to the primers listed in (Ali et al., 2018), the following primers were used in this study:

**Rec8-HA3His6-UD/UD$^{483}$**

| | |
|---|---|
| Rec8_5_neo5_FW | AGGGAACAAAAGCTGGAGCTCTTAATAGATCTAAATGATGGTTAGGC |
| Rec8_5_RV | ATAAGTCTTTGTTAATTAGGAT |
| Rec8_3_FW | AATTAACAAAGACTTATGATGCTTG |
| Rec8_3_neo5_RV | TTCTTCAAATCTCCAACTAGTATGGTGATGGTGATGG |
| Rec8_UD_neo5_FW | CCATCACCATACTAGTTGGAGATTTGAAGAAAAG |
| Rec8_UD_neo5_RV | GACCGATTCAGTTCGCTCAACTAGTTCAGTTTTAGCAAATCTCTACTTTTC |
| Rec8_C183S_GB_RV | ACTCCAGAATCATATCCGTTTTATTAG |

# Abbreviations

| | |
|---|---|
| ATM | ataxia telangiectasia mutated |
| ATR | ataxia telangiectasia- and Rad3 related |
| CO | crossover |
| DAPI | 4',6-diamidino-2-phenylindole |
| DSB | DNA double strand break |
| FISH | fluorescence in situ hybridization |
| GFP | green fluorescent protein |
| IF | immunofluorescence |
| IP | immunoprecipitation |
| MS | mass spectrometry |
| RNAi | RNA interference |
| SC | synaptonemal complex |
| SMC | structural maintenance of chromosomes |
| WB | western blot |
| WT | wild type |

# References


Agostinho, A., Manneberg, O., van Schendel, R., Hernández-Hernández, A., Kouznetsova, A., Blom, H., Brismar, H., and Höög, C. (2016). High density of REC8 constrains sister chromatid axes and prevents illegitimate synaptonemal complex formation. EMBO Rep. *17*, 901–913.

Akematsu, T., Fukuda, Y., Garg, J., Fillingham, J.S., Pearlman, R.E., and Loidl, J. (2017). Post-meiotic DNA double-strand breaks occur in Tetrahymena, and require Topoisomerase II and Spo11. ELife *6*.

Ali, E.I., Loidl, J., and Howard-Till, R.A. (2018). A streamlined cohesin apparatus is sufficient for mitosis and meiosis in the protist Tetrahymena. Chromosoma.

Almedawar, S., Colomina, N., Bermúdez-López, M., Pociño-Merino, I., and Torres-Rosell, J. (2012). A SUMO-Dependent Step during Establishment of Sister Chromatid Cohesion. Curr. Biol. *22*, 1576–1581.

Altschuler, M.I., and Yao, M.C. (1985). Macronuclear DNA of Tetrahymena thermophila exists as defined subchromosomal-sized molecules. Nucleic Acids Res. *13*, 5817–5831.

Arumugam, P., Gruber, S., Tanaka, K., Haering, C.H., Mechtler, K., and Nasmyth, K. (2003). ATP hydrolysis is required for cohesin's association with chromosomes. Curr. Biol. CB *13*, 1941–1953.

Banerji, R., Skibbens, R.V., and Iovine, M.K. (2017). How many roads lead to cohesinopathies?: Mechanisms Underlying Cohesinopathies. Dev. Dyn. *246*, 881–888.

Beckouët, F., Hu, B., Roig, M.B., Sutani, T., Komata, M., Uluocak, P., Katis, V.L., Shirahige, K., and Nasmyth, K. (2010). An Smc3 Acetylation Cycle Is Essential for Establishment of Sister Chromatid Cohesion. Mol. Cell *39*, 689–699.

Ben-Shahar, T.R., Heeger, S., Lehane, C., East, P., Flynn, H., Skehel, M., and Uhlmann, F. (2008). Eco1-Dependent Cohesin Acetylation During Establishment of Sister Chromatid Cohesion. Science *321*, 563–566.

Bermudez, V.P., Farina, A., Higashi, T.L., Du, F., Tappin, I., Takahashi, T.S., and Hurwitz, J. (2012). In vitro loading of human cohesin on DNA by the human Scc2-Scc4 loader complex. Proc. Natl. Acad. Sci. *109*, 9366–9371.

Blackburn, E.H., and Gall, J.G. (1978). A tandemly repeated sequence at the termini of the extrachromosomal ribosomal RNA genes in Tetrahymena. J. Mol. Biol. *120*, 33–53.

Blat, Y., Protacio, R.U., Hunter, N., and Kleckner, N. (2002). Physical and functional interactions among basic chromosome organizational features govern early steps of meiotic chiasma formation. Cell *111*, 791–802.

Brar, G.A., Kiburz, B.M., Zhang, Y., Kim, J.-E., White, F., and Amon, A. (2006). Rec8 phosphorylation and recombination promote the step-wise loss of cohesins in meiosis. Nature *441*, 532–536.

Brar, G.A., Hochwagen, A., Ly-sha, S.E., and Amon, A. (2009). The multiple roles of cohesin in meiotic chromosome morphogenesis and pairing. Mol. Biol. Cell *20*, 1030–1047.

Brooker, A.S., and Berkowitz, K.M. (2014). The Roles of Cohesins in Mitosis, Meiosis, and Human Health and Disease. In Cell Cycle Control, E. Noguchi, and M.C. Gadaleta, eds. (New York, NY: Springer New York), pp. 229–266.

Buheitel, J., and Stemmann, O. (2013). Prophase pathway-dependent removal of cohesin from human chromosomes requires opening of the Smc3–Scc1 gate. EMBO J. *32*, 666–676.

Buonomo, S.B., Clyne, R.K., Fuchs, J., Loidl, J., Uhlmann, F., and Nasmyth, K. (2000). Disjunction of homologous chromosomes in meiosis I depends on proteolytic cleavage of the meiotic cohesin Rec8 by separin. Cell *103*, 387–398.

Canudas, S., and Smith, S. (2009). Differential regulation of telomere and centromere cohesion by the Scc3 homologues SA1 and SA2, respectively, in human cells. J. Cell Biol. *187*, 165–173.

Cassidy-Hanley, D., Bowen, J., Lee, J.H., Cole, E., VerPlank, L.A., Gaertig, J., Gorovsky, M.A., and Bruns, P.J. (1997). Germline and somatic transformation of mating Tetrahymena thermophila by particle bombardment. Genetics *146*, 135–147.

Cech, T.R., Zaug, A.J., and Grabowski, P.J. (1981). In vitro splicing of the ribosomal RNA precursor of Tetrahymena: involvement of a guanosine nucleotide in the excision of the intervening sequence. Cell *27*, 487–496.

Chan, K.-L., Roig, M.B., Hu, B., Beckouët, F., Metson, J., and Nasmyth, K. (2012). Cohesin's DNA Exit Gate Is Distinct from Its Entrance Gate and Is Regulated by Acetylation. Cell *150*, 961–974.

Chao, W.C.H., Murayama, Y., Muñoz, S., Costa, A., Uhlmann, F., and Singleton, M.R. (2015). Structural Studies Reveal the Functional Modularity of the Scc2-Scc4 Cohesin Loader. Cell Rep. *12*, 719–725.

Chao, W.C.H., Murayama, Y., Muñoz, S., Jones, A.W., Wade, B.O., Purkiss, A.G., Hu, X.-W., Borg, A., Snijders, A.P., Uhlmann, F., et al. (2017). Structure of the cohesin loader Scc2. Nat. Commun. *8*, 13952.

Chiang, T., Duncan, F.E., Schindler, K., Schultz, R.M., and Lampson, M.A. (2010). Evidence that Weakened Centromere Cohesion Is a Leading Cause of Age-Related Aneuploidy in Oocytes. Curr. Biol. *20*, 1522–1528.

Ciosk, R., Shirayama, M., Shevchenko, A., Tanaka, T., Toth, A., Shevchenko, A., and Nasmyth, K. (2000). Cohesin's binding to chromosomes depends on a separate complex consisting of Scc2 and Scc4 proteins. Mol. Cell *5*, 243–254.

Cole, E., and Sugai, T. (2012). Developmental progression of Tetrahymena through the cell cycle and conjugation. In Methods in Cell Biology, (Elsevier), pp. 177–236.

Conover, R.K., and Brunk, C.F. (1986). Macronuclear DNA molecules of Tetrahymena thermophila. Mol. Cell. Biol. *6*, 900–905.

Covo, S., Westmoreland, J.W., Gordenin, D.A., and Resnick, M.A. (2010). Cohesin Is Limiting for the Suppression of DNA Damage–Induced Recombination between Homologous Chromosomes. PLoS Genet. *6*, e1001006.

Cubeñas-Potts, C., and Matunis, M.J. (2013). SUMO: A Multifaceted Modifier of Chromatin Structure and Function. Dev. Cell *24*, 1–12.

D'Ambrosio, L.M., and Lavoie, B.D. (2014). Pds5 Prevents the PolySUMO-Dependent Separation of Sister Chromatids. Curr. Biol. *24*, 361–371.

Darwiche, N., Freeman, L.A., and Strunnikov, A. (1999). Characterization of the components of the putative mammalian sister chromatid cohesion complex. Gene *233*, 39–47.

Ding, D.-Q., Matsuda, A., Okamasa, K., Nagahama, Y., Haraguchi, T., and Hiraoka, Y. (2016). Meiotic cohesin-based chromosome structure is essential for homologous chromosome pairing in Schizosaccharomyces pombe. Chromosoma *125*, 205–214.

Ding, Y., Kaido, M., Llano, E., Pendas, A.M., and Kitajima, T.S. (2018). The Post-anaphase SUMO Pathway Ensures the Maintenance of Centromeric Cohesion through Meiosis I-II Transition in Mammalian Oocytes. Curr. Biol. *28*, 1661-1669.e4.

Dixon, J.R., Jung, I., Selvaraj, S., Shen, Y., Antosiewicz-Bourget, J.E., Lee, A.Y., Ye, Z., Kim, A., Rajagopal, N., Xie, W., et al. (2015). Chromatin architecture reorganization during stem cell differentiation. Nature *518*, 331–336.

Dixon, J.R., Gorkin, D.U., and Ren, B. (2016). Chromatin Domains: The Unit of Chromosome Organization. Mol. Cell *62*, 668–680.

Doerder, F.P., and Debault, L.E. (1975). Cytofluorimetric analysis of nuclear DNA during meiosis, fertilization and macronuclear development in the ciliate Tetrahymena pyriformis, syngen 1. J. Cell Sci. *17*, 471–493.

Dowen, J.M., Fan, Z.P., Hnisz, D., Ren, G., Abraham, B.J., Zhang, L.N., Weintraub, A.S., Schuijers, J., Lee, T.I., Zhao, K., et al. (2014). Control of Cell Identity Genes Occurs in Insulated Neighborhoods in Mammalian Chromosomes. Cell *159*, 374–387.

Edgar, R.C. (2004). MUSCLE: multiple sequence alignment with high accuracy and high throughput. Nucleic Acids Res. *32*, 1792–1797.

Eeftens, J.M., Bisht, S., Kerssemakers, J., Kschonsak, M., Haering, C.H., and Dekker, C. (2017). Real-time detection of condensin-driven DNA compaction reveals a multistep binding mechanism. EMBO J. *36*, 3448–3457.

Eichinger, C.S., Kurze, A., Oliveira, R.A., and Nasmyth, K. (2013). Disengaging the Smc3/kleisin interface releases cohesin from Drosophila chromosomes during interphase and mitosis. EMBO J. *32*, 656–665.

Eijpe, M., Offenberg, H., Jessberger, R., Revenkova, E., and Heyting, C. (2003). Meiotic cohesin REC8 marks the axial elements of rat synaptonemal complexes before cohesins SMC1β and SMC3. J. Cell Biol. *160*, 657–670.

Eisen, J.A., Coyne, R.S., Wu, M., Wu, D., Thiagarajan, M., Wortman, J.R., Badger, J.H., Ren, Q., Amedeo, P., Jones, K.M., et al. (2006). Macronuclear Genome Sequence of the Ciliate Tetrahymena thermophila, a Model Eukaryote. PLoS Biol. *4*, e286.

Farcas, A.-M., Uluocak, P., Helmhart, W., and Nasmyth, K. (2011). Cohesin's Concatenation of Sister DNAs Maintains Their Intertwining. Mol. Cell *44*, 97–107.

Faure, A.J., Schmidt, D., Watt, S., Schwalie, P.C., Wilson, M.D., Xu, H., Ramsay, R.G., Odom, D.T., and Flicek, P. (2012). Cohesin regulates tissue-specific expression by stabilizing highly occupied cis-regulatory modules. Genome Res. *22*, 2163–2175.

Fernius, J., Nerusheva, O.O., Galander, S., Alves, F. de L., Rappsilber, J., and Marston, A.L. (2013). Cohesin-Dependent Association of Scc2/4 with the Centromere Initiates Pericentromeric Cohesion Establishment. Curr. Biol. *23*, 599–606.

Fudenberg, G., Imakaev, M., Lu, C., Goloborodko, A., Abdennur, N., and Mirny, L.A. (2016). Formation of Chromosomal Domains by Loop Extrusion. Cell Rep. *15*, 2038–2049.

Fukuda, T., Pratto, F., Schimenti, J.C., Turner, J.M.A., Camerini-Otero, R.D., and Höög, C. (2012). Phosphorylation of chromosome core components may serve as axis marks for the status of chromosomal events during mammalian meiosis. PLoS Genet. *8*, e1002485.

Fukuda, T., Fukuda, N., Agostinho, A., Hernández-Hernández, A., Kouznetsova, A., and Höög, C. (2014). STAG3-mediated stabilization of REC8 cohesin complexes promotes chromosome synapsis during meiosis. EMBO J. *33*, 1243–1255.

Gandhi, R., Gillespie, P.J., and Hirano, T. (2006). Human Wapl is a cohesin-binding protein that promotes sister-chromatid resolution in mitotic prophase. Curr. Biol. CB *16*, 2406–2417.

Gassler, J., Brandão, H.B., Imakaev, M., Flyamer, I.M., Ladstätter, S., Bickmore, W.A., Peters, J.-M., Mirny, L.A., and Tachibana, K. (2017). A mechanism of cohesin-dependent loop extrusion organizes zygotic genome architecture. EMBO J. *36*, 3600–3618.

Gerlich, D., Koch, B., Dupeux, F., Peters, J.-M., and Ellenberg, J. (2006). Live-Cell Imaging Reveals a Stable Cohesin-Chromatin Interaction after but Not before DNA Replication. Curr. Biol. *16*, 1571–1578.

Gibbons, I.R., and Rowe, A.J. (1965). Dynein: A Protein with Adenosine Triphosphatase Activity from Cilia. Science *149*, 424–426.

Gligoris, T., and Löwe, J. (2016). Structural Insights into Ring Formation of Cohesin and Related Smc Complexes. Trends Cell Biol. *26*, 680–693.

Gligoris, T.G., Scheinost, J.C., Burmann, F., Petela, N., Chan, K.-L., Uluocak, P., Beckouet, F., Gruber, S., Nasmyth, K., and Lowe, J. (2014). Closing the cohesin ring: Structure and function of its Smc3-kleisin interface. Science *346*, 963–967.

Greider, C.W., and Blackburn, E.H. (1985). Identification of a specific telomere terminal transferase activity in Tetrahymena extracts. Cell *43*, 405–413.

Gruber, S., Arumugam, P., Katou, Y., Kuglitsch, D., Helmhart, W., Shirahige, K., and Nasmyth, K. (2006). Evidence that Loading of Cohesin Onto Chromosomes Involves Opening of Its SMC Hinge. Cell *127*, 523–537.

Guacci, V., and Koshland, D. (2012). Cohesin-independent segregation of sister chromatids in budding yeast. Mol. Biol. Cell *23*, 729–739.

Gyuricza, M.R., Manheimer, K.B., Apte, V., Krishnan, B., Joyce, E.F., McKee, B.D., and McKim, K.S. (2016). Dynamic and Stable Cohesins Regulate Synaptonemal Complex Assembly and Chromosome Segregation. Curr. Biol. *26*, 1688–1698.

Haarhuis, J.H.I., Elbatsh, A.M.O., and Rowland, B.D. (2014). Cohesin and Its Regulation: On the Logic of X-Shaped Chromosomes. Dev. Cell *31*, 7–18.

Haarhuis, J.H.I., van der Weide, R.H., Blomen, V.A., Yáñez-Cuna, J.O., Amendola, M., van Ruiten, M.S., Krijger, P.H.L., Teunissen, H., Medema, R.H., van Steensel, B., et al. (2017). The Cohesin Release Factor WAPL Restricts Chromatin Loop Extension. Cell *169*, 693-707.e14.

Haering, C.H., Löwe, J., Hochwagen, A., and Nasmyth, K. (2002). Molecular architecture of SMC proteins and the yeast cohesin complex. Mol. Cell *9*, 773–788.

Haering, C.H., Schoffnegger, D., Nishino, T., Helmhart, W., Nasmyth, K., and Löwe, J. (2004). Structure and Stability of Cohesin's Smc1-Kleisin Interaction. Mol. Cell *15*, 951–964.

Haering, C.H., Farcas, A.-M., Arumugam, P., Metson, J., and Nasmyth, K. (2008). The cohesin ring concatenates sister DNA molecules. Nature *454*, 297–301.

Hamilton, E.P., Kapusta, A., Huvos, P.E., Bidwell, S.L., Zafar, N., Tang, H., Hadjithomas, M., Krishnakumar, V., Badger, J.H., Caler, E.V., et al. (2016). Structure of the germline genome of Tetrahymena thermophila and relationship to the massively rearranged somatic genome. ELife *5*, e19090.

Hara, K., Zheng, G., Qu, Q., Liu, H., Ouyang, Z., Chen, Z., Tomchick, D.R., and Yu, H. (2014). Structure of cohesin subcomplex pinpoints direct shugoshin-Wapl antagonism in centromeric cohesion. Nat. Struct. Mol. Biol. *21*, 864–870.

Hauf, S., and Watanabe, Y. (2004). Kinetochore orientation in mitosis and meiosis. Cell *119*, 317–327.

Hauf, S., Roitinger, E., Koch, B., Dittrich, C.M., Mechtler, K., and Peters, J.-M. (2005). Dissociation of Cohesin from Chromosome Arms and Loss of Arm Cohesion during Early Mitosis Depends on Phosphorylation of SA2. PLoS Biol. *3*, e69.

Hayashi, A., and Mochizuki, K. (2015). Targeted Gene Disruption by Ectopic Induction of DNA Elimination in Tetrahymena. Genetics *201*, 55–64.

Heidinger-Pauli, J.M., Ünal, E., Guacci, V., and Koshland, D. (2008). The Kleisin Subunit of Cohesin Dictates Damage-Induced Cohesion. Mol. Cell *31*, 47–56.

Heidinger-Pauli, J.M., Ünal, E., and Koshland, D. (2009). Distinct Targets of the Eco1 Acetyltransferase Modulate Cohesion in S Phase and in Response to DNA Damage. Mol. Cell *34*, 311–321.

Heidinger-Pauli, J.M., Mert, O., Davenport, C., Guacci, V., and Koshland, D. (2010). Systematic Reduction of Cohesin Differentially Affects Chromosome Segregation, Condensation, and DNA Repair. Curr. Biol. *20*, 957–963.

Hill, V.K., Kim, J.-S., and Waldman, T. (2016). Cohesin mutations in human cancer. Biochim. Biophys. Acta BBA - Rev. Cancer *1866*, 1–11.

Hinshaw, S.M., Makrantoni, V., Kerr, A., Marston, A.L., and Harrison, S.C. (2015). Structural evidence for Scc4-dependent localization of cohesin loading. Elife *4*, e06057.

Hons, M.T., Huis In 't Veld, P.J., Kaesler, J., Rombaut, P., Schleiffer, A., Herzog, F., Stark, H., and Peters, J.-M. (2016). Topology and structure of an engineered human cohesin complex bound to Pds5B. Nat. Commun. *7*, 12523.

Hopkins, J., Hwang, G., Jacob, J., Sapp, N., Bedigian, R., Oka, K., Overbeek, P., Murray, S., and Jordan, P.W. (2014). Meiosis-specific cohesin component, Stag3 is essential for maintaining centromere chromatid cohesion, and required for DNA repair and synapsis between homologous chromosomes. PLoS Genet. *10*, e1004413.

Hornbeck, P.V., Zhang, B., Murray, B., Kornhauser, J.M., Latham, V., and Skrzypek, E. (2015). PhosphoSitePlus, 2014: mutations, PTMs and recalibrations. Nucleic Acids Res. *43*, D512–D520.

Howard-Till, R., and Loidl, J. (2018). Condensins promote chromosome individualization and segregation during mitosis, meiosis, and amitosis in Tetrahymena thermophila. Mol. Biol. Cell *29*, 466–478.

Howard-Till, R.A., and Yao, M.-C. (2006). Induction of gene silencing by hairpin RNA expression in Tetrahymena thermophila reveals a second small RNA pathway. Mol. Cell. Biol. *26*, 8731–8742.

Howard-Till, R.A., Lukaszewicz, A., and Loidl, J. (2011). The Recombinases Rad51 and Dmc1 Play Distinct Roles in DNA Break Repair and Recombination Partner Choice in the Meiosis of Tetrahymena. PLoS Genet. *7*, e1001359.

Howard-Till, R.A., Lukaszewicz, A., Novatchkova, M., and Loidl, J. (2013). A Single Cohesin Complex Performs Mitotic and Meiotic Functions in the Protist Tetrahymena. PLoS Genet. *9*, e1003418.

Hu, B., Itoh, T., Mishra, A., Katoh, Y., Chan, K.-L., Upcher, W., Godlee, C., Roig, M.B., Shirahige, K., and Nasmyth, K. (2011). ATP Hydrolysis Is Required for Relocating Cohesin from Sites Occupied by Its Scc2/4 Loading Complex. Curr. Biol. *21*, 12–24.

Hunter, N. (2015). Meiotic Recombination: The Essence of Heredity. Cold Spring Harb. Perspect. Biol. *7*.

Ivanov, D., and Nasmyth, K. (2005). A Topological Interaction between Cohesin Rings and a Circular Minichromosome. Cell *122*, 849–860.

Iwamoto, M., Mori, C., Hiraoka, Y., and Haraguchi, T. (2014). Puromycin resistance gene as an effective selection marker for ciliate Tetrahymena. Gene *534*, 249–255.

Johnson, E.S. (2004). Protein Modification by SUMO. Annu. Rev. Biochem. *73*, 355–382.

Kagey, M.H., Newman, J.J., Bilodeau, S., Zhan, Y., Orlando, D.A., van Berkum, N.L., Ebmeier, C.C., Goossens, J., Rahl, P.B., Levine, S.S., et al. (2010). Mediator and cohesin connect gene expression and chromatin architecture. Nature *467*, 430–435.

Kamenz, J., and Hauf, S. (2017). Time To Split Up: Dynamics of Chromosome Separation. Trends Cell Biol. *27*, 42–54.

Kataoka, K., Schoeberl, U.E., and Mochizuki, K. (2010). Modules for C-terminal epitope tagging of Tetrahymena genes. J. Microbiol. Methods *82*, 342–346.

Katis, V.L., Lipp, J.J., Imre, R., Bogdanova, A., Okaz, E., Habermann, B., Mechtler, K., Nasmyth, K., and Zachariae, W. (2010). Rec8 Phosphorylation by Casein Kinase 1 and Cdc7-Dbf4 Kinase Regulates Cohesin Cleavage by Separase during Meiosis. Dev. Cell *18*, 397–409.

Kearse, M., Moir, R., Wilson, A., Stones-Havas, S., Cheung, M., Sturrock, S., Buxton, S., Cooper, A., Markowitz, S., Duran, C., et al. (2012). Geneious Basic: an integrated and extendable desktop software platform for the organization and analysis of sequence data. Bioinforma. Oxf. Engl. *28*, 1647–1649.

Keeney, S. (2008). Spo11 and the Formation of DNA Double-Strand Breaks in Meiosis. In Recombination and Meiosis, R. Egel, and D.-H. Lankenau, eds. (Berlin, Heidelberg: Springer Berlin Heidelberg), pp. 81–123.

Kikuchi, S., Borek, D.M., Otwinowski, Z., Tomchick, D.R., and Yu, H. (2016). Crystal structure of the cohesin loader Scc2 and insight into cohesinopathy. Proc. Natl. Acad. Sci. *113*, 12444–12449.

Kim, K.P., Weiner, B.M., Zhang, L., Jordan, A., Dekker, J., and Kleckner, N. (2010). Sister Cohesion and Structural Axis Components Mediate Homolog Bias of Meiotic Recombination. Cell *143*, 924–937.

Kim, S.T., Lim, D.S., Canman, C.E., and Kastan, M.B. (1999). Substrate specificities and identification of putative substrates of ATM kinase family members. J. Biol. Chem. *274*, 37538–37543.

Kim, S.-T., Xu, B., and Kastan, M.B. (2002). Involvement of the cohesin protein, Smc1, in Atm-dependent and independent responses to DNA damage. Genes Dev. *16*, 560–570.

Kitagawa, R. (2004). Phosphorylation of SMC1 is a critical downstream event in the ATM-NBS1-BRCA1 pathway. Genes Dev. *18*, 1423–1438.

Kitajima, T.S., Miyazaki, Y., Yamamoto, M., and Watanabe, Y. (2003). Rec8 cleavage by separase is required for meiotic nuclear divisions in fission yeast. EMBO J. *22*, 5643–5653.

Kitajima, T.S., Sakuno, T., Ishiguro, K., Iemura, S., Natsume, T., Kawashima, S.A., and Watanabe, Y. (2006). Shugoshin collaborates with protein phosphatase 2A to protect cohesin. Nature *441*, 46–52.

Kleckner, N. (2006). Chiasma formation: chromatin/axis interplay and the role(s) of the synaptonemal complex. Chromosoma *115*, 175–194.

Klein, F., Mahr, P., Galova, M., Buonomo, S.B., Michaelis, C., Nairz, K., and Nasmyth, K. (1999). A central role for cohesins in sister chromatid cohesion, formation of axial elements, and recombination during yeast meiosis. Cell *98*, 91–103.

Kschonsak, M., Merkel, F., Bisht, S., Metz, J., Rybin, V., Hassler, M., and Haering, C.H. (2017). Structural Basis for a Safety-Belt Mechanism That Anchors Condensin to Chromosomes. Cell *171*, 588-600.e24.

Kueng, S., Hegemann, B., Peters, B.H., Lipp, J.J., Schleiffer, A., Mechtler, K., and Peters, J.-M. (2006). Wapl controls the dynamic association of cohesin with chromatin. Cell *127*, 955–967.

Kulemzina, I., Schumacher, M.R., Verma, V., Reiter, J., Metzler, J., Failla, A.V., Lanz, C., Sreedharan, V.T., Rätsch, G., and Ivanov, D. (2012). Cohesin Rings Devoid of Scc3 and Pds5 Maintain Their Stable Association with the DNA. PLoS Genet. *8*, e1002856.

Kurze, A., Michie, K.A., Dixon, S.E., Mishra, A., Itoh, T., Khalid, S., Strmecki, L., Shirahige, K., Haering, C.H., Löwe, J., et al. (2011). A positively charged channel within the Smc1/Smc3 hinge required for sister chromatid cohesion: Positively charged hinge channel required for cohesion. EMBO J. *30*, 364–378.

Lightfoot, J., Testori, S., Barroso, C., and Martinez-Perez, E. (2011). Loading of Meiotic Cohesin by SCC-2 Is Required for Early Processing of DSBs and for the DNA Damage Checkpoint. Curr. Biol. *21*, 1421–1430.

Lister, L.M., Kouznetsova, A., Hyslop, L.A., Kalleas, D., Pace, S.L., Barel, J.C., Nathan, A., Floros, V., Adelfalk, C., Watanabe, Y., et al. (2010). Age-Related Meiotic Segregation Errors in Mammalian Oocytes Are Preceded by Depletion of Cohesin and Sgo2. Curr. Biol. *20*, 1511–1521.

Lo, A.W.I., Sprung, C.N., Fouladi, B., Pedram, M., Sabatier, L., Ricoul, M., Reynolds, G.E., and Murnane, J.P. (2002). Chromosome instability as a result of double-strand breaks near telomeres in mouse embryonic stem cells. Mol. Cell. Biol. *22*, 4836–4850.

Loidl, J. (2004). Organization and pairing of meiotic chromosomes in the ciliate Tetrahymena thermophila. J. Cell Sci. *117*, 5791–5801.

Loidl, J. (2006). S. pombe linear elements: the modest cousins of synaptonemal complexes. Chromosoma *115*, 260–271.

Loidl, J. (2016). Conservation and Variability of Meiosis Across the Eukaryotes. Annu. Rev. Genet. *50*, 293–316.

Loidl, J., and Lorenz, A. (2016). DNA double-strand break formation and repair in Tetrahymena meiosis. Semin. Cell Dev. Biol. *54*, 126–134.

Loidl, J., and Mochizuki, K. (2009). Tetrahymena meiotic nuclear reorganization is induced by a checkpoint Kinase–dependent response to DNA damage. Mol. Biol. Cell *20*, 2428–2437.

Loidl, J., Lukaszewicz, A., Howard-Till, R.A., and Koestler, T. (2012). The Tetrahymena meiotic chromosome bouquet is organized by centromeres and promotes interhomolog recombination. J. Cell Sci. *125*, 5873–5880.

Lorenz, A. (2004). S. pombe meiotic linear elements contain proteins related to synaptonemal complex components. J. Cell Sci. *117*, 3343–3351.

Losada, A., Hirano, M., and Hirano, T. (1998). Identification of Xenopus SMC protein complexes required for sister chromatid cohesion. Genes Dev. *12*, 1986–1997.

Losada, A., Yokochi, T., Kobayashi, R., and Hirano, T. (2000). Identification and characterization of SA/Scc3p subunits in the Xenopus and human cohesin complexes. J. Cell Biol. *150*, 405–416.

Lukaszewicz, A., Howard-Till, R.A., Novatchkova, M., Mochizuki, K., and Loidl, J. (2010). MRE11 and COM1/SAE2 are required for double-strand break repair and efficient chromosome pairing during meiosis of the protist Tetrahymena. Chromosoma *119*, 505–518.

Mazumdar, C., and Majeti, R. (2017). The role of mutations in the cohesin complex in acute myeloid leukemia. Int. J. Hematol. *105*, 31–36.

McAleenan, A., Cordon-Preciado, V., Clemente-Blanco, A., Liu, I.-C., Sen, N., Leonard, J., Jarmuz, A., and Aragón, L. (2012). SUMOylation of the α-Kleisin Subunit of Cohesin Is Required for DNA Damage-Induced Cohesion. Curr. Biol. *22*, 1564–1575.

McDonald, B.B. (1966). The exchange of RNA and protein during conjugation in Tetrahymena. J. Protozool. *13*, 277–285.

McGuinness, B.E., Hirota, T., Kudo, N.R., Peters, J.-M., and Nasmyth, K. (2005). Shugoshin prevents dissociation of cohesin from centromeres during mitosis in vertebrate cells. PLoS Biol. *3*, e86.

Mehta, G.D., Rizvi, S.M.A., and Ghosh, S.K. (2012). Cohesin: A guardian of genome integrity. Biochim. Biophys. Acta BBA - Mol. Cell Res. *1823*, 1324–1342.

Merkenschlager, M., and Nora, E.P. (2016). CTCF and Cohesin in Genome Folding and Transcriptional Gene Regulation. Annu. Rev. Genomics Hum. Genet. *17*, 17–43.

Miao, W., Xiong, J., Bowen, J., Wang, W., Liu, Y., Braguinets, O., Grigull, J., Pearlman, R.E., Orias, E., and Gorovsky, M.A. (2009). Microarray Analyses of Gene Expression during the Tetrahymena thermophila Life Cycle. PLoS ONE *4*, e4429.

Michaelis, C., Ciosk, R., and Nasmyth, K. (1997). Cohesins: Chromosomal Proteins that Prevent Premature Separation of Sister Chromatids. Cell *91*, 35–45.

Mishra, A., Hu, B., Kurze, A., Beckouët, F., Farcas, A.-M., Dixon, S.E., Katou, Y., Khalid, S., Shirahige, K., and Nasmyth, K. (2010). Both Interaction Surfaces within Cohesin's Hinge Domain Are Essential for Its Stable Chromosomal Association. Curr. Biol. *20*, 279–289.

Mochizuki, K., Novatchkova, M., and Loidl, J. (2008). DNA double-strand breaks, but not crossovers, are required for the reorganization of meiotic nuclei in Tetrahymena. J. Cell Sci. *121*, 2148–2158.

Murayama, Y., and Uhlmann, F. (2014). Biochemical reconstitution of topological DNA binding by the cohesin ring. Nature *505*, 367–371.

Nasir, A.M., Yang, Q., Chalker, D.L., and Forney, J.D. (2015). SUMOylation Is Developmentally Regulated and Required for Cell Pairing during Conjugation in Tetrahymena thermophila. Eukaryot. Cell *14*, 170–181.

Nasmyth, K., and Haering, C.H. (2009). Cohesin: Its Roles and Mechanisms. Annu. Rev. Genet. *43*, 525–558.

Nayak, A., and Müller, S. (2014). SUMO-specific proteases/isopeptidases: SENPs and beyond. Genome Biol. *15*.

NCBI Resource Coordinators (2012). Database resources of the National Center for Biotechnology Information. Nucleic Acids Res. *41*, D8–D20.

Neuwald, A.F. (2000). HEAT Repeats Associated with Condensins, Cohesins, and Other Complexes Involved in Chromosome-Related Functions. Genome Res. *10*, 1445–1452.

Nishiyama, T., Ladurner, R., Schmitz, J., Kreidl, E., Schleiffer, A., Bhaskara, V., Bando, M., Shirahige, K., Hyman, A.A., Mechtler, K., et al. (2010). Sororin Mediates Sister Chromatid Cohesion by Antagonizing Wapl. Cell *143*, 737–749.

Noto, T., and Mochizuki, K. (2017). Whats, hows and whys of programmed DNA elimination in *Tetrahymena*. Open Biol. *7*, 170172.

Novak, I., Wang, H., Revenkova, E., Jessberger, R., Scherthan, H., and Höög, C. (2008). Cohesin Smc1β determines meiotic chromatin axis loop organization. J. Cell Biol. *180*, 83–90.

Orias, E., Cervantes, M.D., and Hamilton, E.P. (2011). Tetrahymena thermophila, a unicellular eukaryote with separate germline and somatic genomes. Res. Microbiol. *162*, 578–586.

Pampalona, J., Roscioli, E., Silkworth, W.T., Bowden, B., Genescà, A., Tusell, L., and Cimini, D. (2016). Chromosome Bridges Maintain Kinetochore-Microtubule Attachment throughout Mitosis and Rarely Break during Anaphase. PLOS ONE *11*, e0147420.

Panizza, S., Mendoza, M.A., Berlinger, M., Huang, L., Nicolas, A., Shirahige, K., and Klein, F. (2011). Spo11-Accessory Proteins Link Double-Strand Break Sites to the Chromosome Axis in Early Meiotic Recombination. Cell *146*, 372–383.

Parelho, V., Hadjur, S., Spivakov, M., Leleu, M., Sauer, S., Gregson, H.C., Jarmuz, A., Canzonetta, C., Webster, Z., Nesterova, T., et al. (2008). Cohesins Functionally Associate with CTCF on Mammalian Chromosome Arms. Cell *132*, 422–433.

Pasierbek, P., Födermayr, M., Jantsch, V., Jantsch, M., Schweizer, D., and Loidl, J. (2003). The Caenorhabditis elegans SCC-3 homologue is required for meiotic synapsis and for proper chromosome disjunction in mitosis and meiosis. Exp. Cell Res. *289*, 245–255.

Petela, N.J., Gligoris, T.G., Metson, J., Lee, B.-G., Voulgaris, M., Hu, B., Kikuchi, S., Chapard, C., Chen, W., Rajendra, E., et al. (2018). Scc2 Is a Potent Activator of Cohesin's ATPase that Promotes Loading by Binding Scc1 without Pds5. Mol. Cell *70*, 1134-1148.e7.

Peters, J.-M., and Nishiyama, T. (2012). Sister Chromatid Cohesion. Cold Spring Harb. Perspect. Biol. *4*, a011130–a011130.

Piazza, I., Rutkowska, A., Ori, A., Walczak, M., Metz, J., Pelechano, V., Beck, M., and Haering, C.H. (2014). Association of condensin with chromosomes depends on DNA binding by its HEAT-repeat subunits. Nat. Struct. Mol. Biol. *21*, 560–568.

Rankin, S., and Dawson, D.S. (2016). Recent advances in cohesin biology. F1000Research *5*, 1909.

Rao, S.S.P., Huntley, M.H., Durand, N.C., Stamenova, E.K., Bochkov, I.D., Robinson, J.T., Sanborn, A.L., Machol, I., Omer, A.D., Lander, E.S., et al. (2014). A 3D Map of the Human Genome at Kilobase Resolution Reveals Principles of Chromatin Looping. Cell *159*, 1665–1680.

Rao, S.S.P., Huang, S.-C., Glenn St Hilaire, B., Engreitz, J.M., Perez, E.M., Kieffer-Kwon, K.-R., Sanborn, A.L., Johnstone, S.E., Bascom, G.D., Bochkov, I.D., et al. (2017). Cohesin Loss Eliminates All Loop Domains. Cell *171*, 305-320.e24.

Remeseiro, S., Cuadrado, A., Carretero, M., Martínez, P., Drosopoulos, W.C., Cañamero, M., Schildkraut, C.L., Blasco, M.A., and Losada, A. (2012). Cohesin-SA1 deficiency drives aneuploidy and tumourigenesis in mice due to impaired replication of telomeres. EMBO J. *31*, 2076–2089.

Rhodes, J., Haarhuis, J., Grimm, J., Rowland, B., Lavis, L., and Nasmyth, K. (2017a). Cohesin Can Remain Associated With Chromosomes During DNA Replication. BioRxiv 124107.

Rhodes, J., Mazza, D., Nasmyth, K., and Uphoff, S. (2017b). Scc2/Nipbl hops between chromosomal cohesin rings after loading. ELife *6*.

Riedel, C.G., Katis, V.L., Katou, Y., Mori, S., Itoh, T., Helmhart, W., Gálová, M., Petronczki, M., Gregan, J., Cetin, B., et al. (2006). Protein phosphatase 2A protects centromeric sister chromatid cohesion during meiosis I. Nature *441*, 53–61.

Roig, M.B., Löwe, J., Chan, K.-L., Beckouët, F., Metson, J., and Nasmyth, K. (2014). Structure and function of cohesin's Scc3/SA regulatory subunit. FEBS Lett. *588*, 3692–3702.

Rong, M., Matsuda, A., Hiraoka, Y., and Lee, J. (2016). Meiotic cohesin subunits RAD21L and REC8 are positioned at distinct regions between lateral elements and transverse filaments in the synaptonemal complex of mouse spermatocytes. J. Reprod. Dev. *62*, 623–630.

Rowland, B.D., Roig, M.B., Nishino, T., Kurze, A., Uluocak, P., Mishra, A., Beckouët, F., Underwood, P., Metson, J., Imre, R., et al. (2009). Building Sister Chromatid Cohesion: Smc3 Acetylation Counteracts an Antiestablishment Activity. Mol. Cell *33*, 763–774.

Sacristan, C., and Kops, G.J.P.L. (2015). Joined at the hip: kinetochores, microtubules, and spindle assembly checkpoint signaling. Trends Cell Biol. *25*, 21–28.

Sakuno, T., and Watanabe, Y. (2015). Phosphorylation of Cohesin Rec11/SA3 by Casein Kinase 1 Promotes Homologous Recombination by Assembling the Meiotic Chromosome Axis. Dev. Cell *32*, 220–230.

Sanyal, S., Molnarova, L., Richterova, J., Huraiova, B., Benko, Z., Polakova, S., Cipakova, I., Sevcovicova, A., Gaplovska-Kysela, K., Mechtler, K., et al. (2018). Mutations that prevent methylation of cohesin render sensitivity to DNA damage in *S. pombe*. J. Cell Sci. *131*, jcs214924.

Scherthan, H. (2007). Telomeres and meiosis in health and disease: Telomere attachment and clustering during meiosis. Cell. Mol. Life Sci. *64*, 117–124.

Schmitz, J., Watrin, E., Lénárt, P., Mechtler, K., and Peters, J.-M. (2007). Sororin Is Required for Stable Binding of Cohesin to Chromatin and for Sister Chromatid Cohesion in Interphase. Curr. Biol. *17*, 630–636.

Schwarzer, W., Abdennur, N., Goloborodko, A., Pekowska, A., Fudenberg, G., Loe-Mie, Y., Fonseca, N.A., Huber, W., Haering, C., Mirny, L., et al. (2017). Two independent modes of chromatin organization revealed by cohesin removal. Nature.

Seitan, V.C., and Merkenschlager, M. (2012). Cohesin and chromatin organisation. Curr. Opin. Genet. Dev. *22*, 93–100.

Seitan, V.C., Hao, B., Tachibana-Konwalski, K., Lavagnolli, T., Mira-Bontenbal, H., Brown, K.E., Teng, G., Carroll, T., Terry, A., Horan, K., et al. (2011). A role for cohesin in T-cell-receptor rearrangement and thymocyte differentiation. Nature *476*, 467–471.

Shodhan, A., Kataoka, K., Mochizuki, K., Novatchkova, M., and Loidl, J. (2017). A Zip3-like protein plays a role in crossover formation in the SC-less meiosis of the protist *Tetrahymena*. Mol. Biol. Cell *28*, 825–833.

Sjögren, C., and Nasmyth, K. (2001). Sister chromatid cohesion is required for postreplicative double-strand break repair in Saccharomyces cerevisiae. Curr. Biol. CB *11*, 991–995.

States, D.J., and Gish, W. (1994). QGB: Combined Use of Sequence Similarity and Codon Bias for Coding Region Identification. J. Comput. Biol. *1*, 39–50.

Stead, K., Aguilar, C., Hartman, T., Drexel, M., Meluh, P., and Guacci, V. (2003). Pds5p regulates the maintenance of sister chromatid cohesion and is sumoylated to promote the dissolution of cohesion. J. Cell Biol. *163*, 729–741.

Storlazzi, A., Tesse, S., Ruprich-Robert, G., Gargano, S., Pöggeler, S., Kleckner, N., and Zickler, D. (2008). Coupling meiotic chromosome axis integrity to recombination. Genes Dev. *22*, 796–809.

Stover, N.A. (2006). Tetrahymena Genome Database (TGD): a new genomic resource for Tetrahymena thermophila research. Nucleic Acids Res. *34*, D500–D503.

Ström, L., Lindroos, H.B., Shirahige, K., and Sjögren, C. (2004). Postreplicative recruitment of cohesin to double-strand breaks is required for DNA repair. Mol. Cell *16*, 1003–1015.

Ström, L., Karlsson, C., Lindroos, H.B., Wedahl, S., Katou, Y., Shirahige, K., and Sjögren, C. (2007). Postreplicative formation of cohesion is required for repair and induced by a single DNA break. Science *317*, 242–245.

Subramanian, V.V., and Hochwagen, A. (2014). The Meiotic Checkpoint Network: Step-by-Step through Meiotic Prophase. Cold Spring Harb. Perspect. Biol. *6*, a016675–a016675.

Sumara, I., Vorlaufer, E., Gieffers, C., Peters, B.H., and Peters, J.-M. (2000). Characterization of vertebrate cohesin complexes and their regulation in prophase. J. Cell Biol. *151*, 749–762.

Sumara, I., Vorlaufer, E., Stukenberg, P.T., Kelm, O., Redemann, N., Nigg, E.A., and Peters, J.-M. (2002). The Dissociation of Cohesin from Chromosomes in Prophase Is Regulated by Polo-like Kinase. Mol. Cell *9*, 515–525.

Tedeschi, A., Wutz, G., Huet, S., Jaritz, M., Wuensche, A., Schirghuber, E., Davidson, I.F., Tang, W., Cisneros, D.A., Bhaskara, V., et al. (2013). Wapl is an essential regulator of chromatin structure and chromosome segregation. Nature *501*, 564–568.

Tusell, L., Soler, D., Agostini, M., Pampalona, J., and Genescà, A. (2008). The number of dysfunctional telomeres in a cell: one amplifies; more than one translocate. Cytogenet. Genome Res. *122*, 315–325.

Uhlmann, F., Lottspeich, F., and Nasmyth, K. (1999). Sister-chromatid separation at anaphase onset is promoted by cleavage of the cohesin subunit Scc1. Nature *400*, 37–42.

Uhlmann, F., Wernic, D., Poupart, M.-A., Koonin, E.V., and Nasmyth, K. (2000). Cleavage of Cohesin by the CD Clan Protease Separin Triggers Anaphase in Yeast. Cell *103*, 375–386.

Unal, E., Heidinger-Pauli, J.M., and Koshland, D. (2007). DNA Double-Strand Breaks Trigger Genome-Wide Sister-Chromatid Cohesion Through Eco1 (Ctf7). Science *317*, 245–248.

U nal, E., Heidinger-Pauli, J.M., Kim, W., Guacci, V., Onn, I., Gygi, S.P., and Koshland, D.E. (2008). A Molecular Determinant for the Establishment of Sister Chromatid Cohesion. Science *321*, 566–569.

Van Bortle, K., Nichols, M.H., Li, L., Ong, C.-T., Takenaka, N., Qin, Z.S., and Corces, V.G. (2014). Insulator function and topological domain border strength scale with architectural protein occupancy. Genome Biol. *15*, R82.

Visnes, T., Giordano, F., Kuznetsova, A., Suja, J.A., Lander, A.D., Calof, A.L., and Ström, L. (2014). Localisation of the SMC loading complex Nipbl/Mau2 during mammalian meiotic prophase I. Chromosoma *123*, 239–252.

Waizenegger, I.C., Hauf, S., Meinke, A., and Peters, J.-M. (2000). Two distinct pathways remove mammalian cohesin from chromosome arms in prophase and from centromeres in anaphase. Cell *103*, 399–410.

Wang, F., Yoder, J., Antoshechkin, I., and Han, M. (2003). Caenorhabditis elegans EVL-14/PDS-5 and SCC-3 Are Essential for Sister Chromatid Cohesion in Meiosis and Mitosis. Mol. Cell. Biol. *23*, 7698–7707.

Watrin, E., Schleiffer, A., Tanaka, K., Eisenhaber, F., Nasmyth, K., and Peters, J.-M. (2006). Human Scc4 Is Required for Cohesin Binding to Chromatin, Sister-Chromatid Cohesion, and Mitotic Progression. Curr. Biol. *16*, 863–874.

Weitzer, S., Lehane, C., and Uhlmann, F. (2003). A Model for ATP Hydrolysis-Dependent Binding of Cohesin to DNA. Curr. Biol. *13*, 1930–1940.

Wendt, K.S., Yoshida, K., Itoh, T., Bando, M., Koch, B., Schirghuber, E., Tsutsumi, S., Nagae, G., Ishihara, K., Mishiro, T., et al. (2008). Cohesin mediates transcriptional insulation by CCCTC-binding factor. Nature *451*, 796–801.

Winter, A., Schmid, R., and Bayliss, R. (2015). Structural Insights into Separase Architecture and Substrate Recognition through Computational Modelling of Caspase-Like and Death Domains. PLOS Comput. Biol. *11*, e1004548.

Winters, T., McNicoll, F., and Jessberger, R. (2014). Meiotic cohesin STAG3 is required for chromosome axis formation and sister chromatid cohesion. EMBO J.

Woodman, J., Fara, T., Dzieciatkowska, M., Trejo, M., Luong, N., Hansen, K.C., and Megee, P.C. (2014). Cell cycle-specific cleavage of Scc2 regulates its cohesin deposition activity. Proc. Natl. Acad. Sci. *111*, 7060–7065.

Wu, N., Kong, X., Ji, Z., Zeng, W., Potts, P.R., Yokomori, K., and Yu, H. (2012). Scc1 sumoylation by Mms21 promotes sister chromatid recombination through counteracting Wapl. Genes Dev. *26*, 1473–1485.

Wutz, G., Várnai, C., Nagasaka, K., Cisneros, D.A., Stocsits, R.R., Tang, W., Schoenfelder, S., Jessberger, G., Muhar, M., Hossain, M.J., et al. (2017). Topologically associating domains and

chromatin loops depend on cohesin and are regulated by CTCF, WAPL, and PDS5 proteins. EMBO J. *36*, 3573–3599.

Xiong, J., Lu, Y., Feng, J., Yuan, D., Tian, M., Chang, Y., Fu, C., Wang, G., Zeng, H., and Miao, W. (2013). Tetrahymena Functional Genomics Database (TetraFGD): an integrated resource for Tetrahymena functional genomics. Database *2013*.

Yakisich, J.S., Sandoval, P.Y., Morrison, T.L., and Kapler, G.M. (2006). TIF1 Activates the Intra-S-Phase Checkpoint Response in the Diploid Micronucleus and Amitotic Polyploid Macronucleus of *Tetrahymena*. Mol. Biol. Cell *17*, 5185–5197.

Yazdi, P.T., Wang, Y., Zhao, S., Patel, N., Lee, E.Y.-H.P., and Qin, J. (2002). SMC1 is a downstream effector in the ATM/NBS1 branch of the human S-phase checkpoint. Genes Dev. *16*, 571–582.

Zhan, Y., Giorgetti, L., and Tiana, G. (2017). Modelling genome-wide topological associating domains in mouse embryonic stem cells. Chromosome Res. Int. J. Mol. Supramol. Evol. Asp. Chromosome Biol. *25*, 5–14.

Zhang, J., Shi, X., Li, Y., Kim, B.-J., Jia, J., Huang, Z., Yang, T., Fu, X., Jung, S.Y., Wang, Y., et al. (2008a). Acetylation of Smc3 by Eco1 Is Required for S Phase Sister Chromatid Cohesion in Both Human and Yeast. Mol. Cell *31*, 143–151.

Zhang, N., Kuznetsov, S.G., Sharan, S.K., Li, K., Rao, P.H., and Pati, D. (2008b). A handcuff model for the cohesin complex. J. Cell Biol. *183*, 1019–1031.

Zhang, N., Ge, G., Meyer, R., Sethi, S., Basu, D., Pradhan, S., Zhao, Y.-J., Li, X.-N., Cai, W.-W., El-Naggar, A.K., et al. (2008c). Overexpression of Separase induces aneuploidy and mammary tumorigenesis. Proc. Natl. Acad. Sci. *105*, 13033–13038.

Zickler, D., and Kleckner, N. (2015). Recombination, Pairing, and Synapsis of Homologs during Meiosis. Cold Spring Harb. Perspect. Biol. *7*, a016626.

# Appendix : Alignments

All alignments were generated with Geneious software (Ali et al., 2018; Edgar, 2004; Kearse et al., 2012). Tt: *Tetrahymena thermophila*, Sc: *Saccharomyces cerevisiae*, Sp: *Schizosaccharomyces pombe*, At: *Arabidopsis thaliana*, Ce: *Caenorhabditis elegans*, Dm: *Drosophila melanogaster*, Hs: *Homo sapiens*, Xl: *Xenopus laevis* , Mm: *Mus musculus*

## 1. Smc1 alignment

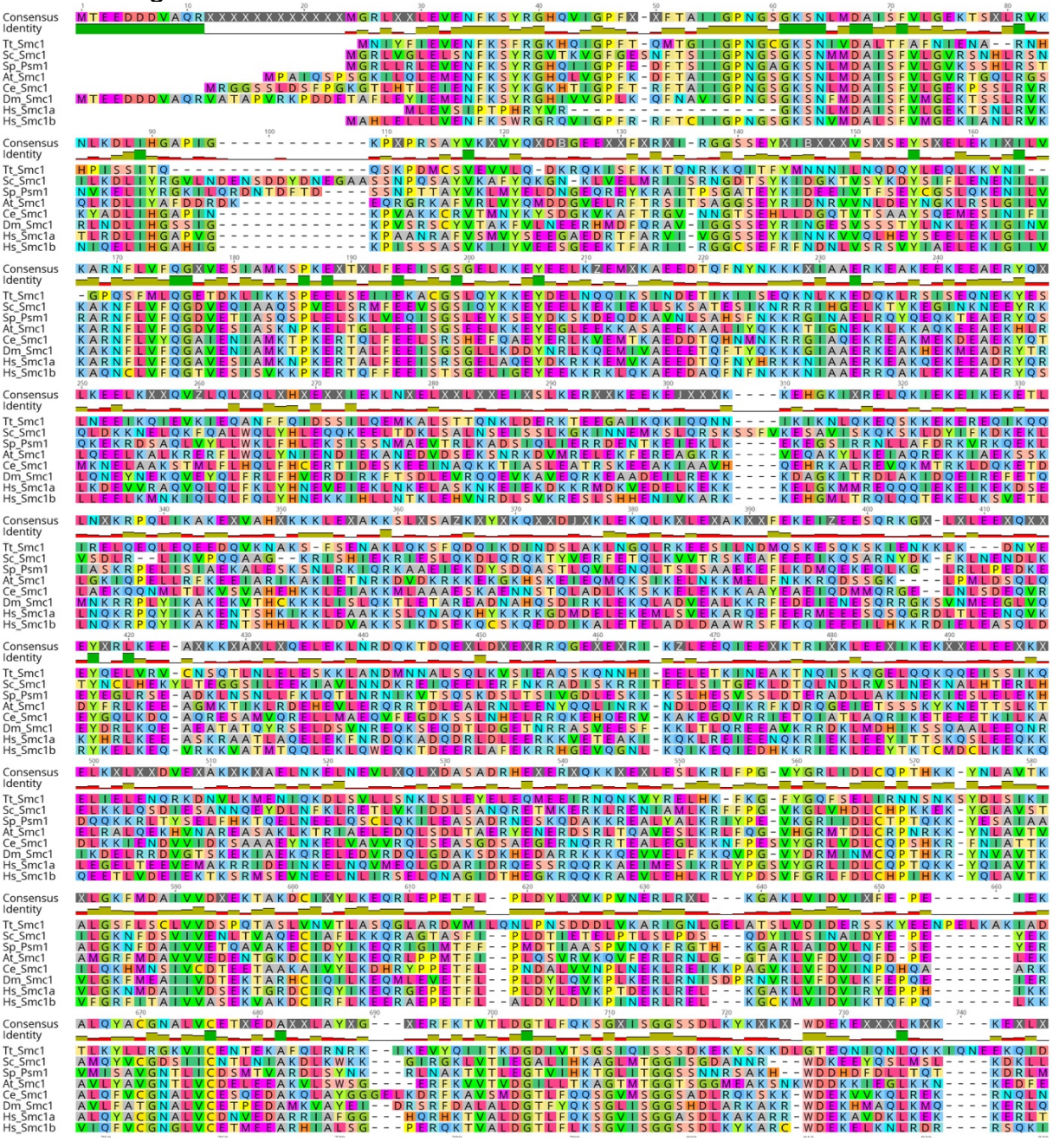


Consensus
Identity
Tt_Smc1
Sc_Smc1
Sp_Psm1
At_Smc1
Ce_Smc1
Dm_Smc1
Hs_Smc1a
Hs_Smc1b

## 2. Smc3 alignment

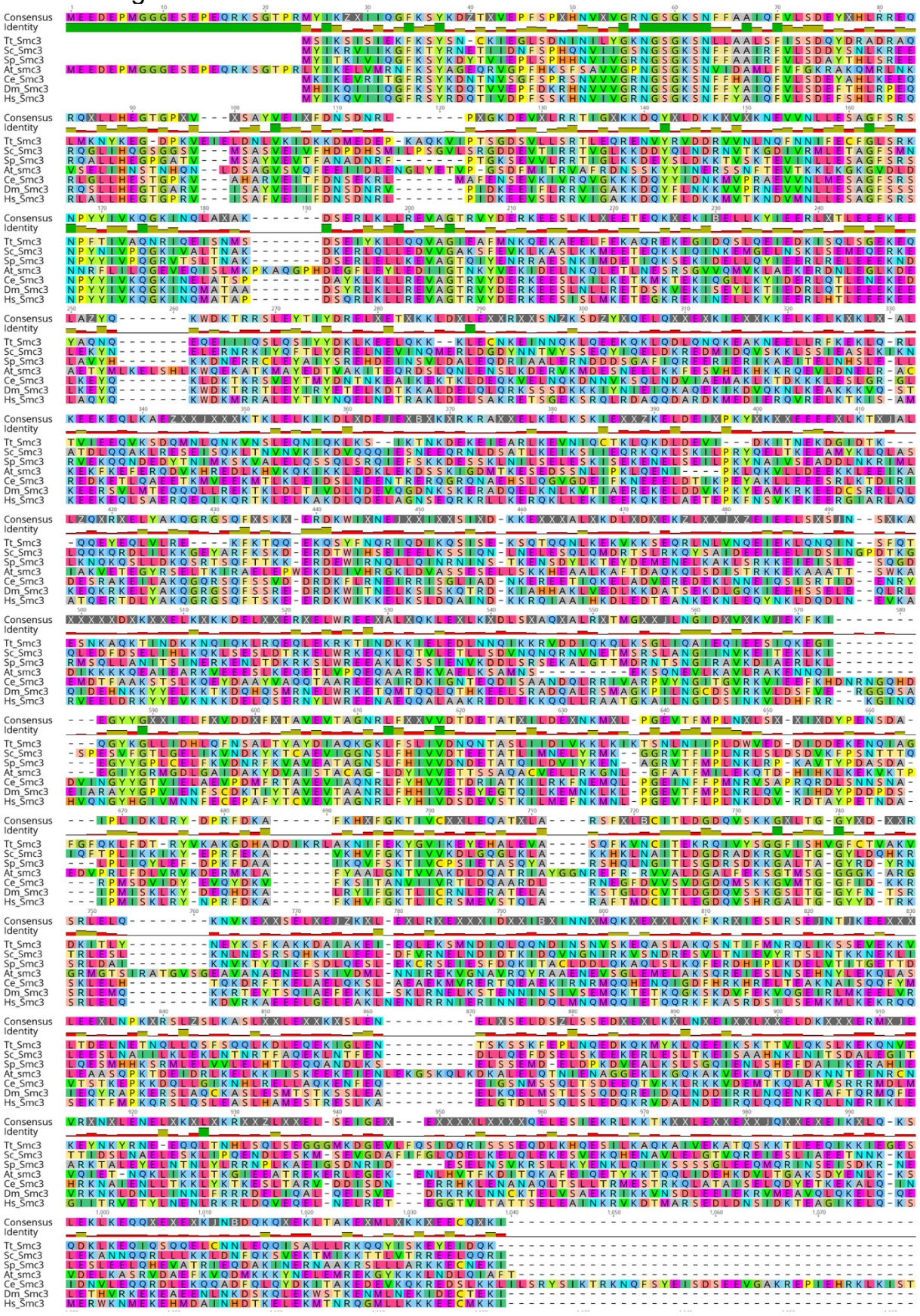

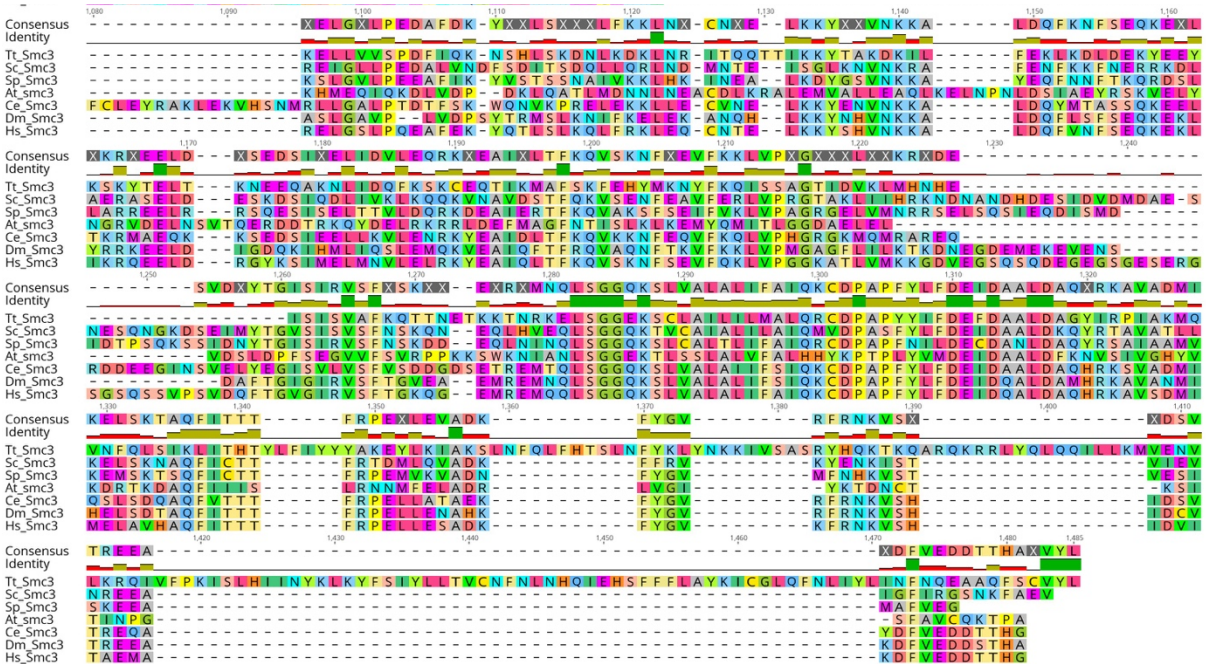
Consensus
Identity
Tt_Smc3
Sc_Smc3
Sp_Smc3
At_smc3
Ce_Smc3
Dm_Smc3
Hs_Smc3

## 3. Rec8 alignment

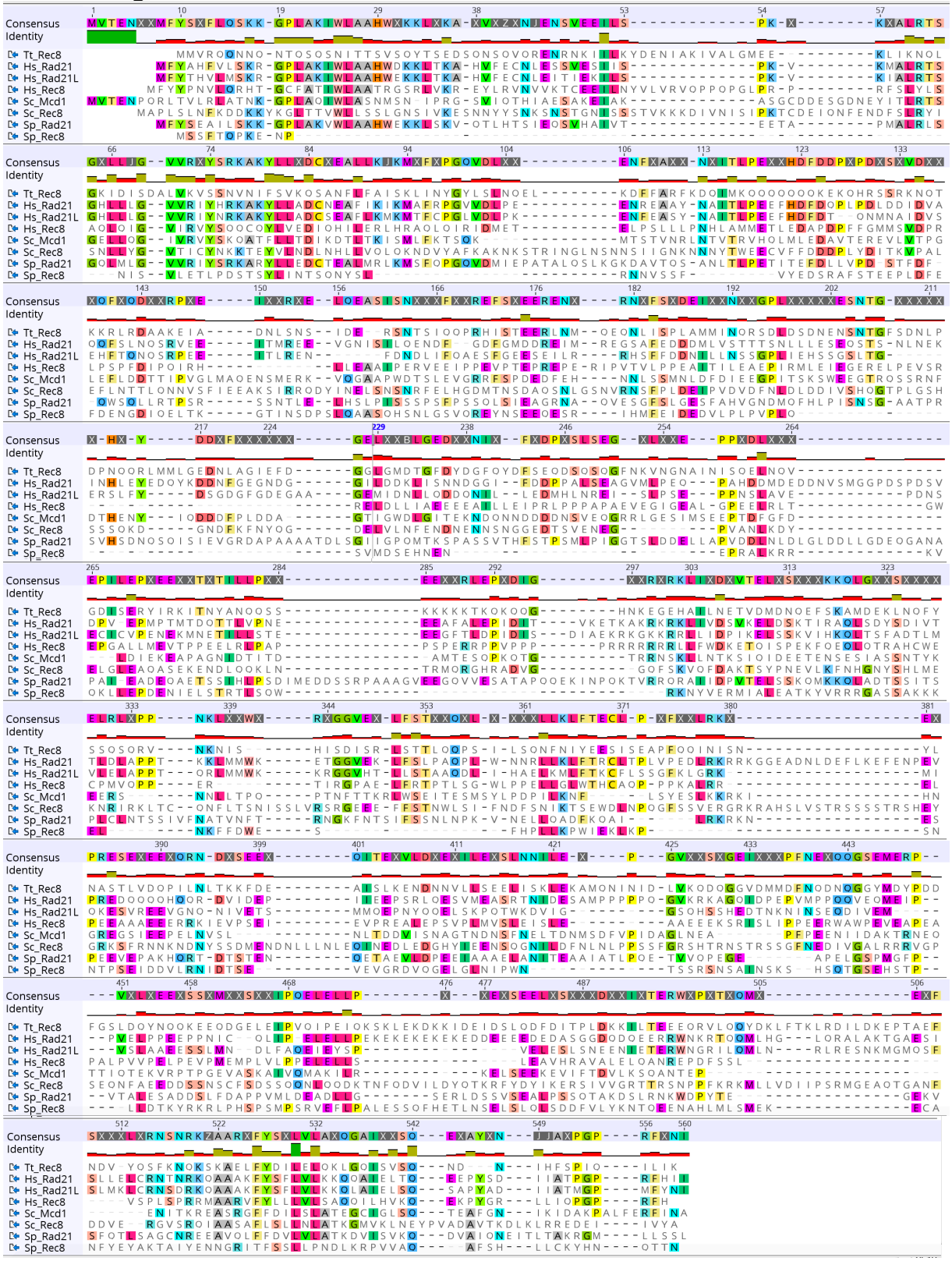

# 4. Scc3 alignment

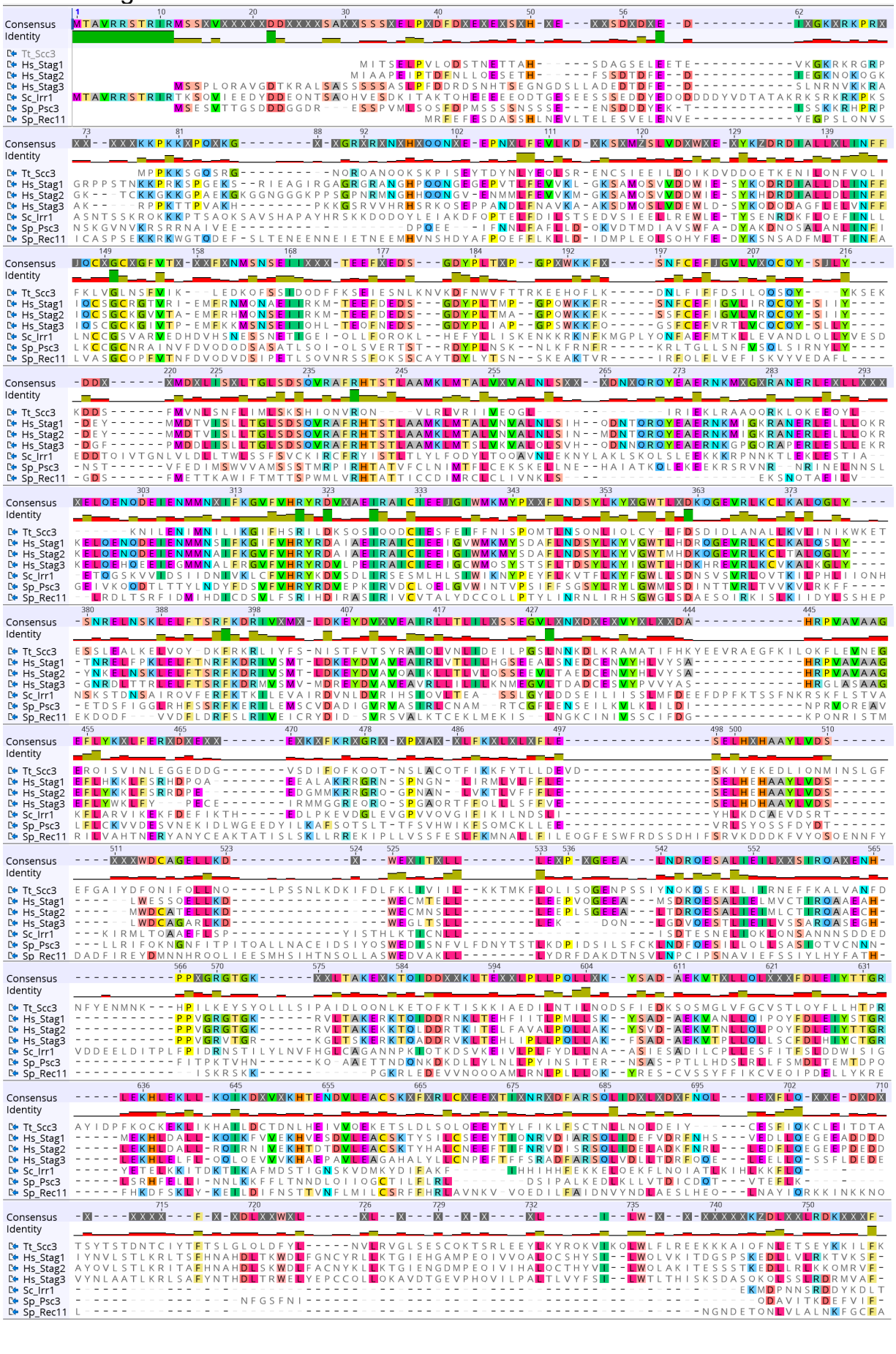

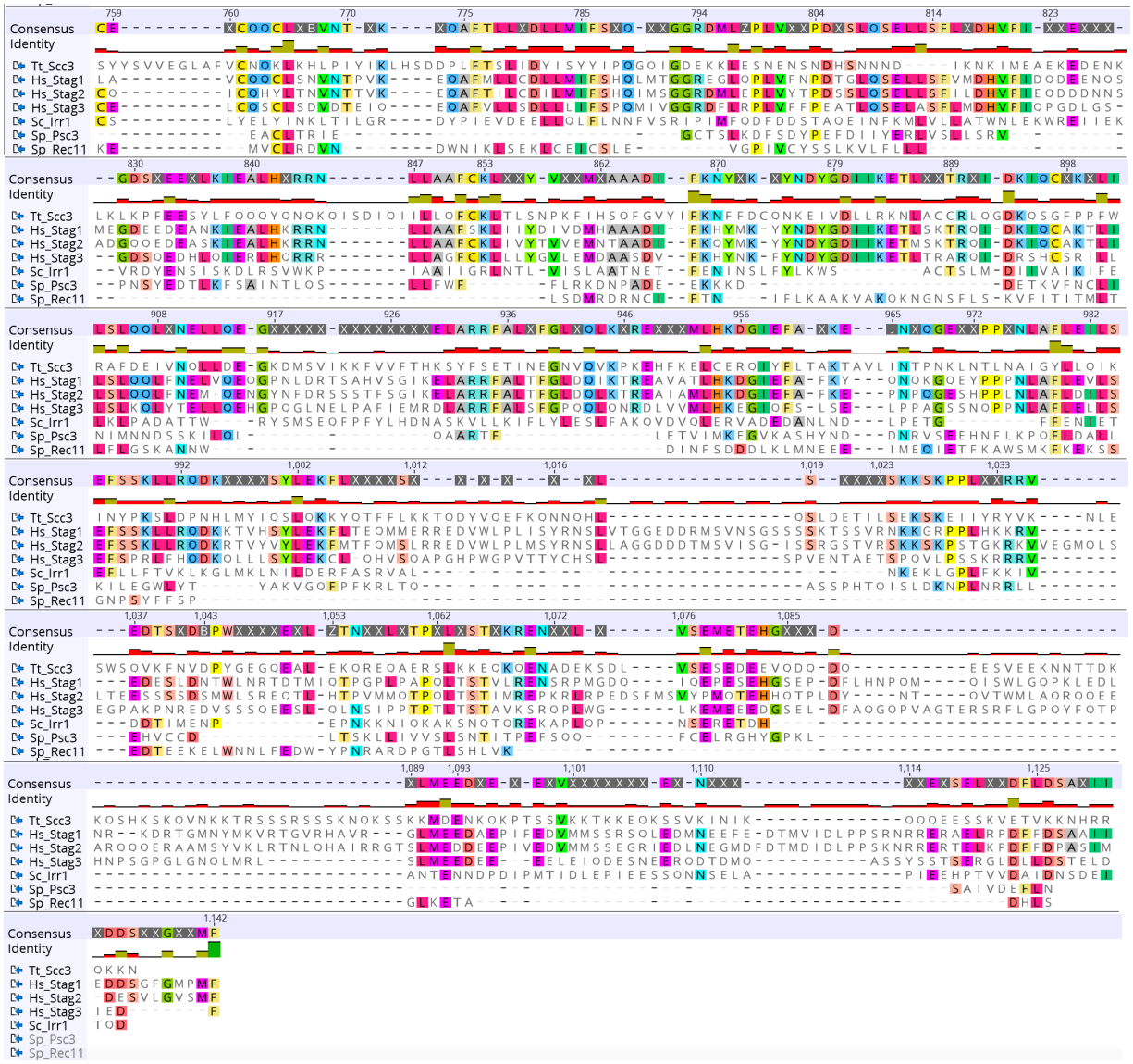
Consensus
Identity
Tt_Scc3
Hs_Stag1
Hs_Stag2
Hs_Stag3
Sc_Irr1
Sp_Psc3
Sp_Rec11

# 5. Scc2 alignment

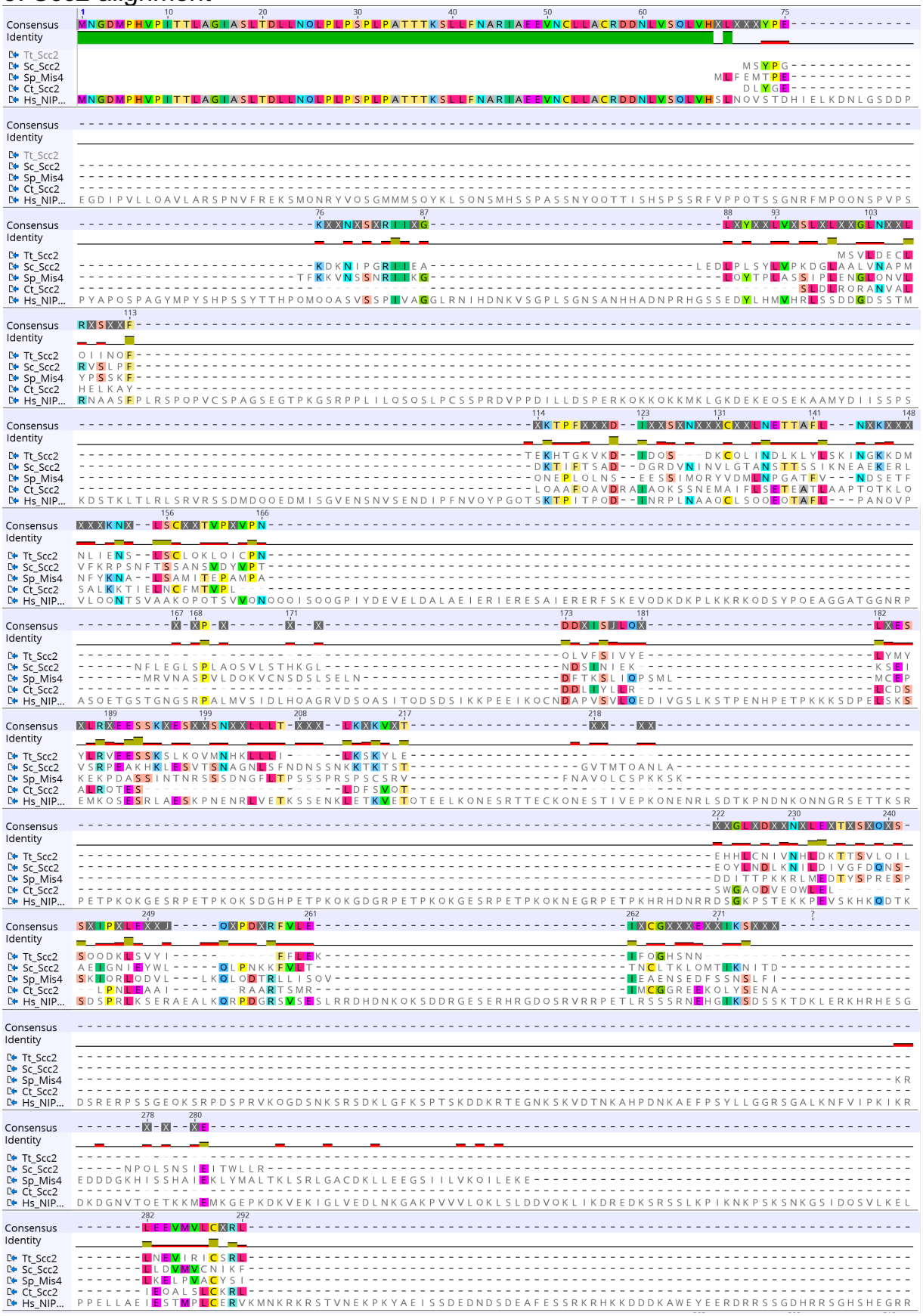

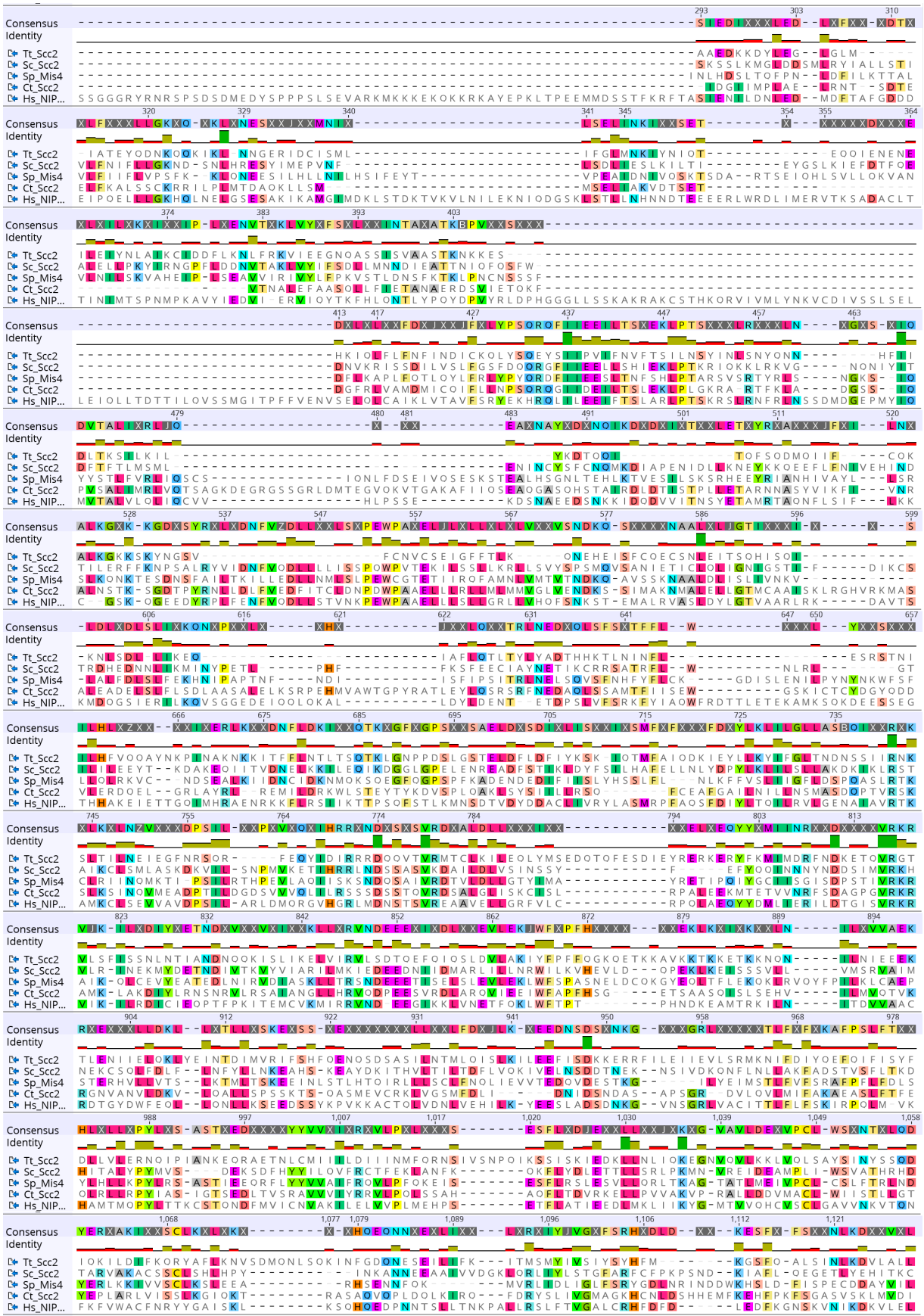
Consensus
Identity
Tt_Scc2
Sc_Scc2
Sp_Mis4
Ct_Scc2
Hs_NIP...

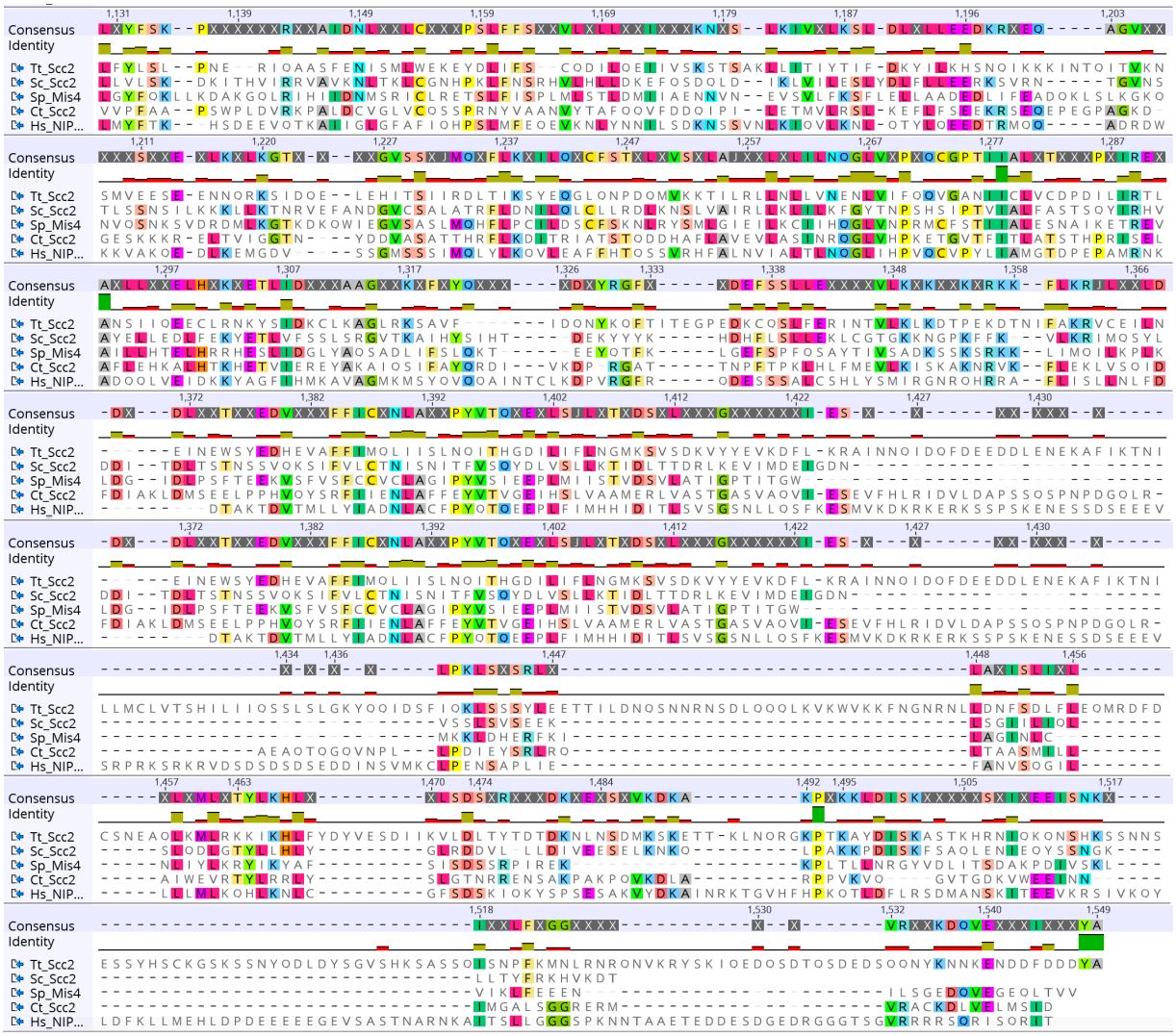
Consensus
Identity
Tt_Scc2
Sc_Scc2
Sp_Mis4
Ct_Scc2
Hs_NIP...

## 6. Ulp1 alignment

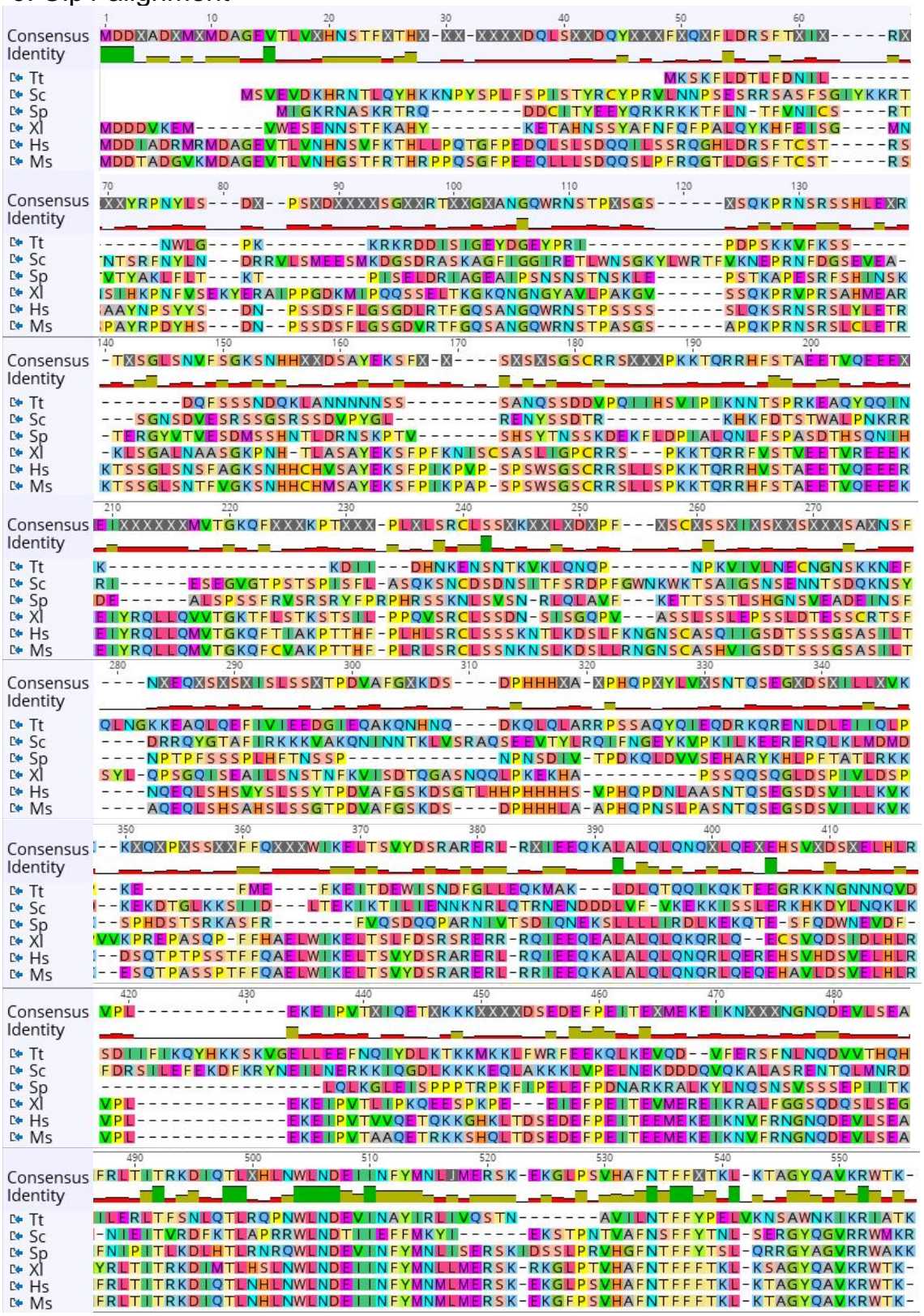

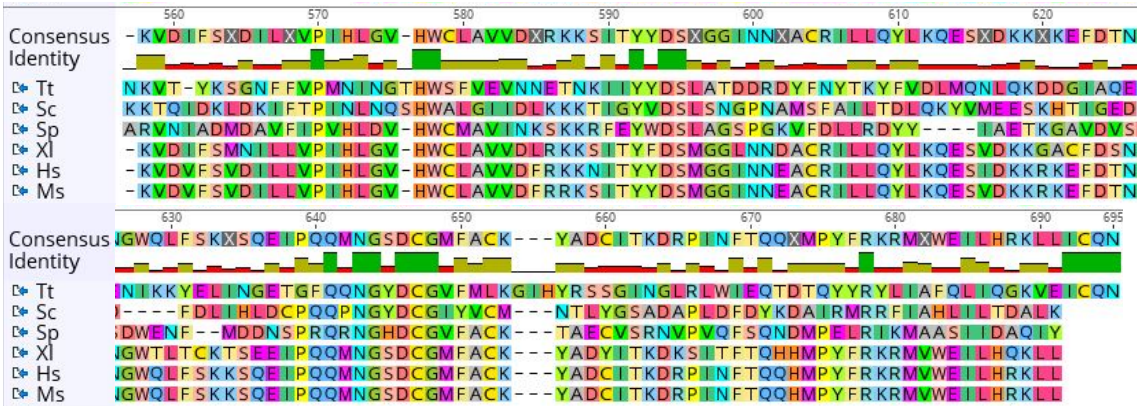
560 570 580 590 600 610 620
Consensus -KVDIIFSXDILXVPIHLGV-HWCLAVVDXRKKSIITYYDSXGGINNXACRILLQYLKQESXDKKXKEFDTN
Identity
Tt NKVT-YKSGNFFVPMNINGTHWSFVEVNNETNKIIYYDSLATDDRDYFNYTKYFVDLMQNLQKDDGIAQF
Sc KKTQIDKLDKIFTPINLNQSHWALGIIDLKKKTIGYVDSLSNGPNAMSFAILTDLQKYVMEESKHTIGED
Sp ARVNIADMDAVFIPVHLDV-HWCMAVINKSKKRFEYWDSLAGSPGKVFDLLRDYY----IAETKGAVDVS
Xl -KVDIFSMNILLVPIHLGV-HWCLAVVDLRKKSITYFDSMGGLNNDACRILLQYLKQESVDKKGACFDSN
Hs -KVDVFSVDILLVPIHLGV-HWCLAVVDFRKKNITYYDSMGGINNEACRILLQYLKQESIDKKRKEFDTN
Ms -KVDVFSVDILLVPIHLGV-HWCLAVVDFRRKSIITYYDSMGGINNEACRILLQYLKQESVDKKRKEFDTN
630 640 650 660 670 680 690 695
Consensus GWQLFSKXSQEIPQQMNGSDCGMFACK---YADCITKDRPINFTQQXMPYFRKRMXWEILHRKLLICQN
Identity
Tt NIKKYELINGETGFQQNGYDCGVFMLKGIHYRSSGINGLRLWIEQTDTQYYRYLIAFQLIQGKVEICQN
Sc I----FDLIHLDCPQQPNGYDCGIYVCM---NTLYGSADAPLDFDYKDAIRMRRFIAHLILTDALK
Sp DWENF--MDDNSPRQRNGHDCGVFACK---TAECVSRNVPVQFSQNDMPELRIKMAASIIDAQIY
Xl GWTLTCKTSEEIPQQMNGSDCGMFACK---YADYITKDKSITFTQHHMPYFRKRMVWEILHQKLL
Hs GWQLFSKKSQEIPQQMNGSDCGMFACK---YADCITKDRPINFTQQHMPYFRKRMVWEILHRKLL
Ms GWQLFSKKSQEIPQQMNGSDCGMFACK---YADCITKDRPINFTQQHMPYFRKRMVWEILHRKLL